UNLV UNIVERSITY LIBRARIES

8-2002

Genesis and morphology of soil pendants in Quaternary landforms of Pahranagat Valley, Nevada

Amy Lynn Brock
University of Nevada, Las Vegas

Follow this and additional works at: https://digitalscholarship.unlv.edu/thesesdissertations

Part of the Desert Ecology Commons, Geology Commons, Geomorphology Commons, and the Soil Science Commons

GENESIS AND MORPHOLOGY OF SOIL PENDANTS IN QUATERNARY

LANDFORMS OF PAHRANAGAT VALLEY, NEVADA

by

Amy L. Brock

Bachelor of Science
Oklahoma State University
1999

A thesis submitted in partial fulfillment
of the requirements for the

Master of Science Degree
Department of Geoscience
College of Sciences

Graduate College
University of Nevada, Las Vegas
August 2002

UNLV
UNIVERSITY OF NEVADA LAS VEGAS

Thesis Approval

The Graduate College
University of Nevada, Las Vegas

_____May 3,_____ , 20_02_

The Thesis prepared by

Amy L. Brock

Entitled

Genesis and Morphology of Soil Pendants in Quaternary Landforms of

Pahranagat Valley, Nevada

is approved in partial fulfillment of the requirements for the degree of

Master of Science

Examination Committee Chair

Dean of the Graduate College

Examination Committee Member

Examination Committee Member

Graduate College Faculty Representative

ABSTRACT

Genesis and morphology of soil pendants in Quaternary landforms of Pahranagat Valley, Nevada

by

Amy L. Brock

Dr. Brenda Buck, Examination Committee Chair
Professor of Geoscience
University of Nevada, Las Vegas

Five geomorphic surfaces present in the northern Pahranagat Valley, Lincoln County,

Nevada range in age from Early Pleistocene to Recent (Q1-Q5) and vary in clast

lithology from dolomite to volcanic tephras. Two chronosequences and 5 lithosequences

were compared to evaluate micro and macromorphic characteristics and development of

soil pendants. This study presents a new interpretation for soil pendant development.

Key features observed in the Pahranagat Valley pendants provide evidence for

precipitation at the clast-pendant contact suggesting that newer deposits are not always

found at the pendant terminus as other studies have assumed. These features include a

void at the clast-pendant contact where precipitates such as calcium carbonate, silica

and/or fibrous silicate clays may precipitate. Other features present in these pendants

include significant amounts of parent clast grains that are incorporated into the pendant,

detrital grain and parent material displacement and/or dissolution and presence of the

fibrous clay sepiolite.

TABLE OF CONTENTS

,

LIST OF FIGURES

ACKNOWLEDGMENTS

CHAPTER I

INTRODUCTION AND BACKGROUND

Purpose of Study

Laminar accumulations of pedogenic material such as calcium carbonate that

accumulates on the bottoms of coarse clasts within a soil profile (pendants) are becoming

increasingly important to Quaternary landform studies throughout the western United

States. Pendants are found in many soils of arid and semi-arid regions of the world. Few

studies have focused on the morphology and genesis of these features although they have

recently provided the material for absolute and relative dating of geomorphic landforms

as well as the timing of Quaternary faulting episodes. Numerous chronosequence studies

pertaining to the genesis of calcic soils have also used pendants for obtaining information

on calcium carbonate development through time. The purpose of this study is to evaluate

soils on a series of landforms that vary with age and clast lithology to determine the

influence of these parameters on the genesis of calcic soil pendant features. This thesis

will address several questions concerning soil pendants found in the Pahranagat Valley of

Lincoln County, Nevada: (1) How are soil pendants formed? (2) What are the

microscopic and macroscopic characteristics of pendants? (3) How do time and lithology

affect pendant genesis?

This thesis will lead to a better understanding of soil pendants, their macro and

micromorphic characteristics and features associated with their development. The results

of this thesis will benefit the fields of Quaternary pedology, geomorphology, agriculture, archaeology and many other soil related areas. Pendants can be applied to these fields to help determine ages (relative and absolute) of landforms, soil fertility and stability, water quality and movement, contaminant transport, biological habitats and air quality.

Significance

Arid soils are becoming increasingly significant as world populations grow. Currently arid and semi-arid soils cover approximately 36% of Earth's surface (Buol et. al., 1997). Landforms found in these areas directly affect and in turn are affected by urbanization and agriculture. Improper management and development may adversely influence soil stability and fertility, water quality, biological habitats and air quality. Poor planning of these surfaces may also promote flooding and increase seismic risks associated with urban development on present or future faults. Secondary carbonate accumulations in soils have been extensively studied throughout the western portion of the continental United States. Carbonate soils stretch as far east as Kansas and Oklahoma and north to Montanta and North Dakota and south into Mexico (Figure 1.1). The overwhelming abundance and variety of calcic soils in the southwestern U.S. provides a unique setting to study their morphological and chemical characteristics and relationships with respect to variations in climate, biota, topography, lithology and time. The lack of comprehensive absolute dating analyses for Quaternary deposits has spurred extensive research on soil carbonate for half of a century (Gile et al., 1965; Gile et al., 1966;
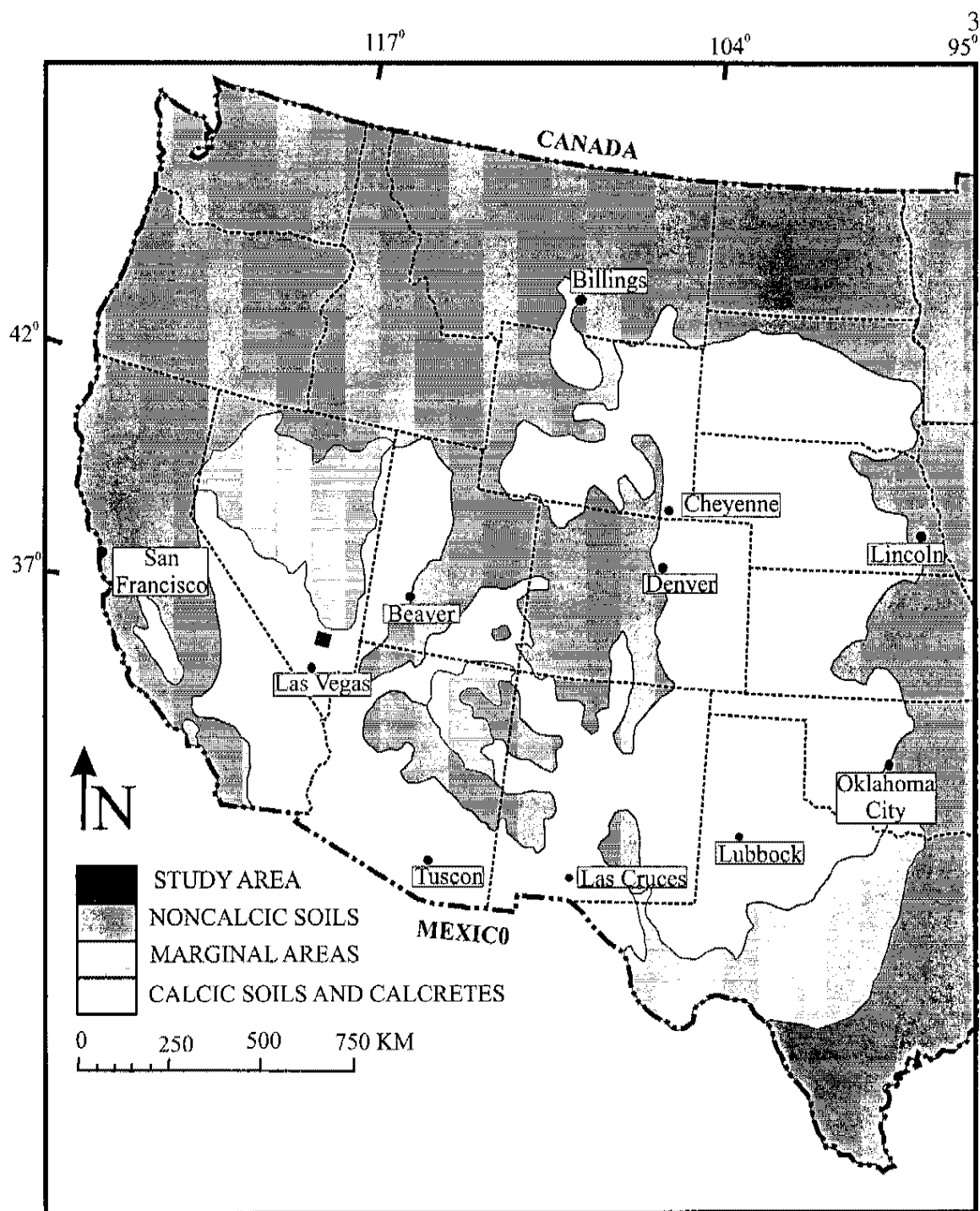
Figure 1.1. Areas of calcic soils and marginal calcic development in the southwestern United States including the Pahranagat Valley shown in red. Modified from Machette, 1985.

Vanden Heuvel, 1966; Wieder and Yaalon, 1974; Bachman and Machette, 1977;

Aguilar et al., 1981; Gile et al., 1981; Pierce and Scott, 1982; Allen, 1985; Blank and

Fosberg, 1990; Boettinger and Southard, 1990; McFadden et al., 1991; Monger et al.,

1991; Reheis et al., 1992; Eghbal and Southard, 1993; Monger and Adams, 1996). The

application of isotopic dating techniques combined with the development of

morphological stages have been used to obtain a better understanding of the temporal

development of calcic soils not only in the southwestern U.S., but the world (Gile et al.,

1965; Gile et al., 1966; Swett, 1974; Bachman and Machette, 1977; Gile et al., 1981;

Pierce and Scott, 1982; Pierce, 1985; Amundson et al., 1989; McFadden et al., 1991;

Reheis et al., 1992; Amundson et al., 1994; Courty et al., 1994; Wang and Anderson,

1998; Khademi and Mermut, 1999; Ludwig and Paces, 2002). Carbonate rich soils found

in the northern portion of the Pahranagat Valley provide an opportunity to contribute to

our understanding of calcium carbonate and silica development in soils. The Pahranagat

Valley is used for this chronosequence and lithosequence study because a number of soil

forming properties are constant. Biota, climate, and topography are consistent between

landforms with local changes in lithology and temporal development. Because of this,

specific changes in soil development can be attributed to lithology and/or time.

An additional significance of this study, although not addressed in detail is the

numerous fault scarps that have been identified in close proximity to the small town of

Hiko, Nevada (Figure 3.1) that could pose a significant seismic hazard for this

community. The valley is also rich in archaeological sites with petroglyphs unique only

to the valley and evidence for prehistoric and paleo-Indian occupation that has yet to be

fully understood. With this study, insight into the geomorphic and developmental history

of the valley may facilitate its overall understanding, sparking new research into the

seismic history and paleo-setting for the Pahranagat Valley.

Study Area Location

The study area is located in the northern Pahranagat Valley of Lincoln County,

Nevada approximately 209 km north of Las Vegas (Figure 1.2). The Pahranagat Valley

spans a length of approximately 48 km and ranges in width from 1-8 km. The study area

covers roughly 8 km^2 in the northern section of the valley. Soil profiles were described

and landforms were evaluated on two, heavily dissected alluvial fans. Each fan contains 5

geomorphic surfaces composed of fan remnants and inset fans associated with multiple

periods of deposition and incision. The sediments that make up these fans are derived

from the North Pahranagat Range and southern Seaman Range located north of the small

town of Hiko, Nevada. Two ephemeral washes extend from the North Pahranagat and

Seaman Ranges as tributaries of the ephemeral White River. The northern Pahranagat

Valley is ideal for studying arid soils because it contains well preserved fan deposits.

Also, the study area has undergone minimal disturbance from anthropogenic sources

including off-road vehicle use, agriculture, grazing and building (with the exception of

two gravel access roads). There is evidence of prehistoric occupation in the area, but

impact appears to be minimal and limited to lithic scatter sites.

Alluvial Fan Formation

Alluvial fans are developed under special tectonic and climatic conditions and

predominantly occur in arid and semi-arid regions of the world. Fluvial debris from steep
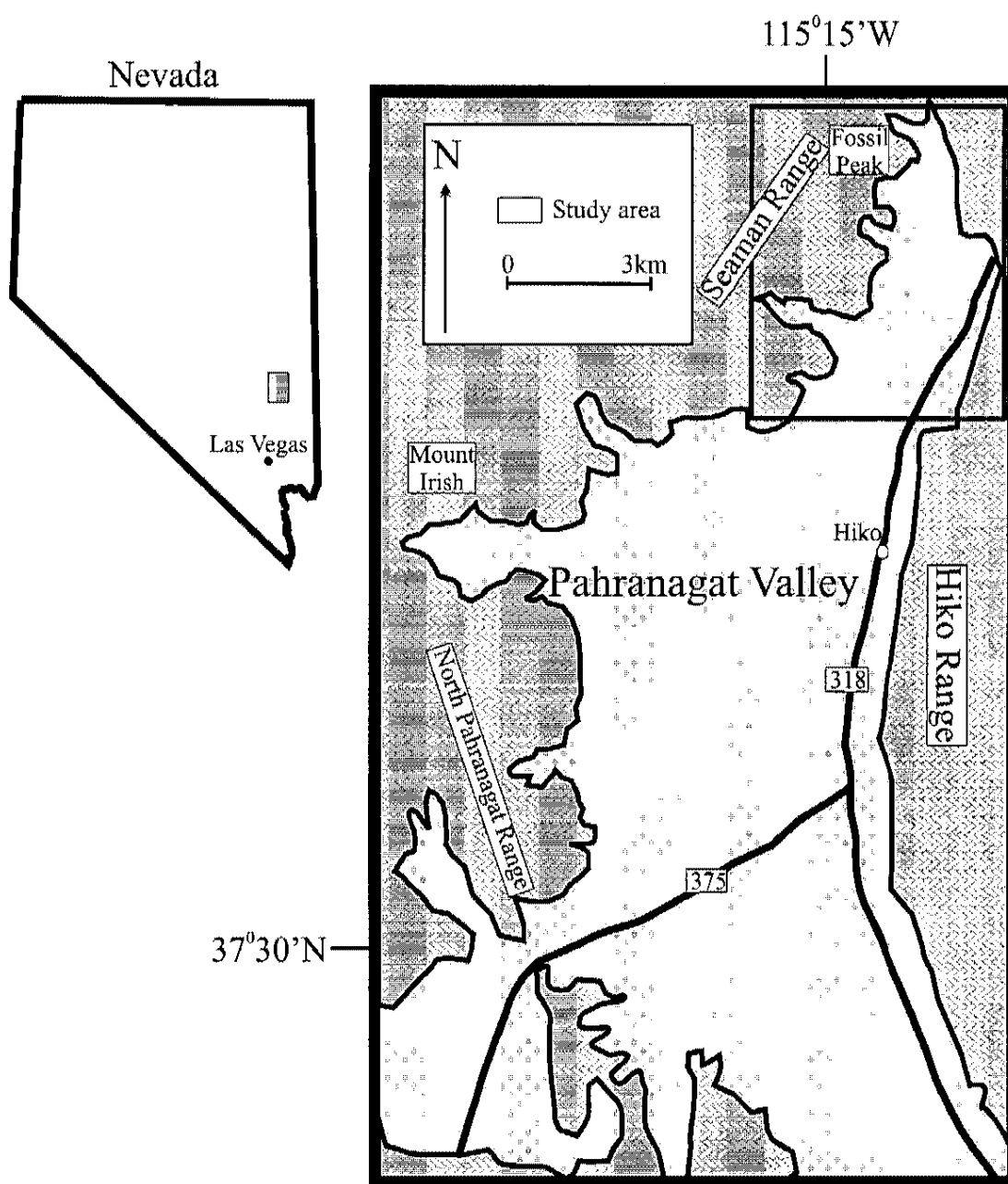
Figure 1.2. Location map showing the upper portion of Pahranagat Valley and study area location.

mountain streams are deposited in adjacent valleys to form these features. Alluvial fans

consist of proximal, mid-fan, and distal portions related to the distance from the mountain

front contact, grainsize, and the type of sediment deposited. Alluvial fans can vary from

small, steep fans to broad and gently sloping, and typically exhibit a cone or triangle

form. Several factors that influence alluvial fan formation in desert environments

include: (1) Faulting along range boundaries that increase stream gradients and/or (2)

Climate changes that affect sediment flux and vegetative cover. Alluvial sediments are

dominantly used in soil studies throughout the southwest (Sowers et al., 1988; Bull,

1991). Terminologies and descriptions of Peterson (1981) are used to describe alluvial

landforms in the Pahranagat Valley study area.

Landforms of the Basin and Range Province

Peterson (1981) describes a series of geomorphic surfaces associated with the

formation of alluvial fans located in the Basin and Range province. The resulting

terminologies used to describe these surfaces are based primarily on topography, relief

and soil development. Descriptions also pertain to shape, geographic scale and genetic

relationship of each landform. Peterson's (1981) terms that will be applied to this study

are ballena, inset fan, and fan remnant (Figure 1.3). Ballenas are defined as erosional

remnants of alluvial fans with rounded tops and extreme soil development consistent with

the convex nature of the surface. These forms are believed to be relicts of surfaces

formed in the Pleistocene. Inset fans are defined as ephemeral stream floodplains that

exist between ballenas or other fan remnant surfaces. They have level surfaces indicating

that they formed by aggradational processes. Fan remnants are the result of alluvial fan
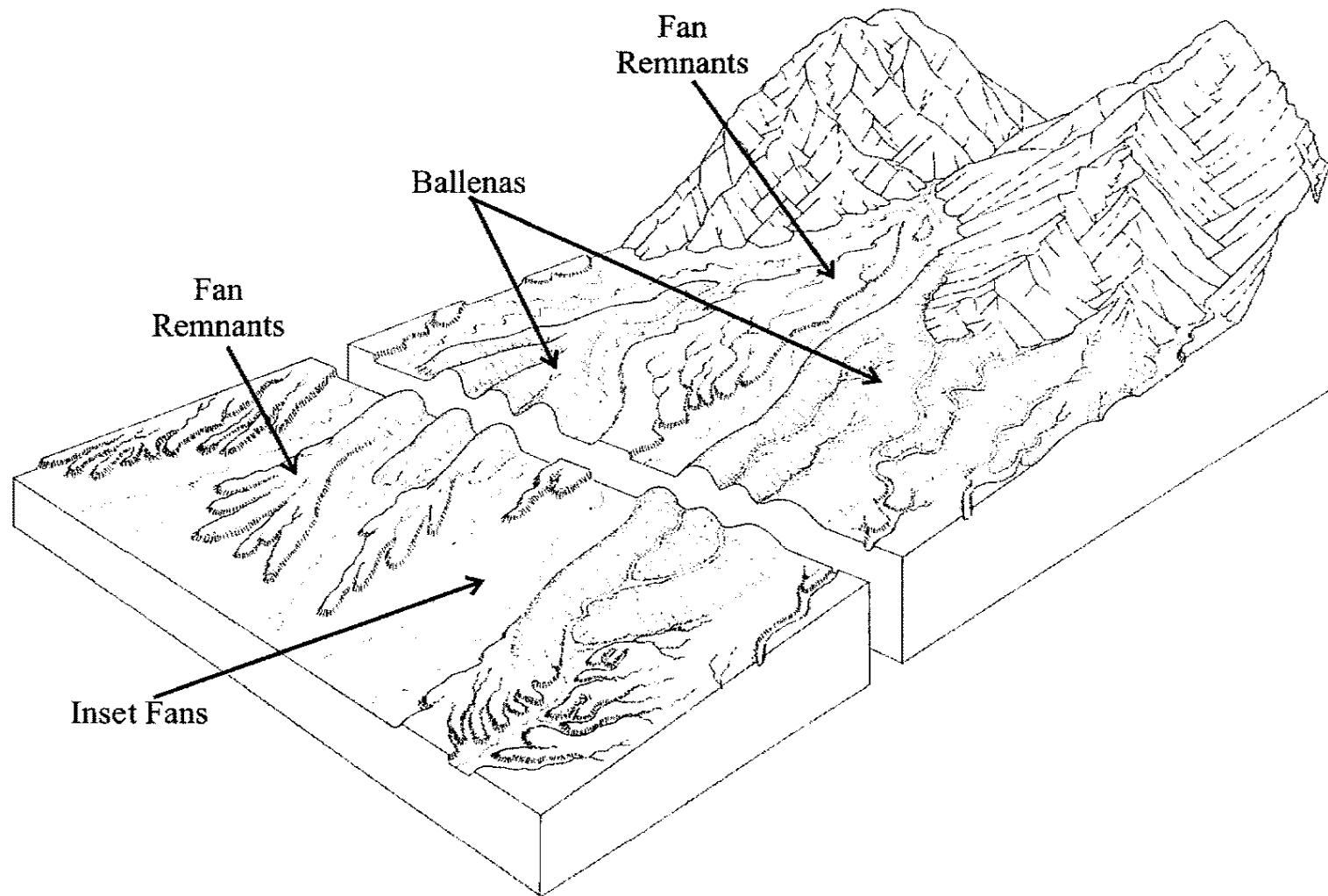
Figure 1.3. Block diagram showing spatial relationships and characteristics associated with ballenas, fan remnants, and inset fans from Peterson (1981) descriptions.

dissection through time. They are located above wash channels or inset fans. After

dissection, the surfaces that remain, including ballenas, can be termed fan remnants.

Ballenas, inset fans and fan remnants combine to form the present day topography of the

northern Pahranagat Valley alluvial fans.

Geologic and Geomorphic History of the Study Area

The Pahranagat Valley is a product of Cenozoic extension of the western United

States and is part of the Basin and Range Physiographic Province. The northern section

of the Pahranagat Valley is bounded by several north-south trending mountain ranges.

Devonian and Mississippian strata underlie Tertiary volcanics where Tschantz and

Pampayan (1970) described a dissected volcanic neck with associated ignimbrites, tuffs

and ash flows. These units are exposed in the Seaman Range that bounds the north and

northwestern side of the field area. For the purpose of this paper, the northernmost

alluvial fan and associated drainage is referred to as BLM fan and BLM wash and the

southernmost fan and drainage is referred to as Mail Summit fan and Mail Summit wash.

The BLM drains rocks exposed in the southern Seaman Range (Figure 3.2). The North

Pahranagat range bounds the western side of the valley and is the main source of material

for alluvial fans in the Mail Summit drainage. The North Pahranagat Range, including

Mount Irish, is composed of the Devonian Simonson dolomite. The northern section of

the range is composed of Tertiary volcanics including undifferentiated volcanics and

ignimbrites (Tschantz and Pampayan, 1970). Fans developed from this range are large

and spread laterally into the valley. The eastern border of the valley is defined by the

tectonically active Hiko range. Many studies have been conducted on the geology and

tectonics of this range (Switzer, 1996; Tschantz and Pampayan, 1970; Taylor et al., 1998). The Hiko Range is composed of Devonian and Mississippian dolomites, quartzites and shales and the southern portion of this range contains few Tertiary volcanics. Fans originating from the Hiko Range are smaller and steeper compared to fans derived from the North Pahranagat and Southern Seaman ranges. The appearance of these fans is presumed to be the result of removal of sediment by the ancestral White River facilitated by Holocene faulting along the range front. Documented normal faulting in the Hiko range and in adjacent Quaternary sediments (Switzer, 1996; Taylor et al., 1998) suggests tectonic control of these alluvial fans. Miocene lacustrine deposits of the Muddy Creek Formation (Tschantz and Pampayan, 1970) underlie Quaternary fan deposits in the northern section of the study area. These deposits are predominantly interbedded siltstone and shale.

As an externally drained valley within the Basin and Range Physiographic Province, the Pahranagat Valley contains the floodplain of the ancestral, now ephemeral, White River that begins in the White Pine Range and joins with Kane Springs Wash and Meadow Valley Wash and flows south to the Colorado River. Several spring-fed lakes are present in the Pahranagat valley. The Frenchy and Maynard lakes, located in the northern section of the valley are used for hunting and fishing nearly year round. The floodplain is widely used for farming and grazing activities that use shallow groundwater wells and local springs to irrigate crops.

Current and Past Climates of the Study Area

The southwest region of the United States has experienced multiple episodes of glacial and interglacial climates since the Early Pleistocene. The glacial episodes are marked by a decrease in temperature and/or increase in rainfall events from a shift of airmass boundaries towards the south (Bull, 1991). This shift brought increased winter precipitation and decreased monsoonal precipitation in the southwest deserts (Bull, 1991). A record of vegetation and climates was put together for the south-central Nevada region, specifically for the Nevada Test Site and vicinity (Spaulding, 1985). This record suggests that the past 45,000 years were marked by major changes in climate. The Wisconsin glacial age with a wetter and cooler climate lasted until about 10,000 years ago. A development of desert vegetation in the Nevada Test Site vicinity began to occur at around 15,000 suggesting an increase in temperatures and decrease in precipitation (Spaulding, 1985). Studies using pack-rat middens and pollen from lacustrine deposits of the Lower Pahranagat Lake have interpreted a detailed, high resolution look at climate changes in the Late Holocene (Isaacs and Tharp, 1996). Alternating wet and dry conditions have occurred over the past several thousand years as told by the Lower Pahranagat Lake sediments (Isaacs and Tharp, 1996). Temperature and precipitation data have been collected between 1964 and 1990 at the Pahranagat Wildlife Refuge approximately 25 km south of the field area. Temperature and precipitation data for this area provided from the 2000 Soil Survey of Lincoln County, Nevada, South Part (Soil Survey Staff, 2000) (Figure 1.4). The Pahranagat Valley receives its highest monthly precipitation in early spring and late summer with averages ranging from 1.5 to 2.0 cm. Summer months receive 0.5 to 1.0 cm on average and winter months get between 1.0 and
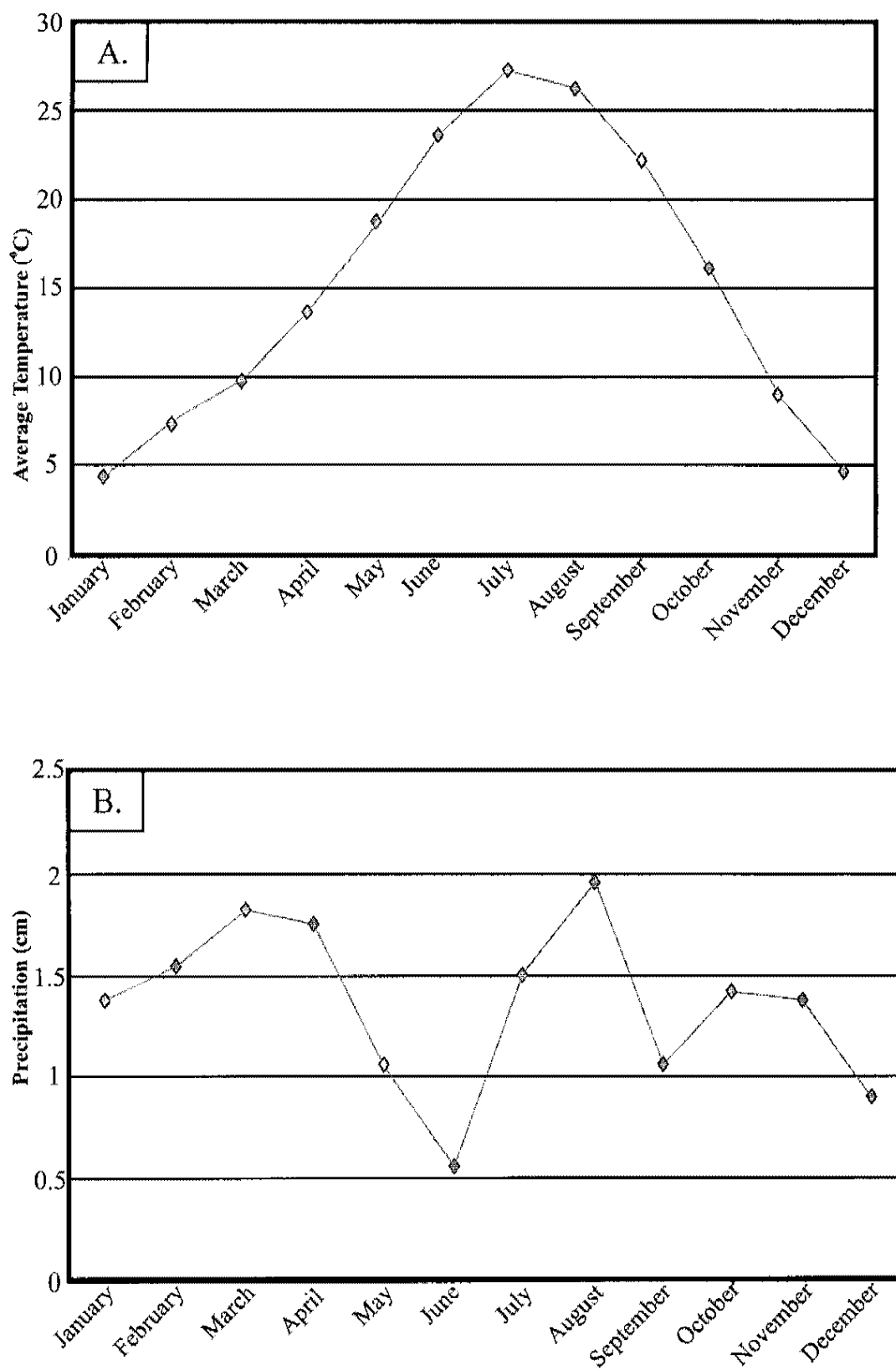
Figure 1.4. (A)Temperature data and (B) precipitation data for the study area.
Data recorded at the Pahranagat Valley Wildlife Refuge from 1964-1990.
After Soil Survey Staff, 2000.

1.8 cm. Temperatures in the Pahranagat average 26.7° Celsius (80°F) in the summer

4.40° (40°F) in the winter. The soils of the study area are classified as having a mesic

soil temperature regime (Soil Survey Staff, 2000).

Vegetation

Blackbrush (*Coleogyne ramosissima*) is the dominant vegetation of the study area and

is present on all landforms except modern drainages. Blackbrush is a component of both

the Great Basin and Mojave desertscrub biomes. The occurrence of blackbrush is

believed to be heavily dependent upon precipitation, limiting its presence in the Mojave

desertscrub biome where precipitation is less than that of the Great Basin biome (Turner,

1982). Other vegetation present on landforms includes Nevada ephedra (*Ephedra*

nevadensis), rabbitbrush (*Chrysothamnus* spp.), red brome (*Bromus rubens*), cholla (O.

cholla), narrow-leafed phacelia (*Phacelia distans*), and purple sage (*Salvia leucophylla*).

Vegetation is considerably different than that of the lower Pahranagat south of Crystal

Spring where creosote is dominant. Areas such as the Pahranagat Valley with arid

climates that exhibit these types of vegetation are commonly characterized by calcic and

or silicious soils.

Calcic Soils and Carbonate Horizon Morphology

Soils containing accumulations of pedogenic carbonate are classified as calcic soils.

Calcic soils with significant accumulation to the point of induration are termed

petrocalcic (Soil Survey Staff, 1998). Pedogenic calcium carbonate forms in the soil

from the combination of calcium ions, CO_2 and water. Calcium is available from dust,

rainwater, and the weathering of parent material. CO_2 is present from diffusion from the atmosphere and plant respiration (Figure 1.5).

Arid and semi-arid soils contain high amounts of calcium carbonate when compared with humid climate soils. The amount and timing of precipitation controls the development of calcic soils. If enough precipitation occurs, calcium ions will be flushed through the soil profile and will not accumulate to form calcic horizons. Similarly, if precipitation occurs in cooler and/or cloudier seasons where soil water is not overwhelmingly effected by evaporation, depths of wetting will be greater, thus calcic horizons may be found much deeper in the soil profile.

The precipitation of minerals including clays, silica, gypsum, halite, and other soluble salts can be directly affected by the presence of calcium carbonate or vice versa. Carbonate can mask clay accumulation making it difficult to see in a soil profile (Allen, 1985). A typical soil profile containing all of the above-mentioned minerals without other complicating factors would exhibit a solubility effect where minerals precipitate out at increasing depths within a soil profile based on increasing solubility. For example, a typical soil would exhibit, from top of profile to bottom: clay (Bt), calcium carbonate (Bk), gypsum (By), and other soluble salts (Bz) (Harden et al., 1991; Birkeland, 1999). The depths at which these constituents accumulate depend upon the depth of soil wetting, which is a function of precipitation (total amount and seasonality), texture, topography and plant cover and type. A change in any of these factors can cause overprinting where, for example, gypsum and calcium carbonate may precipitate at approximately the same depths (Harden et al., 1991).
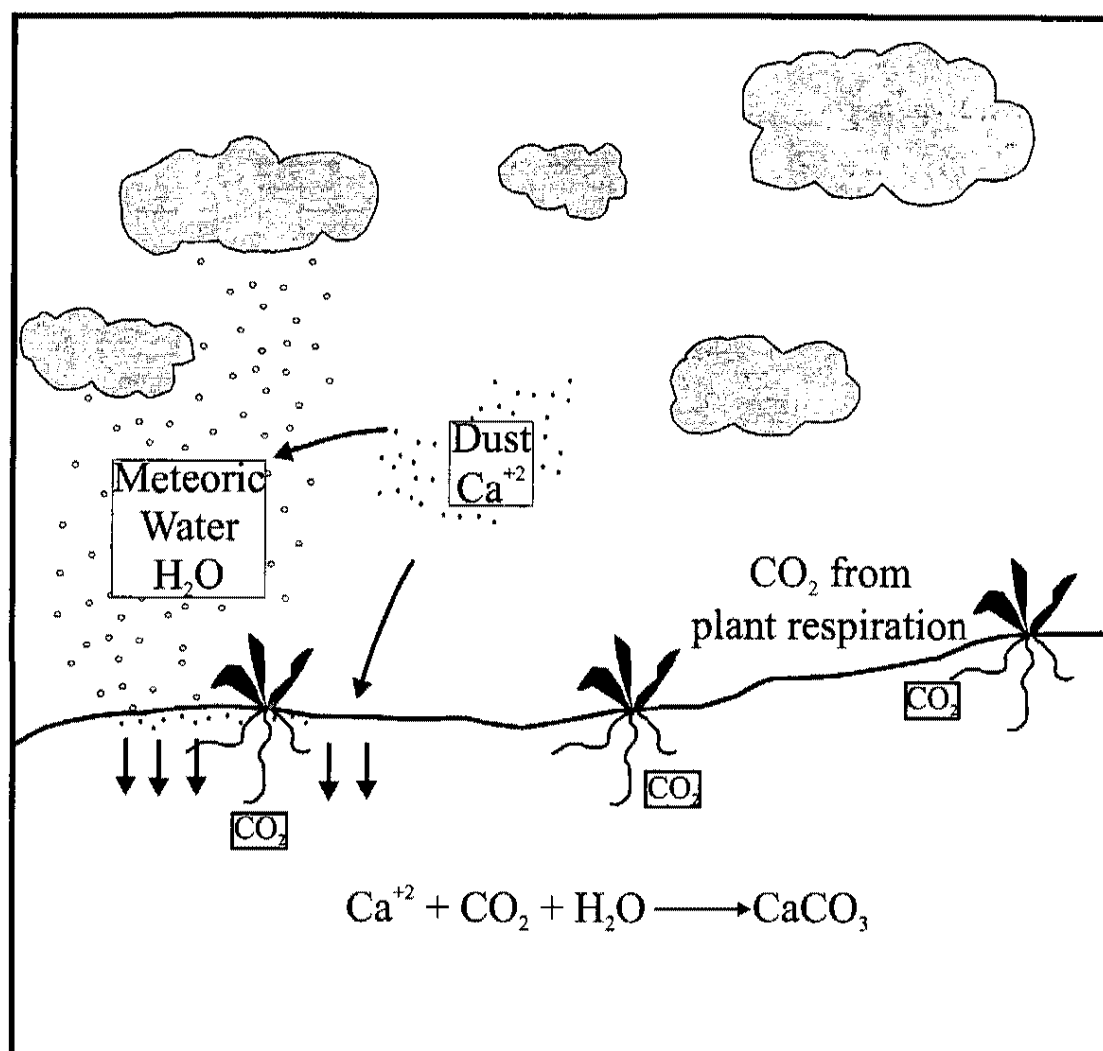
Figure 1.5. The formation of pedogenic calcium carbonate.

In order to compare calcium carbonate development in soils, several factors affecting its genesis must be evaluated. These factors are topography, biota, climate, parent material and time. Depending on environment each factor can dominate the characteristics of a soil. When all but one factor is constant, soil characteristics can be attributed to be the result of that one factor. For example, studies conducted on calcic soils of southern New Mexico have provided information concerning carbonate development through time (Gile et al., 1965, 1966). These studies were conducted as chronosequences where biology, climate, topography and parent material are consistent throughout each landform. Therefore, changes in soil characteristics were attributed to time of soil formation. Gile et al. (1966) were then able to construct four stages of carbonate morphology relating morphological stages of carbonate accumulation in soils to corresponding profiles and associated ages.

The four stages of carbonate development described by Gile et al. (1966) are depicted in Figure 1.6. These stages range from slight coatings on pebble bottoms and filaments to massive horizons that are completely indurated with secondary carbonate with overlying laminar caps. Bachman and Machette (1977) added two more stages (Figure 1.7) described as pisolitic and brecciated features based on studies conducted at Mormon Mesa, Nevada and Roswell, New Mexico. These stages directly relate to the age of the associated landform. This provides a standard for carbonate development through time across arid regions of the world.

Research has indicated that dissolution of limestone parent materials can also contribute to calcic soil development (Rabenhorst and Wilding, 1986; Levine and Hendricks, 1990). Dissolution features include "cupped limestones" and partially
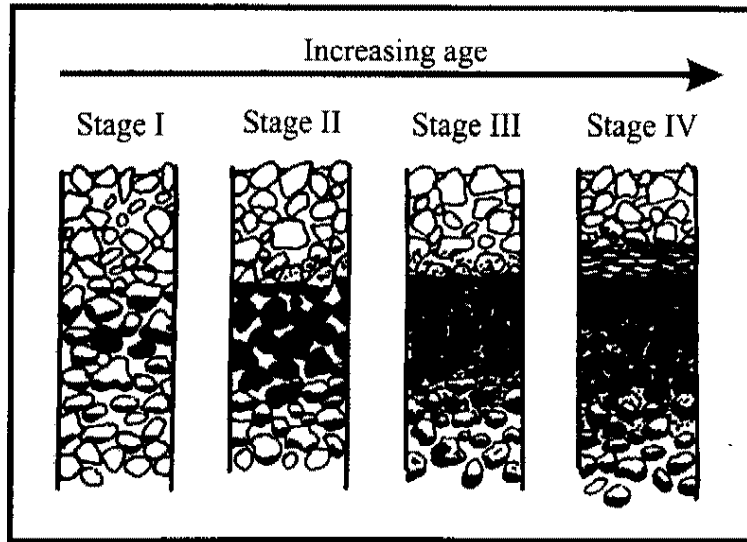
Figure 1.6. Four stages of secondary carbonate development in gravelly soils through time Gile et. al., 1965.

Stage and general character	Diagnostic carbonate morphology
	Gravelly sequence
I Weakest expression of macroscopic carbonate	Thin, discontinuous pebble coatings
II Carbonate segregations separated by low-carbonate material	Continuous pebble coatings, some interpebble fillings
III Carbonate essentially continuous; plugged horizon forms in last parts	Many interpebble fillings
IV Laminar horizon develops	Laminar horizon overlaying plugged horizon
V Thick laminae (>1 cm) and thin to thick pisolites. Vertical faces and fractures are coated with laminated carbonate (case hardening surface).	
VI Brecciated multiple times with pisolites and multiple laminar horizons.	

Figure 1.7. Carbonate morphology and associated stages for gravelly soils (Bachman and Machette, 1977).

dissolved clasts. Evidence for pedogenic reprecipitation include thick carbonate coatings (pendants) on undersides of clasts (Gile et al., 1981; Sowers et al., 1988; Treadwell-Steitz and McFadden, 2000). The dominant limestone lithology of the parent material can cause faster rates of accumulation preventing an accurate correlation of accumulation with time (Sowers et al., 1988).

Gile et al.'s (1966) stages of carbonate morphology have been widely used throughout the southwest United States and other arid regions for relative landform dating, paleoclimate determination, seismic hazard assessment and land sustainability issues. Increasing the understanding of the genesis of calcic soils in arid regions is extremely important because this knowledge can contribute to dating Quaternary landforms found throughout the Basin and Range Province. Organic carbon is rare in desert soils, providing little opportunity for ^{14}C radiometric ages. A few studies have focused on the application of ^{14}C and U-Th dating techniques to calcic soils with some success (Pierce, 1985; Sowers et al., 1988; Amundson et al., 1989; Amundson et al., 1994; Ludwig and Paces, 2002). However, most of these studies did not examine the micromorphology of the pedogenic carbonate in detail (specifically soil pendants) they were dating, thus limiting the success of these techniques. A thorough understanding of the genesis of calcic soils and their relationship to the age of the associated landforms is still greatly needed.

Silica in Calcic Soils

The precipitation of silica in arid soils depends upon soil pH and the presence of other precipitates (i.e. secondary carbonate and other salts) in the soil. Many calcic soils

throughout the southwestern U.S. contain varying amounts of pedogenic silica. A variety of silica polymorphs ranging from well ordered to amorphous can occur as several forms in pedogenic environments: Quartz, opal-C, opal-CT, and opal-A. Quartz is present as silt and sand-sized detrital grains that have been moved into the soil profile from eolian, fluvial or other physical processes (Drees et al., 1989). Opal-C is rare in soils, however opal C-T is commonly found in soils and many of its parent materials (Drees et al., 1989). Opal-A is found in pedogenic duripans and calcretes of silicious soils (Drees et al., 1989). Opal-C, opal-CT and opal-A are differentiated according to their ordered and/or disordered arrangement of silica identified through patterns in X-Ray Diffraction and from this point forward, will be referred to as opaline silica or amorphous silica. Silicious soils in arid environments have been studied but not to the extent of calcium carbonate soils. Silica has been noted to display an increase in accumulation through time and with certain silica rich parent materials (Chadwick et al. 1989). First "stages" of silica accumulation occur as microagglomerates and durinodes (Chadwick et al., 1989) in Holocene soils of Monitor Valley, Nevada. In a study of three soil chronosequences of the western U.S., Harden, et al. (1991) noted an increase in the amount of silica precipitated in soils through time coinciding with calcic and gypsic horizon development. Silica accumulation in these soils ranged from coatings under clasts to indurated, laminar platelets. Opaline pendants in Alfisols of California are assumed to indicate the maximum form of accumulation in those soils and are not related to duripans or their formation (Munk and Southard, 1993). Much more work is needed to constrain the timing and morphology of silica pedogenesis in arid environments.

Increased solubility of amorphous silica occurs at pH 9 (Birkeland, 1999). Many

workers discuss the downward movement and eventual precipitation of silica in profile,

similar to carbonates and other salts. Harden et al. (1991) found opaline silica to

precipitate at or above the Bt horizon similar to soils in Monitor Valley, Nevada

(Chadwick et al., 1989).

Parent material can have a huge impact on silicic soil formation. Volcanic material

such as ash, and other tephra deposits containing high amounts of volcanic glass can be

transported and ultimately deposited into the subsurface where hydrolysis reactions may

take place. Figure 1.8 displays areas covered by Holocene duric formation in soils

coinciding with the ash fall area covered by Mazama ash 6900 years ago as well as the

area of the Great Basin florisitic zone (Chadwick et al., 1985). Chadwick et al. (1989)

found Holocene silicification of soils is heavily influenced by volcanic glass and

determined that soils of Monitor Valley, Nevada, had enough moisture to cause

hydrolysis and release silica into solution, but was not enough to flush silica out of the

profile. As silica in solution moves through soil, it can do one of three things: (1) it can

be used by plants to form phytoliths, which are used in buried soils to interpret

paleoclimates, (2) precipitate out as durinodes or cement or lamina of stage IV horizons

or (3) bond with other ions to produce silicate clays (Chadwick et al., 1989).

Silicate Clays in Calcic Soils

Clay accumulation in soils occurs through several processes: (1) translocation, (2)

transformation, and (3) neoformation. Translocation is the process where by clays are
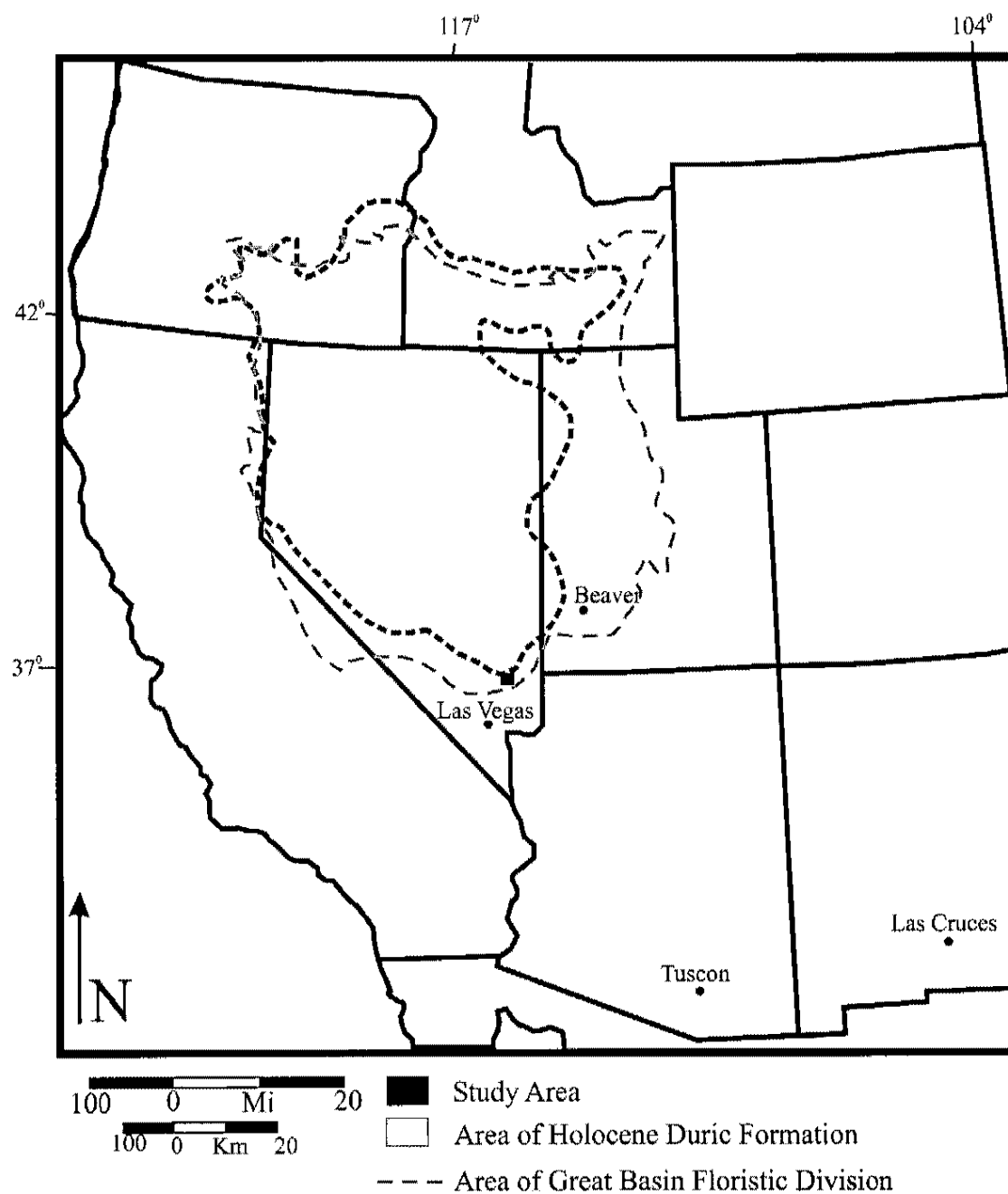
Figure 1.8. Map of southwestern United States displaying areas of Holocene duric soil formation and area covered by the Great Basin Floristic division (Chadwick, 1985).

physically transported through the profile under the influence of gravity and meteoric water. No chemical reactions or changes take place with translocation. These clays have collected on the surface through eolian, fluvial and other physical processes. Evidence for translocation is the presence of clay films called "argillans" on ped surfaces (Birkeland, 1999). Through time, the amount of clay that accumulates creates an increase in clay in subsurface horizons. The amount of clay in subsurface horizons can be used to indicate the degree of development of the soil. In arid environments, a significant portion of silicate clays that are present and available for movement from the surface come from dust. Such clays include kaolinite, chlorite, smectites, illite and mixed layer clays. The type of clay present in a soil profile is often dependent upon nearby sources containing these clay minerals that are carried by eolian processes.

Transformations occur below the surface, in the soil profile. Transformation occurs where one mineral changes to another mineral through a series of solid state alterations (Birkeland, 1999). Transformation commonly occurs at grain edges or along layers and then continues inward (Birkeland, 1999). This process is limited by available moisture and available ions through parent material, other clays and/or other downward moving ions in solution such as aluminum and magnesium. In petrocalcic horizons, pressure dissolution of incorporated feldspars, quartz, and other grains may also lead to clay formation and cause clay to accumulate around areas of dissolved grains. Ions may also be incorporated back into solution to be available for later precipitation where neoformation may take place (Monger and Daugherty, 1991; Wang et al., 1994; Birkeland, 1999).

Neoformation occurs where ions in solution combine to precipitate out as secondary minerals including clay minerals. Neoformation of clays from combined ions in a solution or through reactions with amorphous minerals is different from that of transformation processes because it is not a solid state transformation (Birkeland, 1999). Evidence for neoformation in arid soils includes perfect-nearly perfect, undisturbed structures such as tunnel-like fibers of sepiolite and palygorskite. Fibers radiating into pore spaces is also evidence of neoformation (Monger and Daugherty, 1991). Smectite or forms of 2:1 smectite clays such as illite and chlorite tend to be the most abundant clay minerals found in soils of arid and semi-arid regions (Borchardt, 1989). Any soil environment high in silica may contain smectite clays. In petrocalcic horizons of arid soils, ions of Al and Mg may precipitate with silica to form the fibrous clay minerals sepiolite and palygorskite. In calcic soils, depending on parent material lithologies, ions found in solution include, but are not limited to Al, Mg, K, Na, and Si. In these soils, calcium tends to precipitate out with CO_2 and water to form secondary calcium carbonate. The remaining ions in solution then precipitate out with silica to form clay minerals characteristic of arid environments. Figure 1.9 displays a basic clay assemblage found in calcic soils in arid and semi-arid climates. The relationships between secondary carbonate and clay minerals in soils are sometimes difficult to characterize (Aguilar et al., 1981; Allen, 1985). The dominant observation has been that of secondary carbonate of petrocalcic horizons "consuming" clay minerals and grains (Reheis, 1988; Halitim et al., 1993). However, Aguilar et al. (1981) noticed several zones in calcic horizons where the clay appears to "invade" the carbonate. In the petrocalcic horizon of a Texas Aridisol, the banded appearance of crystalline calcite has been interpreted to be a product of
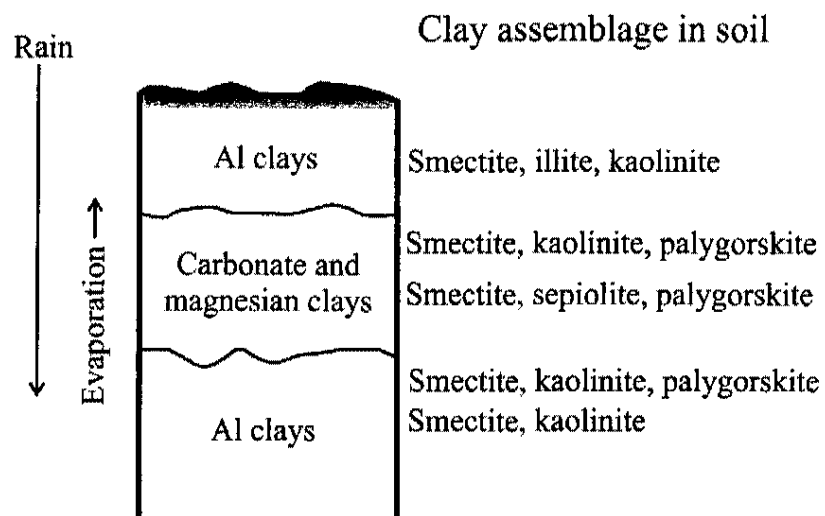
Figure 1.9. A typical carbonate-bearing soil in a semi-arid or arid climate. Smectite dominates the clay assemblages (Velde, 1992).

exclusion of clay and other particles into a band of its own (Allen, 1985). Petrocalcic

horizons can also provide an environment for the preservation of other illuvial clays

because they are protected from some weathering processes (Khademi and Mermut,

1999).

Sepiolite and Palygorskite

Magnesium and aluminum silicate clays, such as sepiolite

$[Si_{12}Mg_8O_{30}(OH)_4(OH_2)_4 \bullet 8H_2O]$ and palygorskite $[Si_8Mg_5O_{20}(OH)_2(OH_2)_4 \bullet 2H_2O)]$

(Singer, 1989), occur in several types of environments including marine and lacustrine

environments, deposits that have been influenced by hydrothermal activity and

petrocalcic horizons of arid soils (Singer, 1984). The presence of dolomite parent

material can provide the necessary magnesium needed to produce sepiolite and

palygorskite in the soil profile (Singer, 1984). An inverse relationship between the

occurrences of smectite and palygorskite suggest some pedogenic environments favor the

formation of one mineral over the other (Mackenzie et al., 1984; Singer, 1984). Some

authors have suggested the transformation of montmorillonite and illite to sepiolite and

palygorskite with increasing soil development (in petrocalcic horizons) (Hay and

Wiggens, 1980). The occurrence of neoformed sepiolite and palygorskite in pedogenic

environments with stage III or greater carbonate development are indicative of Middle to

Early Pleistocene-aged soils (Bachman and Machette, 1977). Bachman and Machette

suggest that the formation of these clays first requires the petrocalcic horizon to form,

and remain with enough time for grain dissolution and clay neoformation. Hay and

Wiggins (1980) attribute the dominance of opal and sepiolite to volcanic parent material

rather than the presence of carbonate material because of the high glass and quartz content of volcanic tephras.

Sepiolite can also be found as coatings on soil pellets (Hay and Wiggens, 1980; Sowers et al., 1988). Sepiolite has been found to preferentially encompass grains such as quartz, feldspar, rhyolite, and calcite (Vanden Heuvel, 1966; Hay and Wiggins, 1980). These pellet features occur above the laminar cap of Stage IV carbonate horizons (Sowers et al., 1988) and in fracture fillings (Hay and Wiggins, 1980). Pellets are made up of sepiolite and/or opal, which surrounds grains, pieces of carbonate and/or soil matrix (Hay and Wiggins, 1980).

Soil Pendants

Multiple, laminar layers of secondary calcium carbonate and/or silica that have accumulated on the bottoms of clasts in coarse or gravelly soils have been given various names by several authors. In this study, these features will be referred to as pendants and/or coatings. Pendants have also been called carbonate coats, beards, gravel coatings, and pebble bottom coatings (Sowers et al., 1988; Chadwick et al., 1988; Admunson et al., 1989; Ducloux and Laouina, 1989; Blank and Fosberg, 1990; Levine and Hendricks, 1990; Munk and Southard, 1993; Vincent, et. al., 1994; Treadwell-Steitz and McFadden, 2000). These are important yet poorly understood features of calcic and duric soils of the western United States and other arid and semi-arid regions of the world, including cryic temperature areas (Forman and Miller, 1984; Sletten, 1988; Courty et al., 1994; Wang and Anderson, 1998). Pendants are described as multiple carbonate and/or silica coatings

ranging from pure carbonate to pure opaline silica that have accumulated on the bottom

of coarse clasts in the subsurface of a soil.

Pendant formation is assumed to resemble a stalactite-style process with an initial

accumulation adjacent to the underside of the clast (Pierce and Scott, 1982; Pierce, 1985;

Chadwick et al., 1988; Sowers et al., 1988; Amundson et al., 1989; McFadden et al.,

1991; Reheis et al., 1992; Amundson et al., 1994; Courtey et al., 1994; Wang and

Anderson, 1998; Birkeland, 1999; Treadwell-Steitz and McFadden, 2000; Ludwig and

Paces, 2002). As additional accumulation continues, layers of carbonate and/or silica

form an order of lamina with the oldest immediately adjacent to the clast and youngest at

the terminus of the pendant.

Throughout development of the pendant, continued precipitation results in multiple

layers of $CaCO_3$ with occasional laminae that contain other materials such as detrital

grains, silica or clays (Amundson et al 1989; Blank and Fosberg, 1990; Amundson et al.,

1994; Courtey et al., 1994; Wang and Anderson, 1998; Treadwell-Steitz and McFadden,

2000; Ludwig and Paces, 2002). Alternating layers are suggested to be a product of

changes to and from arid and wet seasons or climates (Chadwick et al., 1988; Amundson

et al., 1994; Courtey et al., 1994; Ludwig and Paces, 2002).

Soil forming processes begin once a landform is stable. By obtaining ages for the

first, "inner" layers of pendant, it may be possible to estimate minimum ages for stability

of the landforms where the pendants formed. Several studies have explored the use of

pendants as potential aids in determining age of landforms. U-Th and ^{14}C dating has

been used to analyze the oldest lamina (those closest to the clast) to estimate ages of

formation (Pierce, 1985; Amundson et al., 1989; Ludwig and Paces, 2002). However, the

use of pendants as relative dating tools has not been entirely successful. The dating of "inner" and "outer" lamina has revealed many inconsistencies. In some studies, the inner lamina (believed to be oldest) reveal younger ages when compared with the outer lamina (believed to be youngest) (Pierce, 1985; Sowers et al., 1988; Chadwick et al., 1989). Extensive micromorphic observations of the pendants in these studies were rarely conducted. Several studies have used the innermost layers to obtain absolute ages for the initial development of pendants. Inner carbonate accumulations assumed to be the first deposited are dated to find the age at which the soil began to develop (Amundson et al., 1994; Ludwig and Paces, 2002).

CHAPTER II

METHODOLOGY

Landform Selection and Mapping

Landforms were mapped using 1:40,000, black and white, USGS aerial photograph

stereoscopic pairs. These landforms were input into a Geographic Information System

using the Fossil Peak, NV, NW, Fossil Peak, NV, SW, Fossil Peak, NV, NE, and Mail

Summit, NV, SE, digital orthophoto quadrangles (DOQs) that have a resolution of 1

meter. Landforms were differentiated using degree of desert pavement and desert

varnish development, spatial relationships with other landforms, vegetation differences,

dissection, slope, surface color, curvature, and soil development.

Landforms were grouped according to parent material, represented by the dominant

lithology of surface clasts, and visual observations of the lithologies of gravel in profiles.

Surface clast data was obtained using a method similar to one described by Bull (1991).

A metric tape was randomly tossed on the surface and 100 clasts were measured at their

C-axes. The portion of the clast that the tape crossed was also measured. The lithology of

each clast measured was recorded. At the final clast, the total length of tape used was

noted. Percentages for area of tape covered by clasts were determined, as well as percent

lithologies from all surfaces. This method was used to estimate amount of surface

covered by clasts and to separate the volcanic dominant landforms from the

limestone/dolomite landforms, and also to compare of soil development between soils
of two different parent lithologies. Surface data for landforms is provided in Chapter III.

Pedon Selection and Sampling

One pit per landform was dug using a backhoe provided by the Clark County Natural
Resources Conservation Service and by hand where a backhoe could not reach. Depths
of pits ranged from 30 cm to over 1 m. Pit locations were chosen based on minimal
erosion, desert pavement development and flatness of surface. Pit locations were also
chosen on areas that best represented each landform. In order to sample for chrono and
lithosequences, one profile was sampled from a representative of each landform that had
dolomite and volcanic dominant material, with the exception of the youngest landform in
dolomite material. A total of 9 pits were described and sampled. Samples were collected
from all horizons in each profile, sieved and divided into gravel (>2 mm) and fines (<2
mm). Universal transverse mercator (UTM) coordinates of each pit location were
recorded in the field with a geographic positioning system (Figure 2.1). Horizons
containing pendants or other delicate features such as durinodes were carefully wrapped
and transported in plastic containers back to the laboratory. All soil descriptions were
completed using the 1998 NRCS Field Book for Describing and Sampling Soils (Soil
Survey Staff, 1998), with the exception of Av horizons, where the nomenclature 'v'
represents vesicular features rather than the presence of plinthite (McFadden et al., 1987).
Soil structure, including type, grade and size were recorded in the field as well as roots,
pore spaces, degree of effervescence with HCl and stages of secondary calcium carbonate
development (Gile, 1966; Bachman and Machette, 1977). Silica was observed in the

115°12'30"

37°42'30"

2.5 km   • Location of soil pits with names in boxes
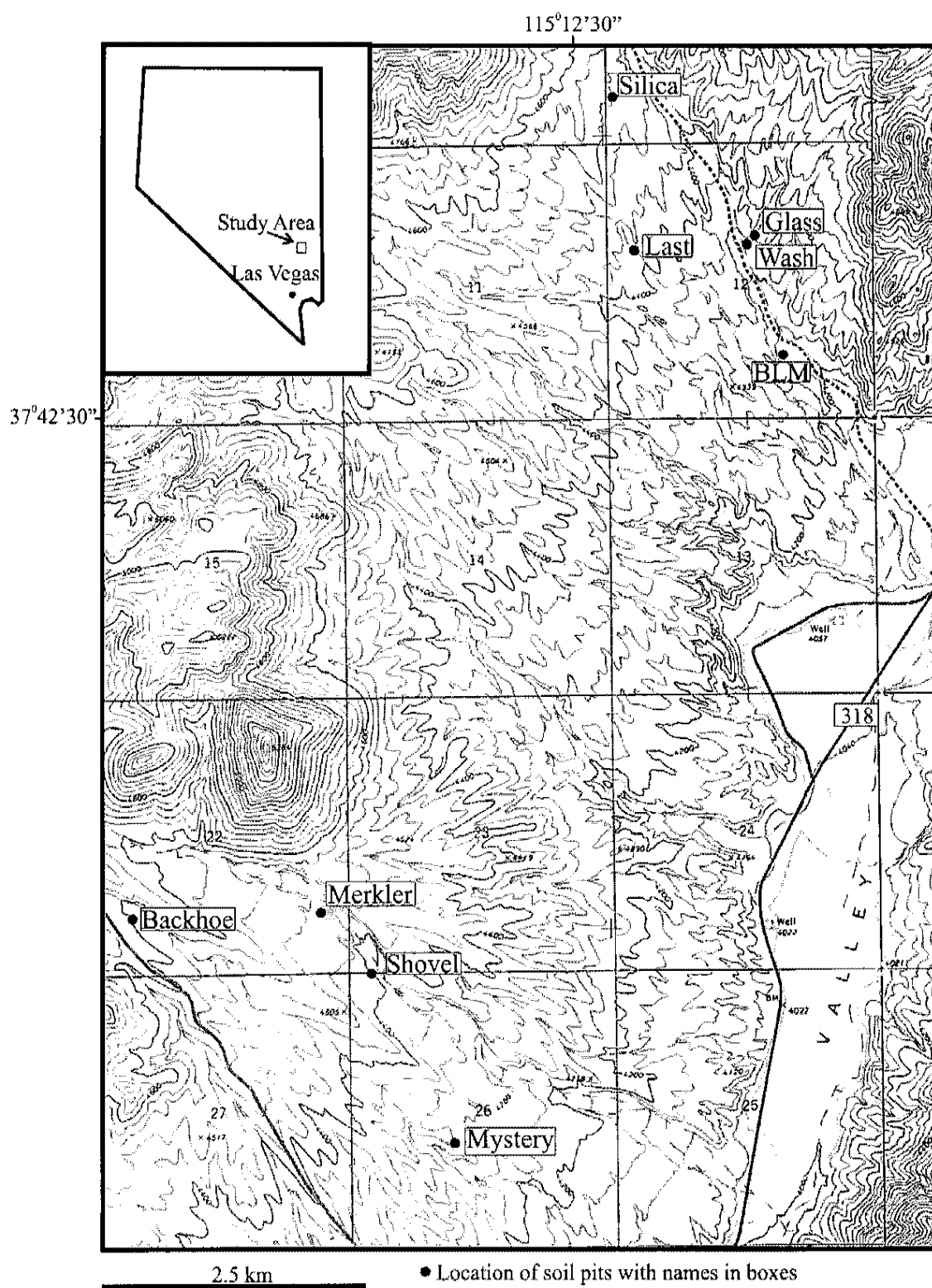
Figure 2.1. Soil pit locations in study area on a portion of the Fossil Peak 7.5 minute quadrangle.

field as patchy, yellow accumulations occurring with carbonate on the underside of clasts. No specific terminology has been published for description of these accumulations. For the purposes of this study, the Ped and Void Surface Features-Distinctness classes from the USDA-NRCS Field Book for Describing and Sampling Soils (Soil Survey Staff, 1998) were used to compare silica accumulation between horizons. Durinodes were tested in the field by soaking them in water and observing their tendency to break apart. If the sample held together after soaking, it was determined to be a durinode (Soil Survey Staff, 1996). Wet and dry colors were determined in the field using the Munsell Soil Color Chart. A qualitative taxonomic classification was determined with the available laboratory data using the USDA's 1998 Keys to Soil Taxonomy (Soil Survey Staff, 1998).

Texture Analysis

Texture analyses were conducted in the UNLV Soil Analysis Laboratory. Secondary calcium carbonate was removed from all sampled horizons, with the exception of Q1 Silica, under the guidelines set by Gee and Bauder (1986). Samples from each horizon were distributed between 4-50 mm plastic test tubes and alternately centrifuged and washed with distilled water and sodium acetate, and then oven dried when removal was complete. Approximately 60 gm of each sample were weighed and combined with distilled water and a mixture of 50 gm to 1 L of Calgon water softener containing sodium hexametaphosphate to facilitate clay dispersion. Texture was determined using the hydrometer method described by Gee and Bauder (1986). Three 40-second readings

were taken to measure the amount of silt and clay in suspension. Clay percent was determined from a six-hour reading of the hydrometer.

Electrical Conductivity and pH

Electrical conductivity (EC) and pH were determined using an Accumet Basic AB30 conductivity meter and a VWR model 8100 pH meter in a saturated paste. These analyses were conducted in the UNLV Soil Analyses Laboratory. Soil water was extracted for EC using a ceramic filter and vacuum. Methods for EC and pH analyses were followed from the Soil Survey Laboratory Methods Manual, (Soil Survey Staff, 1996).

Macroscopic Techniques

A Leica GZC macroscope was used to examine soil features from each horizon. Loose grains and dirt were dusted from pendants with a small paintbrush then observed and photographed at scales ranging from 1 mm to 20 mm. Features such as crystal fibers, structure, glass shards, quartz grains, pellets, secondary carbonate and silica accumulations and pendant structures were observed and recorded using this method. This method was also used when preparing samples for scanning electron microscopy (SEM).

Microscopic Techniques

One or two pendants from each horizon containing pendants, pellet material and durinodes were epoxied using Spurr low-viscosity embedding media to hold pendants

together during thin section preparation. Blue epoxy dye was added to each sample for easier identification of void spaces. Billets of pendants were cut perpendicular to the soil surface in the UNLV Rock Laboratory. A total of 26 pendant, 1 pellet, and 4 durinode billets were sent to Quality Thin Sections in Arizona. Thin sections were then etched with 1.5% HCl and dipped in a mixture of HCl and Azalarin Red for calcite staining (Hutchison, 1974). Twenty-four pendants were also point counted using 1/3mm by 1/3mm grid spacing for up to 600 counts. Points were grouped as carbonate, silica/clay, void spaces and grains incorporated from the soil matrix or from the parent clast.

Scanning Electron Microscopy

Thin sections were analyzed using backscatter electron (BSE) imaging and electron dispersion spectrometry (EDS) to determine pendant composition and relationships between materials. Samples were prepared as stated above, placed in a sonic bath and sputtered with a carbon coating. A gold coating was not used because the coating device was not big enough to accommodate the 2x3 inch thin sections. Samples were analyzed in the UNLV EMIL laboratory with a JEOL-5600 SEM equipped with an Oxford ISIS Electron Dispersion Spectrometer (EDS) system.

EDS was used to determine the composition of minerals found within soil pendants and to identify silica, carbonate, clays, void spaces, grain lithology and parent-clast lithology.

X-Ray Diffraction

X-ray diffraction was used to differentiate clays in pendants from several soil horizons. Because soil pendants are predominantly composed of calcium carbonate, removal of carbonate was necessary before XRD analysis. The sample was crushed into a powder using a rock hammer and large metal file. These techniques were also used to granulate two parent clasts to obtain their compositions. The powder was placed in a 1:10 mixture of distilled water and NaOAc (Gee and Bauder, 1986). Alternating NaOAc treatment and washing with centrifugation was repeated until a reaction no longer took place. The sample was oven dried in low heat to prevent destruction of clay structure. Two parent clasts (Figure 4.2) that held pendants were also crushed and sent through the same processes to obtain a standard for clays that may be derived from the clast. Samples were analyzed at the New Mexico State University Analytical Geochemistry Research Laboratory with a Rigaku X-ray diffractometer.

CHAPTER III

LANDFORM AND PEDON RESULTS

The northern Pahranagat Valley contains a series of five time-variant landforms (Q1-Q5) developed from depositional episodes in the Quaternary. These landforms were identified in two large fans that cover most of the study area and slope 3-6 degrees to the east toward the White River floodplain and Hiko Range. The soils developed on these landforms are typical of those found in desert environments. They contain vesicular horizons (Av), desert pavements and sparse vegetation (Bull, 1991). These landforms are believed to range in age from Early-Middle Pleistocene to Late Holocene. Interpreted relative ages of the landforms in the study area are discussed in Chapter V. Topographically, the highest landforms represent the oldest preserved landforms of the valley. The Q1 landforms are ballenas and are located adjacent to bedrock mountain fronts on the eastern and northern-most parts of the study area. Fan remnants and inset fans represent the Q2 and Q3 landforms. These surfaces are found between ballenas and as terraces to large drainages. Q4 landforms are inset fans found below the Q1-Q3 landforms and approximately 1m above Q5 that include the active drainages of the study area. A detailed geomorphic map of northern Pahranagat Valley landforms is shown in Figure 3.1 and Plate 1. The soil characteristics of these landforms tend to vary through time and exhibit increased pedogenic development corresponding to increased age. Complexity in carbonate, silica and clay accumulation also increase with increasing age.

Map Legend

Undifferentiated faults
solid white lines, dotted
where inferred

Ephemeral drainages

State Route 318

QT White River floodplain

Volcanic dominant parent material	Dolomite dominant parent material
Q4	Q4
Q3	Q3
Q2	Q2
Q1	Q1

Bedrock

4,172,000m. N

655,000m. E

N

Map projection--Universal transverse mercator
NAD 83, Zone 11

0   1 km   2 km

1:24,000
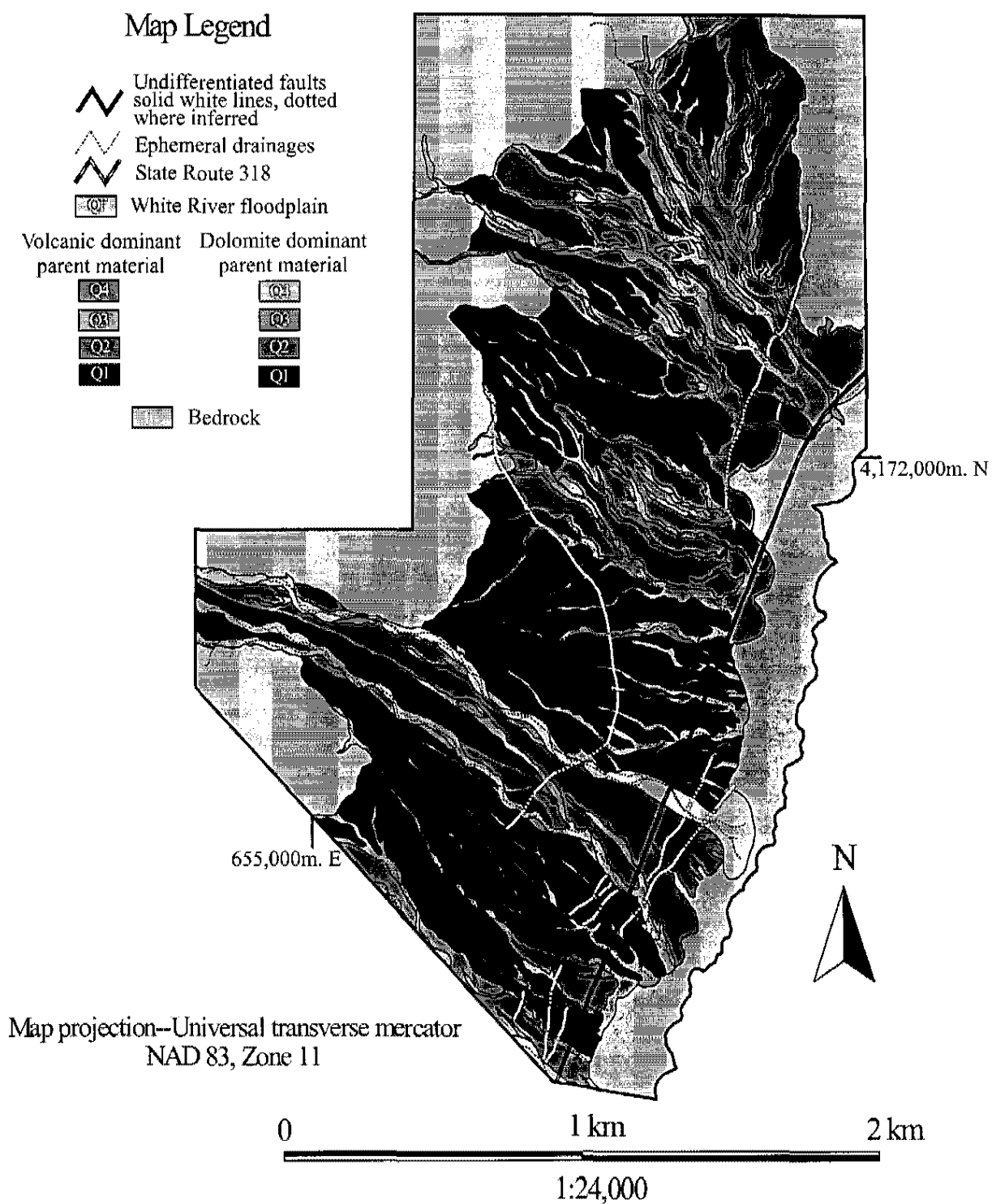
Figure 3.1. Quaternary landform map of northern Pahranagat Valley.

Initial differentiation between landforms was attained by comparing soil development,

degree of dissection, degree of desert varnish, desert pavement development, vegetation

differences, curvature, surface color and topographical position. A chart showing a

summary of landform descriptions, qualitative taxonomic classifications, dominant

vegetation, slope and relative ages for all landforms of the study area is provided in

Chapter V (Figure 5.1).

Parent Material Lithology and Surface Characteristics

Two drainages, BLM and Mail Summit washes, are present on two fan complexes that

exhibit distinct and separate parent lithologies (Figure 3.2). BLM wash drains Tertiary

volcanic rocks that have provide material for the BLM fan. Landforms of the BLM are

distinguished from Mail Summit fan landforms, with a subscripted V (i.e. $Q1_V$). The

Mail Summit landforms, composed primarily of dolomite, are denoted by a subscripted D

(i.e. $Q1_D$). Surface clast data supports this division of landforms (Figure 3.3). The BLM

fan has volcanic surface clast percentages ranging from 59-94%. The Mail Summit fan

has dominantly dolomite lithologies ranging from 99-100%. Each landform displays a

set of surface characteristics that can be compared through time and with lithology. This

creates two chronosequences and five lithosequences. BLM and Mail Summit fans

provide numerous surface material brought from two different sources. Profiles of

surfaces of the same age but with different parent lithologies (i.e. $Q1_V$ and $Q1_D$) can give

insight into the development of soils and soil features in varying lithologies. The type of

parent material that a soil forms in can greatly influence its pedogenic development. The
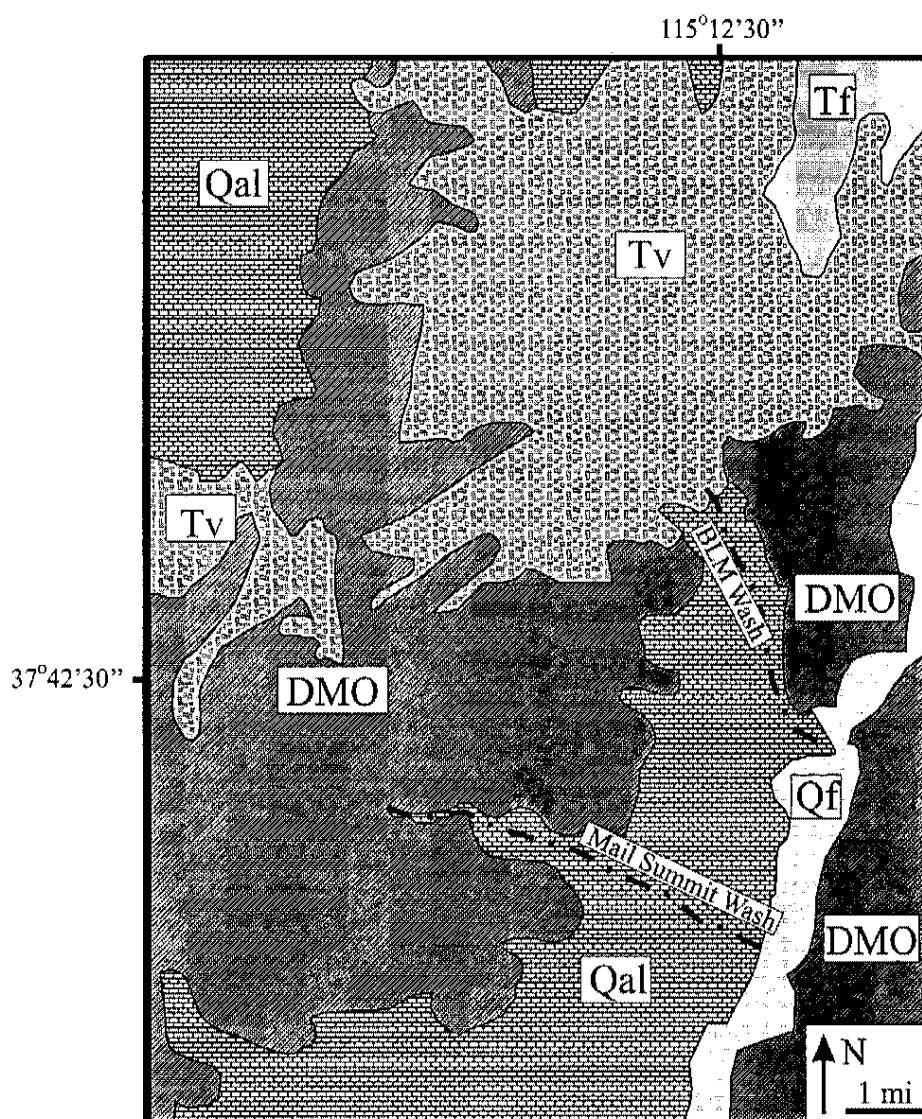
Figure 3.2. Simplified geologic map depicting generalized bedrock lithologies of the study area and vicinity. BLM wash and Mail Summit wash are shown and labeled (Tschantz and Pampayan, 1970).

Surface	Percent of Surface in Pavement	Percent of Bare Ground Between Particles	Stream Channels	Gravel Bars	Mean mm	Sorting	Percent >32 mm	Percent clasts >32mm limestone	Percent Dominant Lithology
$Q1_L$	53.0	47.0	None	None	15.9	Moderate	3	100	99 carbonate
$Q1_v$	45.1	54.9	None	None	15.0	Poor	5	60	71 volcanic
$Q2_L$	45.4	54.6	None	None	14.9	Moderate	3	100	99 carbonate
$Q2_v$	37.4	62.6	None	None	18.2	Poor	12	83	59 volcanic
$Q3_L$	No pavement		Poor	Good	24.2	Moderate	23	100	100 carbonate
$Q3_v$	No pavement		Poor	Good	11.9	Moderate	0	0	65 volcanic
$Q4_L$	No pavement		Good	Excellent	—	Poor	—	—	100 carbonate
$Q4_v$	No pavement		Good	Excellent	—	Moderate	2	—	94 volcanic
$Q5_L$	No pavement		Excellent	Excellent	—	Poor	—	—	100 carbonate
$Q5_v$	No pavement		Excellent	Excellent	—	Moderate	0	—	90 volcanic

Figure 3.3. Data from surface clast observation and measurements of 100 clasts. Dashes represent data not recorded. Percent dominant lithology was calculated by recording the lithology of the clasts that were larger than 32 mm. Table format taken from Bull, 1991.

BLM and Mail Summit fans provide perfect settings to study the effect of time and lithology on soil development.

BLM fan surface characteristics

Landforms associated with the BLM fan include ballenas, fan remnants, inset fans and modern drainages (Peterson, 1981). These landforms are composed of dominantly volcanic material that show pronounced weathering and degradation. Quartz crystals and other grains that have weathered from the volcanic material are present on the surface as 2 mm and smaller grains. Sorting of surface clasts is poor on all five BLM landforms. Surfaces of the BLM fan have a pinkish color inherited from the dominant pink ignimbrite material. Surface clasts on the $Q1_V$-$Q3_V$ landforms range in size from 11.9-18.2 mm. Larger clasts (>32mm) incorporated into pavements on $Q1_V$ and $Q2_V$ landforms are predominantly limestone/dolomite clasts (60% and 80%).

Mail Summit fan surface characteristics

Landforms associated with the Mail Summit fan are equivalent to those of the BLM fan with respect to topographic position, microtopography, vegetation, and temporal development; suggesting similar depositional histories. Mail Summit landforms display a gray-white color inherited from the predominant gray dolomite clasts. Sorting of surface material is moderate and remains moderate on all landforms. Surface clasts on $Q1_D$-$Q3_D$ landforms range in size from 14.9-24.2 mm.

Q1 Landforms and Profile Descriptions

Q1 landforms are found in both volcanic and limestone/dolomite rich parent material. Because these landforms have the highest topographic location, they are easily

distinguished from all other landforms. Q1 landforms are ballenas with well defined rounded, convex surfaces (Peterson, 1981) (Figures 3.4 and 3.5). Q1 landforms are easily identified on aerial photos as lobate and shadow-producing forms sloping $3°$ east toward the White River floodplain. In aerial photos, these landforms are light in color. Desert pavement is moderately to well developed with evidence of erosional disturbance. Overall, little desert varnish is present because this landform lacks material lithologically conducive for desert varnish formation. However, desert varnish is present on clasts other than limestone/dolostone and tephra material. Q1 landforms of the Mail Summit and BLM fans exhibit evidence for exhumation of subsurface calcic and petrocalcic horizons. Partial eroded pieces of carbonate pendants and fragments of a stage IV laminar cap are sitting on the surface, upturned and on their sides. Cupped or dissolved limestone/dolomite clasts are present at the surface (Figure 3.6). Soil development for all Q1 landforms is parallel to the surface with a massive calcic horizon at equal depths on all sides. For example, small test pits dug on the side slopes of the ballena revealed a petrocalcic horizon at equal depth with the petrocalcic horizon that was encountered at the crest. The dominant vegetation is blackbrush. Nevada ephedra is also present on the Q1 landforms of both Mail Summit and BLM fans.

Mail Summit Q1$_D$ Backhoe Pit

The pedon described as Backhoe Pit is found in the gravelly, limestone/dolomite material of the Q1 Mail Summit landforms. The pedon described is located at UTM coordinates 655037 east and 4170233 north. Pedon depth reaches 82 cm and is divided into 7 horizons and qualitatively classified as a Calcic Petrocalcid. All horizons are skeletal with gravel percents ranging from 37 to 95%. Carbonate horizons begin at 13 cm

43
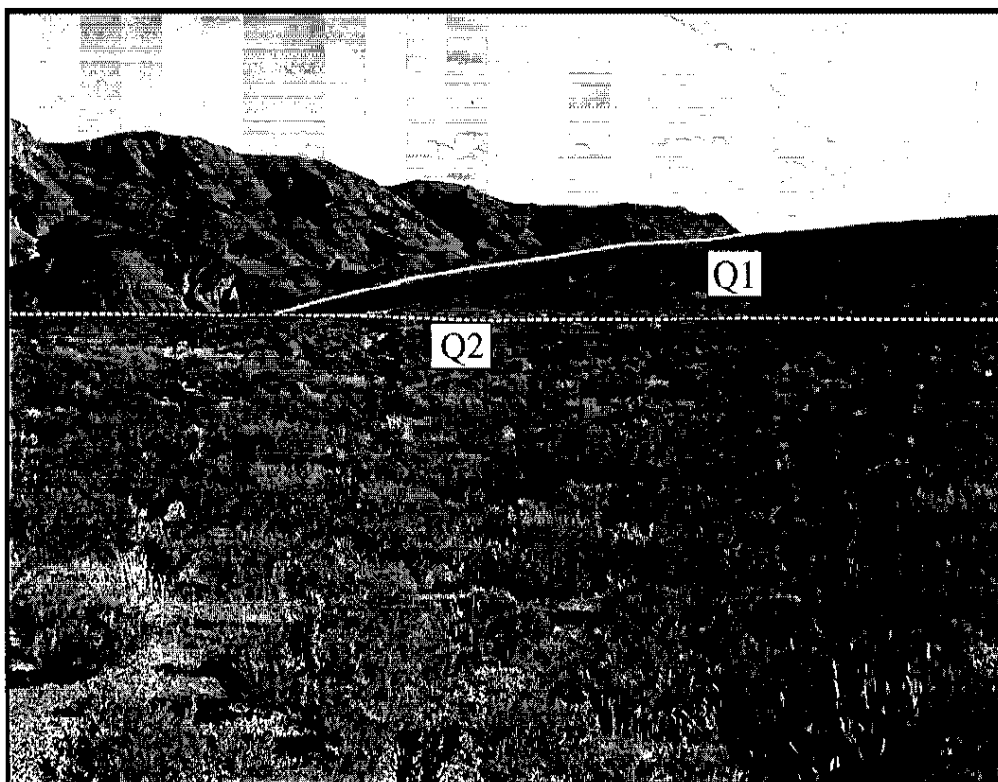
Figure 3.4. $Q1_D$ and $Q2_D$ landforms located on the Mail Summit fan. $Q1_D$ is outlined with a solid line. White dashed line shows $Q2_D$ landform outline.
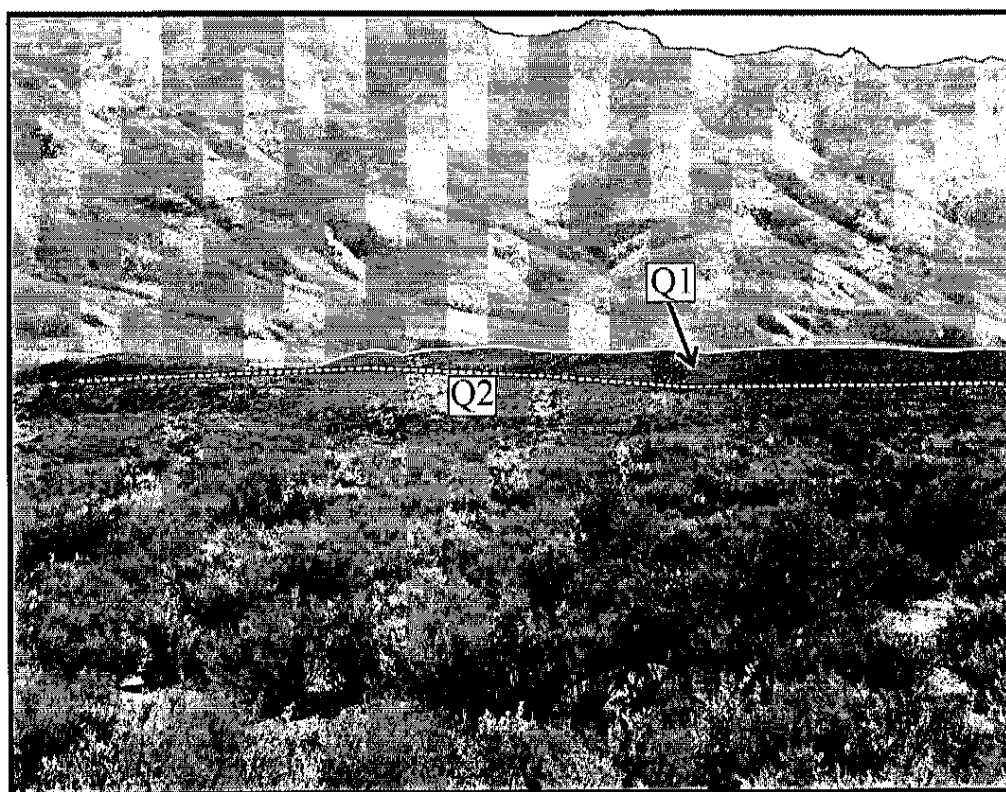
Figure 3.5. Rounded ballenas of the $Q1_V$ landform. $Q1_V$ is highlighted with the solid line. White dashed line shows $Q2_V$ landform outline.

Figure 3.6. Surface clasts of $Q1_D$ landforms. Box outlines "cupped" limestone clast common on the Q1 surfaces.

depth and continue, with increasing stages of morphology, through the rest of the profile

(Figure 3.7). Stage II carbonate begins at 13 cm exhibiting thick coatings on the

undersides of clasts and between gravels. Carbonate accumulation increases downward

through the profile with stage III at 33 cm depth, continuing at 57 cm with stage III with

incipient development of a stage IV laminar cap encountering a stage IV horizon at 82

cm. Pendants were observed in all horizons of the profile except for Av1 and Av2.

Pendants were also found at the surface overturned and on their sides. A thin layer of

ovoid shaped pellets overly the stage IV laminar cap at 81 cm. These pellets ranged in

size from ~250µm to 1 mm. BSE compositional imaging and EDS methods show that

these pellets were composed of detrital grains composed of quartz and sphene, pieces of

carbonate material and masses of sepiolite all encompassed by a layer of sepiolite clay or

other clay (Figure 3.8). Texture varied from very gravelly loam in the Av1 and Av2

horizons, to very to extremely gravelly sandy loam in the Bk, Bkqm1, Bkqm2 and

Bkqm3 horizons and is gravelly with a fine fraction texture of loamy sand in the Bkqm4

horizon. pH values range from 7.92 to 8.28. EC values range from 325.2µs/cm to

4120µs/cm (Figure 3.25).

BLM Q1v Silica Pit

Silica Pit is located at UTM coordinates 658135 east and 4174745 north. Silica Pit

represents soils found in the Q1v landform. Pit depth reached only 29 cm due to

increased hardpan strength and inability to reach area with a backhoe (Figure 3.9).

Carbonate development begins at 10 cm with a well developed stage III with incipient

stage IV petrocalcic horizon. Below 23 cm the stage III horizon overlies a stage IV

horizon at 29 cm. Soils associated with this profile are qualitatively classified as Calcic

$Q1_D$ Backhoe Pit

Horizon	Depth (cm)	Structure	Texture (< 2mm fraction)	[a]Silica	*CaCO$_3$
Av1	0-10	Moderate, Fine-Med., Subangular Blocky	Loam	N/A	None
	Abrupt Smooth				
Av2	10-13	Strong, Coarse, Platy	Loam	None	None
	Abrupt Smooth				
Bk	13-33	Strong, Med.-Coarse, Subangular Blocky	Sandy Loam	Distinct	Stage II
	Abrupt Wavy				
Bkqm1	33-57	Massive	Sandy Loam	Distinct	Stage III
	Abrupt Wavy				
Bkqm2	57-65	Massive	Sandy Loam	Distinct	Stage III incipient IV
	Abrupt Wavy				
Bkqm3	65-82	Massive	Sandy Loam	Prominent	Stage III
	Pellet Horizon 81-82 cm				
	Abrupt Wavy				
Bkqm4	82+	Massive	Loamy Sand	Faint	Stage IV

Profile Depth (cm)

Figure 3.7. Soil profile and associated data from $Q1_D$ Backhoe pit. [a]Silica descriptions from Soil Survey Staff (1998). *Stages of carbonate morphology (Gile et al., 1966; Bachman and Machette, 1977)
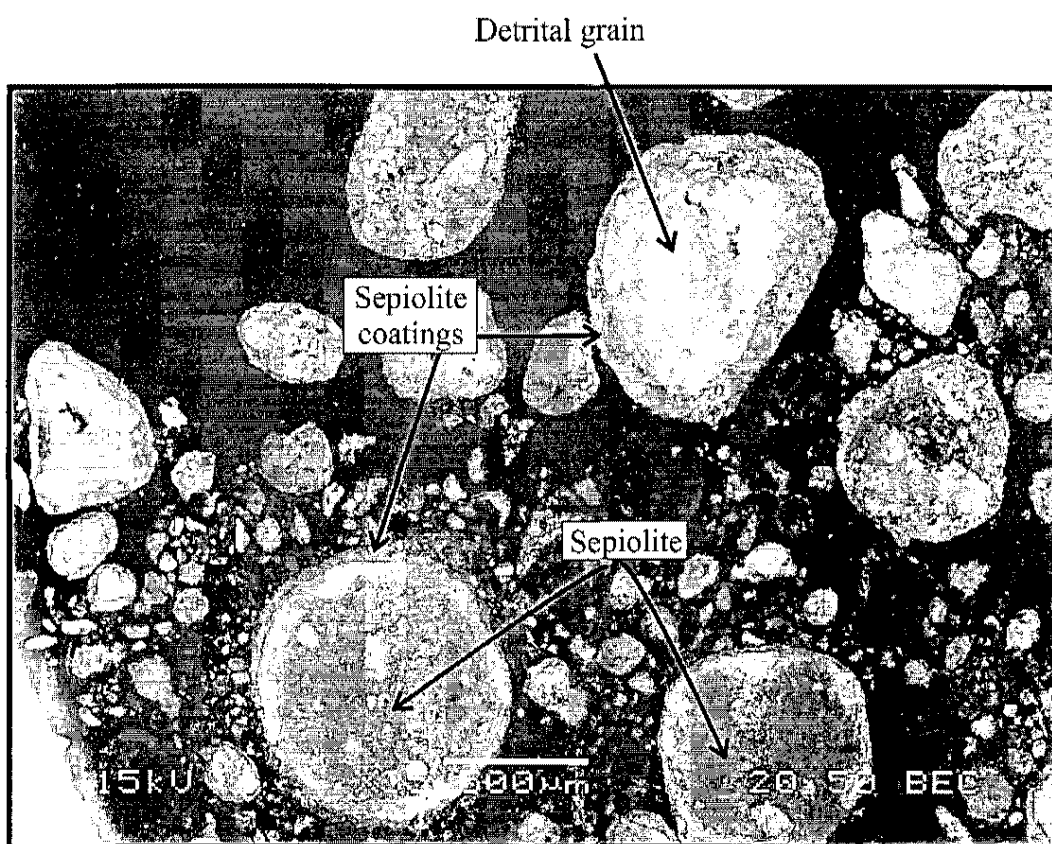
Figure 3.8. Pellets from Q1$_D$ Backhoe pit. Notice sepiolite coatings surrounding rounded masses of sepiolite and detrital grains.

Q1$_V$ Silica Pit

Horizon	Depth (cm)	Structure	Texture (< 2mm fraction)	[k]Silica	*CaCO$_3$
Av	0-10	#	#	None	None
	Abrupt Smooth				
Bkq	10-23	#	#	Distinct	Stage III incipient IV
	Abrupt Wavy				
Bkqm1	23-29	#	#	Distinct	Stage III
	Abrupt Wavy				
Bkqm2		#	#	Prominent	Stage IV

Profile Depth (cm): 10, 20, 30

Figure 3.9. Soil profile for Q1V Silica pit. # analyses were not performed. [k]Silica descriptions from Soil Survey Staff (1998). *Stages of carbonate morphology (Gile et al., 1966; Bachman and Machette, 1977).

Petrocalcids. Texture, pH, and EC were not measured for this profile because of sampling difficulty.

Q2 Landforms and Pedon Descriptions

The second oldest landforms present in the study area are found in both limestone/dolostone and volcanic parent material. The Q2 geomorphic surfaces are located below and inset against Q1 ballena surfaces and are recognized as topographically flat, moderately dissected, inset fans (Figures 3.4 and 3.5) (Peterson, 1981). Soil development is parallel with this planar surface, which is different and easily distinguished from the rounded development of the Q1 surfaces. Vegetation is predominantly blackbrush, similar to Q1 landforms. Degree of desert pavement is high but not as great as the older surfaces (Figure 3.10 and 3.11). Desert varnish is present on clasts other than limestone although there is limited material for varnish development. The best preserved inset fans of Q2 are found near the larger drainages of the study area in BLM and Mail Summit Washes.

Mail Summit Q1$_D$ Merkler Pit

Merkler Pit is located on a Q2 inset fan surface of the Mail Summit fan at UTM coordinates 659196 meters east and 4173482 meters north. Pedon depth reaches 72 cm and was divided into four separate soil horizons (Figure 3.12). Carbonate accumulation increases with depth with initial accumulation as stage II at 13 cm forming a stage IV at 40 cm decreasing to a stage III massive carbonate horizon at 55 cm. The laminar cap of the stage IV horizon at 40 cm has a thin layer of pellets that sit on top. Pellets are similar to those described in the Q1$_D$ Backhoe Pit profile discussion. Soil pendants are observed

Figure 3.10. Surface clasts of Q2$_0$ landform on Mail Summit fan.
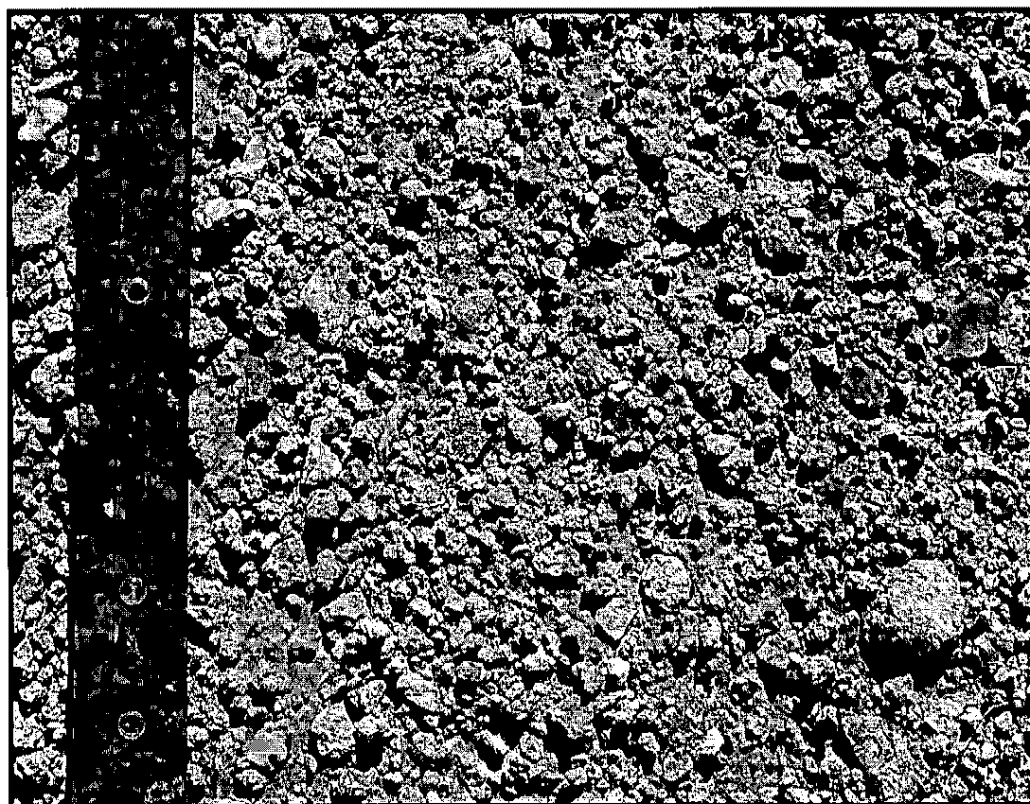
Figure 3.11. Surface clasts of Q2$_v$ landform on BLM fan.

Q2$_D$ Merkler Pit

Horizon	Depth (cm)	Structure	Texture (< 2mm fraction)	[a]Silica	*CaCO$_3$
Av	0-13	Strong, Very Coarse, Platy	Sandy Loam	None	None
		Abrupt Smooth			
Bk	13-40	Weak, Medium, Subangular Blocky	Sandy Loam	Faint	Stage II
		Pellet Horizon 40-41cm			
		Abrupt Wavy			
Bkqm	40-55	Massive	Loamy Sand	Distinct	Stage IV
		Abrupt Wavy			
Bkm	55-72	Massive	Loamy Sand	Faint	Stage III

Profile Depth (cm)
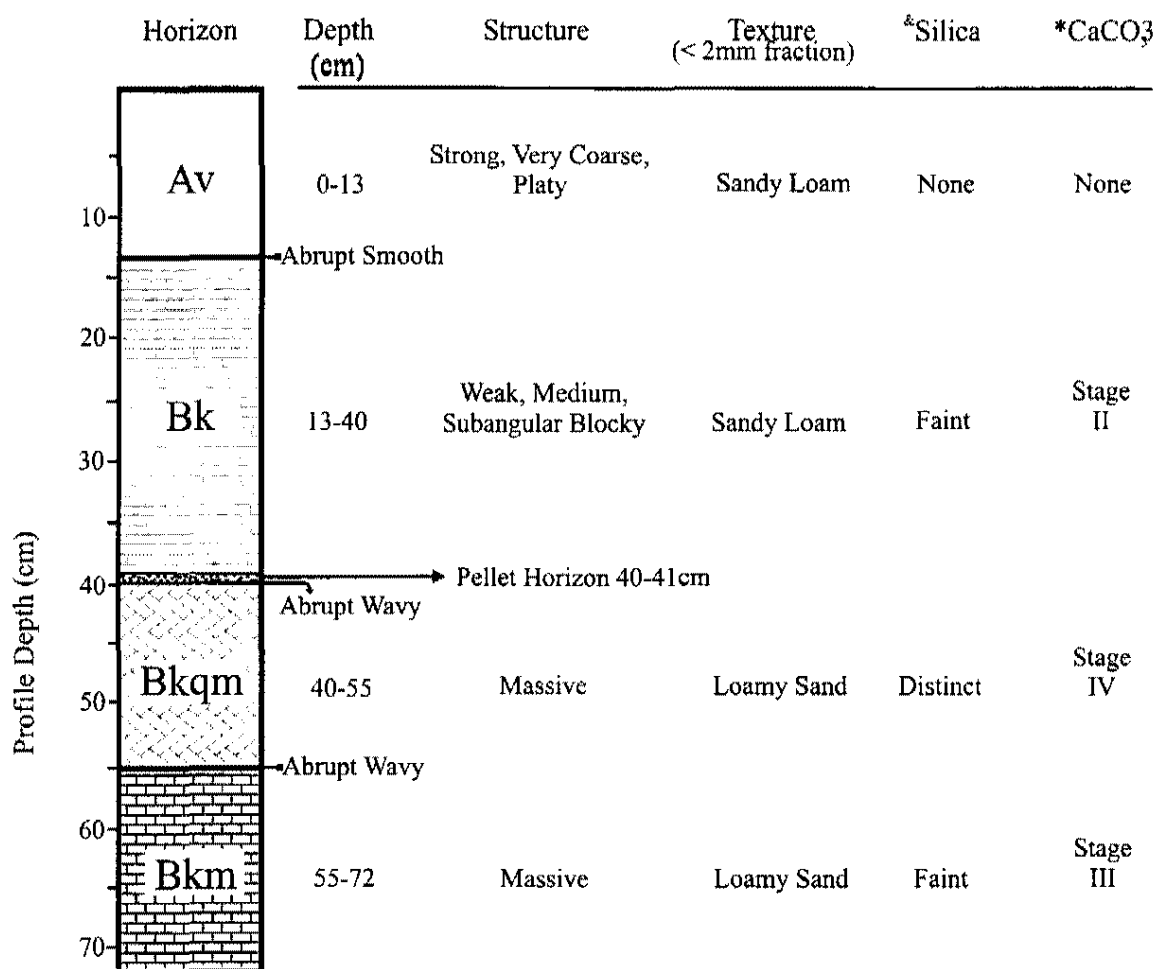
Figure 3.12. Soil profile of Q2$_D$ Merkler pit and associated descriptions.[a]Silica descriptions from Soil Survey Staff (1998). *Stages of carbonate morphology (Gile et al., 1966; Bachman and Machette, 1977).

throughout the calcic horizons of the profile. Pendants are relatively thick and are similar to those of the Q1 landforms. Gravel content is high with percentages ranging from 43-70%. Soil texture is very gravelly loam for the Av horizon, extremely gravelly sandy loam for the Bk and extremely gravelly loamy sand for the remaining horizons. Soils associated with Merkler Pit are qualitatively classified as Calcic Petrocalcids. pH ranges from 8.13-8.28 and EC values range 310.9µs/cm to 352.5µs/cm (Figure 3.24).

BLM Q2$_v$ BLM Pit

BLM Pit is located on a Q2 inset fan surface of the BLM fan at UTM coordinates 659196 meters east and 4173400 meters north and is dominated by volcanic parent material with some dolomite at the surface. The profile depth reached 90 cm with carbonate accumulation beginning at 13 cm with faint carbonate present on the undersides of clasts continuing with a stage III and incipient stage IV at 40 cm. Below 51 cm, calcium carbonate morphology decreased to stage III and continued to the base of the profile (Figure 3.13). Gravel percentages were not measured for this profile. Five horizons were designated in the field with textures ranging from sandy loam to sand at 40 cm depth. Soils associated with this profile are qualitatively classified as Calcic Petrocalcic. pH values range from 8.4 to 8.9 with EC between 288.5µs/cm and 412.0µs/cm (Figure 3.24).

Q3 Landforms and Profile Descriptions

Q3 landforms are inset fan remnants, dissecting Q2 and some areas of Q1 landforms (Figures 3.14 and 3.15). Slight bar and swale topography is present. However, there is no desert varnish or desert pavement development. The Q3 landforms contain more

Q2ᵥ BLM Pit

Horizon	Depth (cm)	Structure	Texture	ᵃSilica	*CaCO₃
Av	0-12	Strong, Fine, Subangular Blocky	Sandy Loam	None	None
Bk	12-40	Moderate, Med.-Coarse, Subangular Blocky	Sandy Loam	Faint	Faint
Bkqm1	40-51	Massive	Sand	Distinct	Stage III incipient IV
Bkqm2	51-70	Massive	Sand	Distinct	Stage III
Bkqm3	70-90	Single Grain	Sand	Prominent	Stage III

Profile markers (left axis, Profile Depth (cm)):
- Abrupt Wavy (~12 cm)
- Abrupt Smooth (~40 cm)
- Abrupt Smooth (~51 cm)
- Abrupt Smooth (~70 cm)

Figure 3.13. Soil profile of Q2ᵥ BLM pit and associated data. ᵃSilica descriptions from Soil Survey Staff (1998). *Stages of carbonate morphology (Gile et al., 1966; Bachman and Machette, 1977).
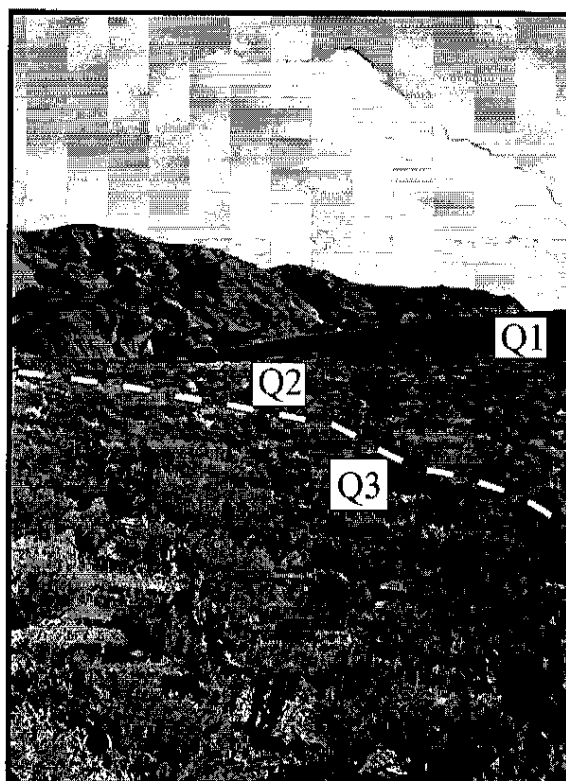
Figure 3.14. $Q3_D$ landform outlined in white dashed line. Notice $Q1_D$ landform in distance.
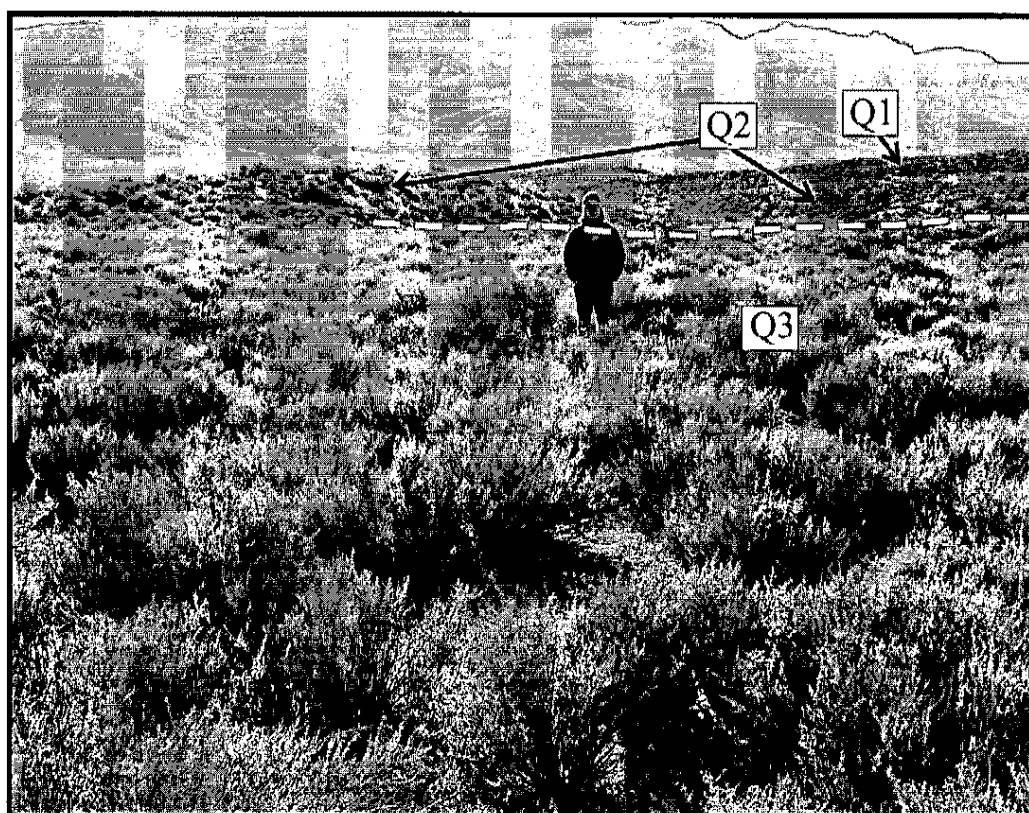
Figure 3.15. $Q3_v$ landform of the BLM fan outlined with dashed line. Notice $Q1_v$ and $Q2_v$ landforms in background.

effedra than the older Q1 and Q2 landforms. However, blackbrush, is still the dominant vegetation. Q3 landforms can be identified on aerial photographs as darker (when compared to Q1 and Q2) with shallower stream channel areas that have not been dissected by the Q4-forming event(s). The distal ends of the Q3 landforms were dissected by fluvial episodes of the ancient White River, leaving no fans on the modern floodplain. Q3 landforms are also found upstream of some smaller tributary channels where headcutting of Q4 has not occurred.

Mail Summit Q3$_D$ Mystery Pit

Mystery Pit is located on a Q3 inset surface of the Mail Summit fan at UTM coordinates 656575 meters east and 4169884 meters north. The profile is 118 cm deep with gravel percents varying between 51-77% and texture ranging from very to extremely gravely sandy loam in the A, Bk1 and Bk3 horizons to extremely gravelly loamy sand in the Bk2 and Bk4 horizons. No massive carbonate horizons exist in this profile. Stage I carbonate begins at 11 cm and continues to 100 cm where it increases to stage II. Carbonate accumulation occurs as thin pendants throughout the profile (Figure 3.16). Soils associated with this profile are qualitatively classified as Typic Haplocalcids. pH values range from 8.15-8.34 and EC from 282.9μs/cm to 650.1μs/cm (Figure 3.24).

BLM Q3$_V$ Last Pit

Last Pit is located on a Q3 inset surface of the BLM fan at UTM coordinates 658237 meters east and 4174376 meters north. This profile contains 46-91% gravel and all horizons have a very to extremely gravelly loamy sand texture. The profile is 118 cm deep. Carbonate accumulation begins at 10 cm with stage I and increases to a stage II accumulation at 68 cm. Thin carbonate coatings on clasts (pendants) are present in the Bk

Q3$_D$ Mystery Pit

Horizon	Depth (cm)	Structure	Texture (< 2mm fraction)	[a]Silica	*CaCO$_3$
A	0-11	Mod., Fine-Med., Subangular Blocky	Sandy Loam	None	None
		Clear Wavy			
Bk1	11-38	Weak, Fine, Subangular Blocky	Sandy Loam	None	Stage I
		Clear Wavy			
Bk2	38-73	Weak, Very Fine-Fine, Subangular Blocky	Loamy Sand	Faint	Stage I
		Clear Wavy			
Bk3	73-100	Mod., Fine-Med., Subangular Blocky	Sandy Loam	None	Stage I
		Clear Wavy			
Bk4	100-118	Single Grain	Loamy Sand	None	Stage II

Profile Depth (cm)

Figure 3.16. Diagram of Q3$_D$ Mystery profile and associated information. [a]Silica descriptions from Soil Survey Staff (1998). *Stages of carbonate morphology (Gile et al., 1966; Bachman and Machette, 1977).

horizons with stage II carbonate morphology (Figure 3.17). Durinodes occur between

68-100 cm depth. Soils associated with this profile are qualitatively classified as

Durinodic Haplocalcids. pH measurements range from 6.6 to 7.23 and EC from

304μs/cm-481.5μs/cm.

Q4 Landform and Profile Descriptions

Q4 landforms are inset fans found in deeply dissected drainages of the study area

approximately 1 meter above the modern channels. Strong bar and swale surface

topography is present with no desert varnish or desert pavement development (Figures

3.18 and 3.19). Cryptogamic crust is common and the dominant vegetation is blackbush

and Nevada ephedra, with less common rabbitbrush and cholla. Few, large boulder-sized

rocks are present on this landform. There is a significant (~20 meter) change in elevation

from adjacent, Q2 inset fans to the Q4 inset fans. Q4 is easily identified on aerial

photographs as channel shaped, sinuous forms, dark in color, that have transported and

deposited alluvium onto the White River floodplain.

Mail Summit Q4$_D$ Shovel Pit

Shovel Pit is located on a Q4 inset fan at UTM coordinates 657003 meters east and

4169005 meters north. It lies in the Mail Summit fan and is 90 cm deep. Shovel Pit

profile contains a sporadic, weak Av horizon overlying a Bw and two Bk horizons

(Figure 3.20). Stage I carbonate development begins at 13 cm and remains throughout

the profile. Thin carbonate gravel coatings are present throughout the profile in the Bk1,

Bk2 and Bk3 horizons. Soils associated with this profile are qualitatively classified as

Typic Haplocalcids. Gravel content varies from 29 to 58% and has textures of gravelly to

Q3$_V$ Last Pit

Horizon	Depth (cm)	Structure	Texture (< 2mm fraction)	*Silica	*CaCO$_3$
A	0-10	Weak, Medium, Subangular Blocky	Loamy Sand	None	None
		Clear Smooth			
Bk1	10-22	Moderate, Medium, Subangular Blocky	Loamy Sand	None	Stage I
		Clear Wavy			
Bk2	22-68	Single Grain	Loamy Sand	Faint	Stage I
		Clear Wavy			
Bk3	68-100	Single Grain	Loamy Sand	Faint Durinodes	Stage II

Profile Depth (cm): 10, 20, 30, 40, 50, 60, 70, 80, 90, 100

Figure 3.17. Diagram of Q3$_V$ Last profile and associated data. *Silica descriptions from Soil Survey Staff (1998). *Stages of carbonate morphology (Gile et al., 1966; Bachman and Machette, 1977).
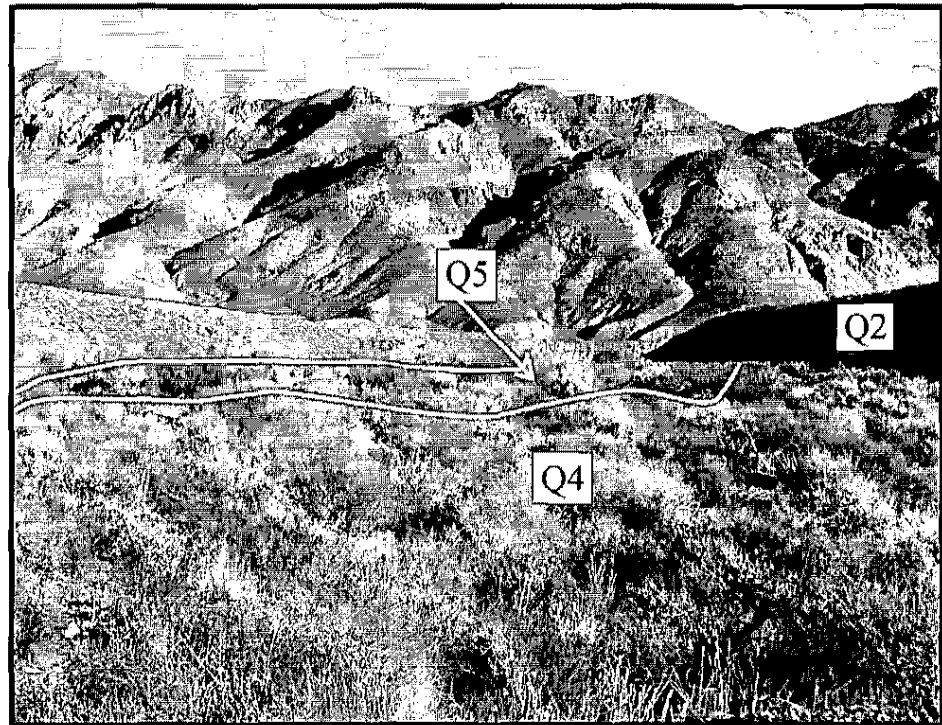
Figure 3.18. $Q4_D$ landform of Mail Summit fan. Photo taken facing east looking towards Hiko Range. Notice $Q2_D$ landforms at higher elevations on left and right edges of photo.
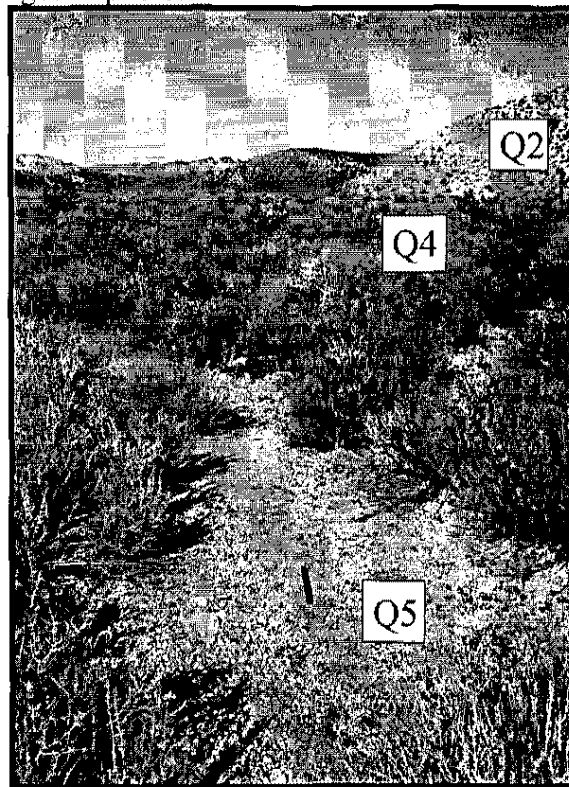
Figure 3.19. $Q4_V$ landform of BLM fan. Photo taken looking west. Notice $Q2_V$ landform at higher elevation on right edge of photo.

Q4$_D$ Shovel Pit

Horizon	Depth (cm)	Structure	Texture (<2mm fraction)	[&]Silica	*CaCO$_3$
Av	0-6	Weak, Fine-Med. Subangular Blocky	Sandy Loam	None	None
		Clear Wavy			
Bw	6-28	Weak, Medium, Subangular Blocky	Sandy Loam	None	None
		Clear Wavy			
Bk1	28-37	Single Grain	Sandy Loam	None	Stage 1
		Clear Wavy			
Bk2	37-90	Single Grain	Loamy Sand	None	Stage I

Profile Depth (cm)

Figure 3.20. Soil profile of Q4$_D$ Shovel profile and associated information. [&]Silica descriptions from Soil Survey Staff (1998). *Stages of carbonate morphology (Gile et al., 1966; Bachman and Machette, 1977).

very gravelly sandy loam to very gravelly loamy sand. pH values are 7.91-8.44 and EC values ranging from 270µs/cm-927.4µs/cm (Figure 3.24).

BLM Q4$_V$ Glass Pit

Glass Pit profile is located on a Q4 inset fan at UTM coordinates 658810 meters east and 4174122 meters north and is 122 cm deep. Profile development is similar to that of Q4$_D$ Shovel Pit with stage I carbonate morphology beginning at 26 cm as stage I accumulations throughout the entire profile. (Figure 3.21). Durinodes are present in this profile at 89-122 cm but are not as distinct as those found in the Q3 Last Pit. Soils associated with this profile are qualitatively classified as Durinodic Haplocalcids. Gravel content ranges between 40-64% with textures of extremely gravely sandy loam and very gravely loamy sand with extremely gravely sand in the Bk2 and Bk3 horizons. No vesicular horizon was present with this profile. pH values range from 8.01 to 8.41 with EC values of 1100µs/cm to 382.3µs/cm (Figure 3.24).

Q5 Landform and Profile Description

Q5 is an inset drainage found in areas where ephemeral channels and associated active floodplains create whiter, light colored meandering and braided areas on aerial photographs . Q5 inset fan surfaces are located adjacent to and approximately one meter below the Q4 inset fan surfaces (Figure 3.22). Q5 soil profile is qualitatively classified as a Typic Torriorthent. The one profile associated with this landform is Wash Pit (Figure 3.23) located on a Q5 inset fan surface of the BLM drainage at UTM coordinates 658810 meters east and 4174100 meters north. This profile consists of four C horizons that have undergone little to no pedogenesis. Sedimentary structures are present as fluvial

Q4$_V$ Glass Pit

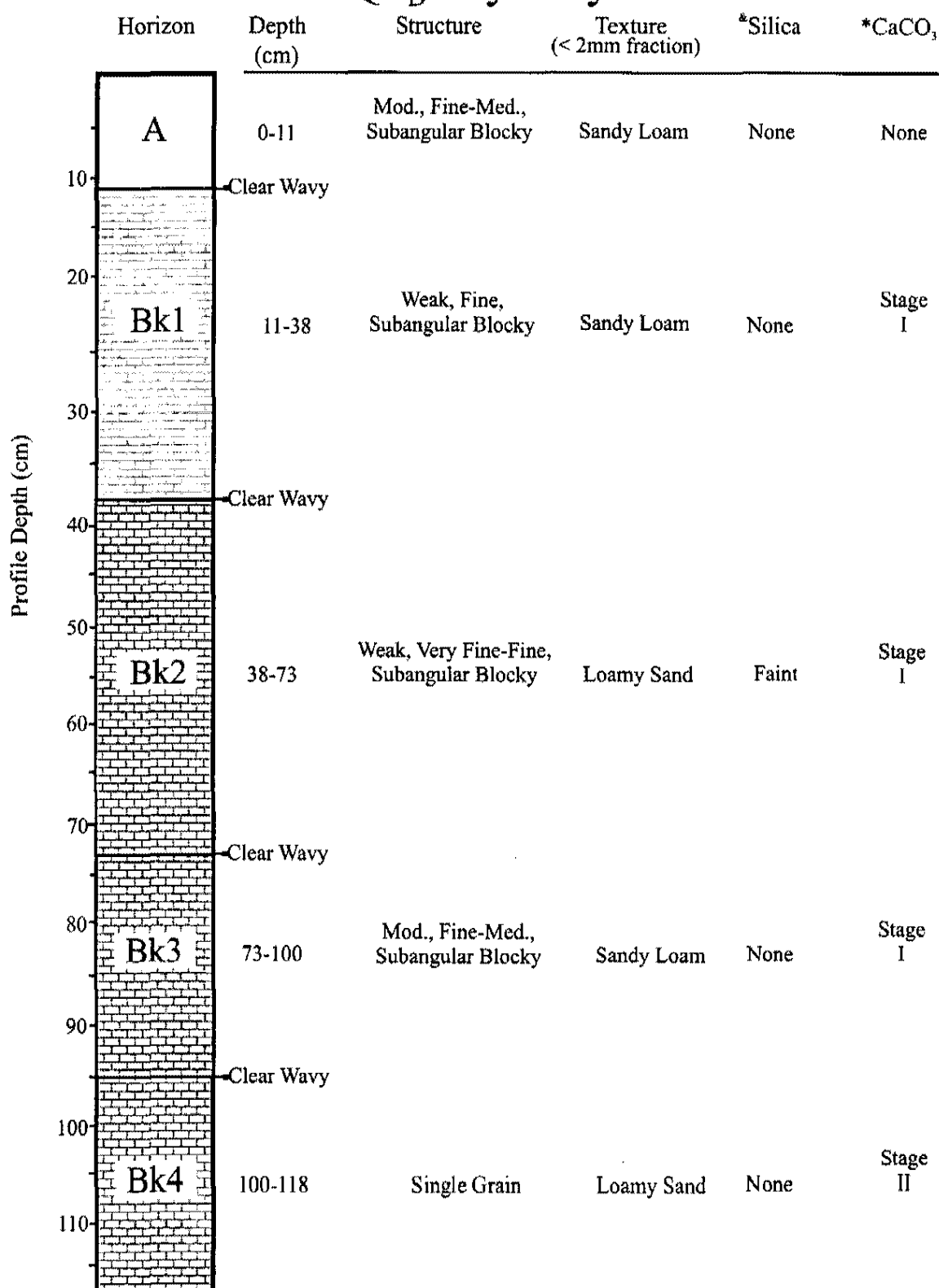| Horizon	Depth (cm)	Structure	Texture (< 2mm fraction)	*Silica	*CaCO$_3$
A	0-2	Weak, Fine-Med., Platy	Loamy sand	None	None
	Abrupt Smooth				
Bw	2-13	Moderate, Very Fine-Fine, Subangular Blocky	Loamy sand	None	None
	Abrupt Wavy				
Bk1	13-46	Moderate, Med-Coarse, Subangular Blocky	Sandy Loam	Distinct	Stage I
	Abrupt Wavy				
Bk2	46-89	Moderate, Med-Coarse, Subangular Blocky	Sand	Distinct	Stage I
	Abrupt Wavy				
Bkq	89-122	Single Grain	Sand	Distinct Durinodes	Stage I

Profile Depth (cm)

Figure 3.21. Diagram of Q4$_V$ Glass profile and associated data. *Silica descriptions from Soil Survey Staff (1998). *Stages of carbonate morphology (Gile et al., 1966; Bachman and Machette, 1977).
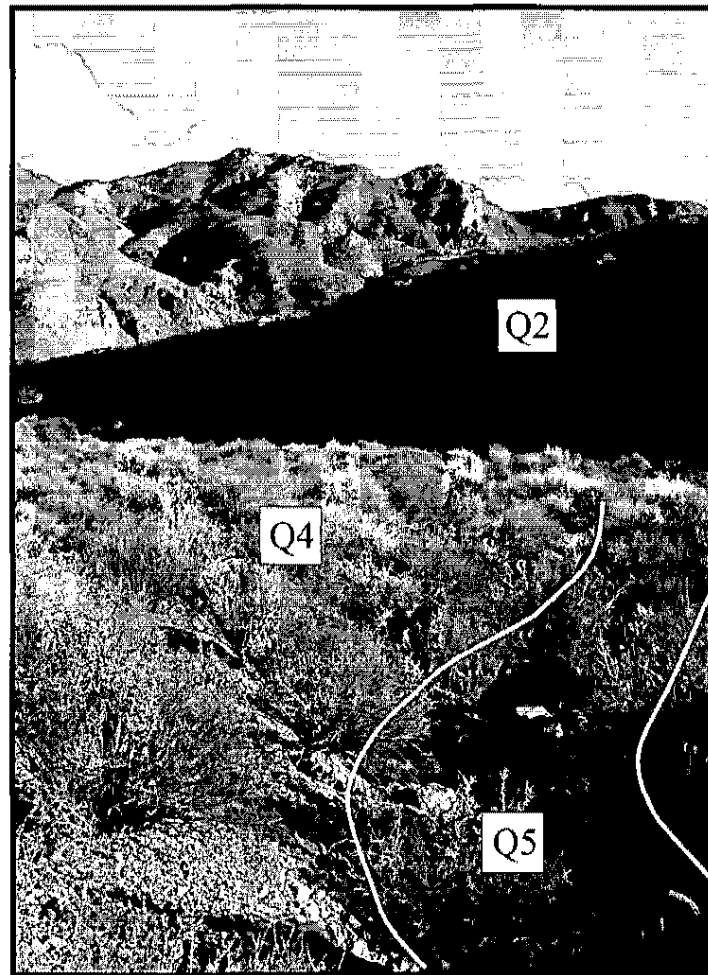
Figure 3.22. $Q5_D$ (active) landform outlined with solid line. Notice $Q4_D$ immediately adjacent to $Q5_D$. $Q2_D$ is in background.

Q5$_V$ Wash Pit

Horizon	Depth (cm)	Structure	Texture (< 2mm fraction)	[a]Silica	*CaCO$_3$
C1	0-3 ◄Abrupt Smooth	Single grain	Sand	None	None
C2	3-20	Single grain	Sand	None	None
	◄Abrupt Smooth				
C3	20-30	Single grain	Sand	None	None
	◄Abrupt Smooth				
C4	30-50	Single grain	Sand	None	None
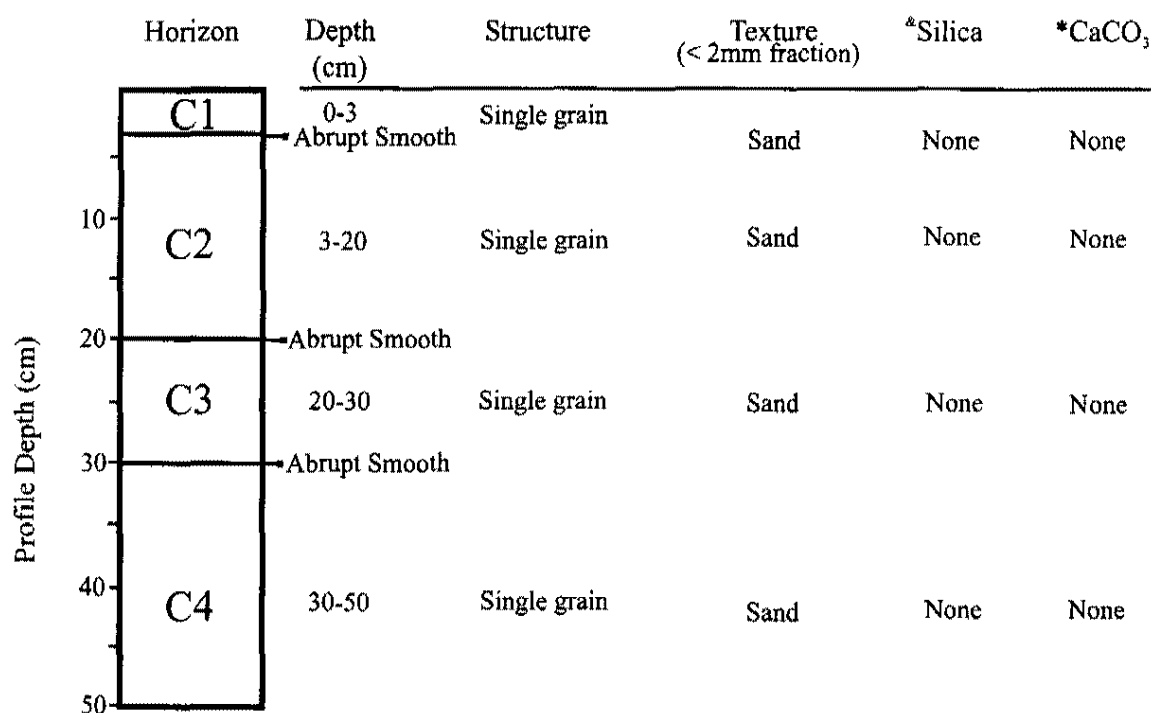
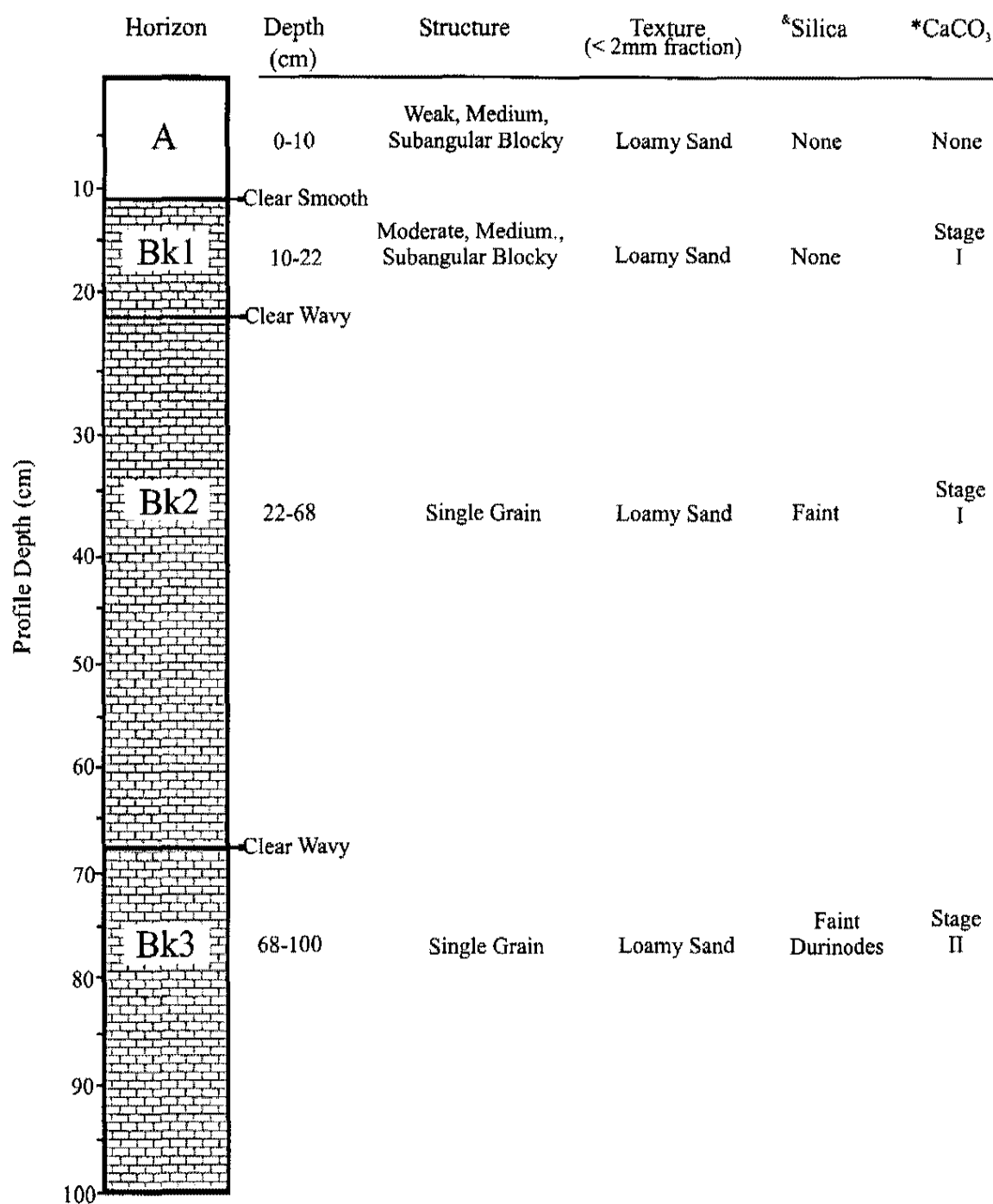Figure 3.23. Soil profile of Q5$_V$ Wash profile and associated data. [a]Silica descriptions from Soil Survey Staff (1998). *Stages of carbonate morphology (Gile et al., 1966; Bachman and Machette, 1977).

crossbedded sands and gravels. The texture is sand for each horizon. pH values range

from 8.2 to 9 and EC values from 302.6μs/cm to 510.4μs/cm (Figure 3.24).

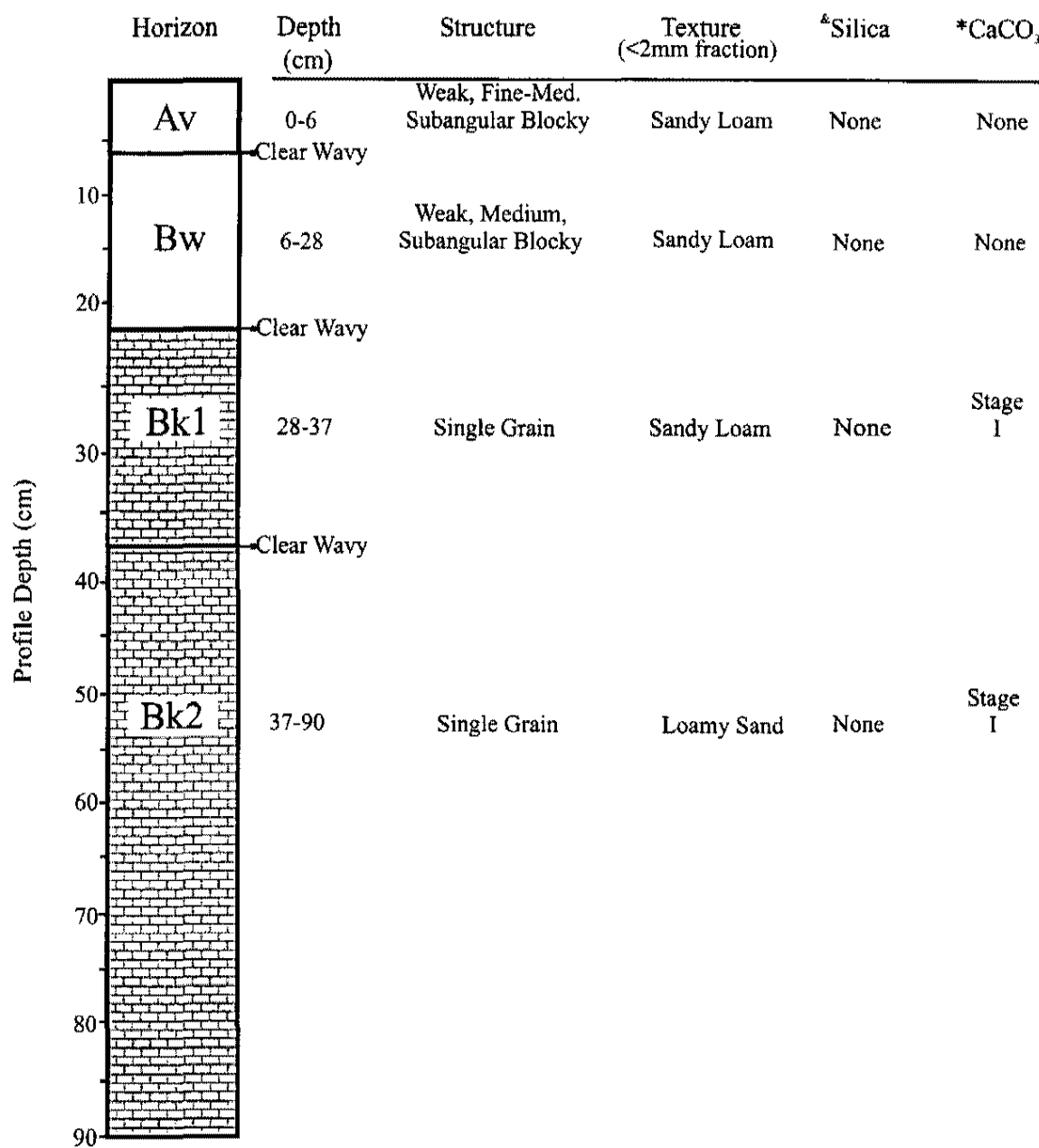| Pedon Name	Depth	Horizon	Texture	Gravel %	Dry Color	pH	EC(μs/cm)
Q1 Backhoe	0-10	Av1	Loam	51	7.5yr7/2	8.22	479.5
Q1 Backhoe	10-13	Av2	Loam	37	7.5yr6/3	8.28	365.2
Q1 Backhoe	13-33	Bk	Sandy Loam	50	7.5yr6/3	8.22	325.2
Q1 Backhoe	33-57	Bkqm1	Sandy Loam	74	7.5yr7/3	8.24	358.6
Q1 Backhoe	57-65	Bkqm2	Sandy Loam	76	7.5yr7/2	8.23	362
Q1 Backhoe	65-82	Bkqm3	Sandy Loam	77	7.5yr7/2	8.11	819.9
Q1 Backhoe	82+	Bkqm4	Loamy Sand	95	7.5yr7/3	7.92	4121
Q1 Silica	0-10	Av	*	*	*	*	*
Q1 Silica	10-23	Bkq	*	*	*	*	*
Q1 Silica	23-29	Bkqm1	*	*	*	*	*
Q1 Silica	29+	Bkqm2	*	*	*	*	*
Q2 Merkler	0-13	Av	Loam	43	10yr6/2	8.13	334.5
Q2 Merkler	13-40	Bk	Sandy Loam	68	10yr7/3	8.18	310.9
Q2 Merkler	40-55	Bkqm	Loamy Sand	75	10yr6/2	8.22	336.9
Q2 Merkler	55-72	Bkm	Loamy Sand	70	10yr7/3	8.28	352.5
Q2 BLM	0-12	Av	Sandy Loam	*	10yr6/3	8.4	320
Q2 BLM	12-40	Bk	Sandy Loam	*	10yr7/2	8.9	288.5
Q2 BLM	40-51	Bkqm1	Sand	*	10yr6/2	8.6	382.6
Q2 BLM	51-70	Bkqm2	Sand	*	10yr6/2	8.8	295.5
Q2 BLM	70-90	Bkqm3	Sand	*	10yr6/3	8.9	412
Q3 Mystery	0-11	A	Sandy Loam	51	10yr6/4	8.15	650.1
Q3 Mystery	11-38	Bk1	Sandy Loam	66	10yr6/3	8.34	297
Q3 Mystery	38-73	Bk2	Loamy Sand	77	10yr6/3	8.32	282.9
Q3 Mystery	73-100	Bk3	Sandy Loam	65	10yr7/3	8.31	378.8
Q3 Mystery	100-118	Bk4	Loamy Sand	67	10yr7/3	8.21	500.7
Q3 Last	0-10	A	Loamy Sand	48	7.5yr6/3	7.19	481.5
Q3 Last	10-22	Bk1	Loamy Sand	46	7.5yr6/3	7.23	409.3
Q3 Last	22-68	Bk2	Loamy Sand	52	7.5yr6/3	6.6	304
Q3 Last	68-100	Bk3	Loamy Sand	91	7.5yr6/3	7.15	382.1
Q4 Shovel	0-6	Av	Sandy Loam	58	10yr5/4	7.91	927.4
Q4 Shovel	6-28	Bw	Sandy Loam	47	10yr6/4	8.38	323.4
Q4 Shovel	28-37	Bk1	Sandy Loam	29	10yr5/3	8.44	296.1
Q4 Shovel	37-90	Bk2	Loamy Sand	44	10yr5/3	8.35	270.5
Q4 Glass	0-2	A	Loamy Sand	48	10yr6/2	8.01	1103
Q4 Glass	2-13	Bw	Loamy Sand	40	10yr6/3	8.39	355.2
Q4 Glass	13-46	Bk1	Sandy Loam	64	10yr6/2	8.35	317.5
Q4 Glass	46-89	Bk2	Sand	62	10yr6/3	8.35	317.2
Q4 Glass	89-122	Bkq	Sand	64	10yr6/2	8.41	382.3

Pedon Name	Depth	Horizon	Texture	Gravel %	Dry Color	pH	EC(µs/cm)
Q5 Wash	0-3	C1	Sand	*	*	8.2	510.4
Q5 Wash	3-20	C2	Sand	*	*	8.6	466
Q5 Wash	20-30	C3	Sand	*	*	9	317.6
Q5 Wash	30-50	C4	Sand	*	*	8.2	302.6

Figure 3.24. Combined data from all profiles sampled. (*-analyses were not performed)

CHAPTER IV

SOIL PENDANT RESULTS

Soil pendants collected from the Quaternary landforms in the northern Pahranagat

Valley display a variety of unique morphologies and characteristics. Pendants were

examined from each soil horizon in which they appeared. This chapter summarizes field

descriptions, macromorphology and micromorphology from pendants sampled in the

northern Pahranagat Valley. The information obtained from these analyses is given in

Figures 4.1-4.4.

General Description and Characteristics

Soil pendants are present in all Quaternary landforms of the study area except for

active inset drainages (Q5). Pendants were collected from horizons with stage I and

greater carbonate development where carbonate and or other material has accumulated on

the undersides of gravel or cobbles in the soil profile. Pendants are commonly seen in the

soil profile with distinct, white, carbonate accumulating below each clast (Figure 4.5).

When pendants are removed from soil profiles, they retain the same form as seen in place

(Figure 4.6). Each pendant has a set of features and associated terminology that will be

used throughout this chapter (Figure 4.6). All pendants have a parent clast and associated

clast-pendant contact. Parent clasts are the gravel to cobble sized clasts, located in the

Unit	Sample ID	Depth	Total$	Carbonate*	Clay/Silica*	Voids*	Grains*	Thickness&
Q1 Backhoe	Q1B2	10-13	600	20.33	32.33	27.66	19.66	17
Q1 Backhoe	Q1B3	13-33	600	56.33	34.66	4.5	5	11
Q1 Backhoe	Q1B4	33-57	600	44.66	33.5	12.83	9	6
Q1 Backhoe	Q1B5	57-65	600	17.82	8.83	35.16	0.33	10
Q1 Backhoe	Q1B6	65-82	600	54.33	19.33	25	1.33	5
Q1 Backhoe	Q1B7	82+	600	4.33	52.16	8.33	35.16	12
Q1 Silica	Q1S3a	29+	300	37.33	28.33	29.33	5	4
Q2 BLM	Q2B2	12-40	500	54.6	21	1.6	22.8	2
Q2 BLM	Q2B3	40-51	600	12.83	27.5	6.33	53.33	11
Q2 BLM	Q2B3a	40-51	600	36.83	13	6.16	43.99	11
Q2 BLM	Q2B4	51-70	600	29.82	17.5	14.16	38.5	7
Q2 BLM	Q2B5	70-90	600	10.66	45.16	22.66	21.5	15
Q2 BLM	Q2B5a	70-90	600	30.83	16.83	13.16	39.16	15
Q2 Merkler	Q2M2	13-40	600	68.83	11.16	10.33	9.66	6
Q2 Merkler	Q2M3	40-55	600	21.83	27.83	4.16	46.16	14
Q2 Merkler	Q2M4	55-72	600	25.66	17	11.83	45.5	17
Q3 Mystery	Q3MY1	0-11	600	37.5	32.5	13.66	16.33	4
Q3 Mystery	Q3MY1a	0-11	600	65.99	17.39	8.33	12.83	4
Q3 Mystery	Q3MY2	11-38	405	75.3	14.56	8.88	1.23	2
Q3 Mystery	Q3MY3	38-73	not enough pendant to count					1
Q3 Mystery	Q3MY4	73-100	600	53.83	17.83	18.16	10.66	4
Q3 Mystery	Q3MY4a	73-100	600	68	15.66	13.66	2.66	3
Q3 Mystery	Q3MY5	100-118	600	60.33	31	7	1.66	1
Q3 Last	Q3L3	22-68	not enough pendant to count					1
Q3 Last	Q3L4	68-100	276	73.18	17.39	9.42	0	2
		0-2						
Q5 Glass	Q5G5	89-122	600	63.33	11	5	20.66	4

Figure 4.1. Point count data with sample thicknesses. $total number of points counted in a 1/3x1/3 grid. *Percentages, &Measurement of pendant at thickest vertical point.

Unit	Depth	Ls Parent	Dolomite Parent	Vocanic Parent	EDS Silica	EDS Illite	EDS Sepiolite	EDS Other	XRD Chl.-Mont.	XRD Illite	XRD Dolomite	XRD Quartz	XRD Silica	XRD Sepiolite	XRD Paly.	XRD Mont.	XRD Orthoclase	XRD Muscovite	XRD Kaolinite
Q1 Backhoe	0-10																		
Q1 Backhoe	10-13																		
Q1 Backhoe	13-33	X							—	—	—	—	—	—	—	—	—	—	—
Q1 Backhoe	33-57		X				X	X	—	—	—	—	—	—					
Q1 Backhoe	57-65		X				X					X		X					
Q1 Backhoe	65-82	X					X				X	X	X	X	X				
Q1 Backhoe	82+	X					X	X	—	—	—							—	
Q1 Silica	0-10																		
Q1 Silica	10-23																		
Q1 Silica	23-29																		
Q1 Silica	29+			X	X		X						X				X		
Q2 Merkler	0-12																		
Q2 Merkler	12-40		X					X		X	X	X			X				
Q2 Merkler	40-55	X				X		X	—	—	—	—	—	—	—	—	—	—	—
Q2 Merkler	55-72		X				X	X			X	X		X				X	X
Q2 BLM	0-12																		
Q2 BLM	12-40			X	X		X	X	—	—	—	—	—	—	—	—	—	—	—
Q2 BLM*	40-51		XZ		X		X				X	X				X	X		
Q2 BLM	51-70		X				X		—	—	—	—	—	—	—	—	—	—	—
Q2 BLM*	70-90		XZ		X		X	X			X	X	X		X				
Q3 Mystery*	0-11	X	Z				X	X	—	—	—	—	—	—	—	—	—	—	—
Q3 Mystery	11-38		X		X			X	—	—	—	—	—	—	—	—	—	—	—
Q3 Mystery	38-73	X						XZ	—	—	—	—	—	—	—	—	—	—	—
Q3 Mystery*	73-100		XZ					X	X	X		X							X
Q3 Mystery	100-118	X							—	—	—	—	—	—	—	—	—	—	—
Q3 Last	0-10																		
Q3 Last	10-22																		
Q3 Last	22-68	X			X				—	—	—	—	—	—	—	—	—	—	—
Q3 Last	68-100	X			X			X											
Q4 Glass	0-2																		
Q4 Glass	2-13																		
Q4 Glass	13-46																		
Q4 Glass	46-89																		
Q4 Glass	89-122		X		X		X												
Total Count		9	14	2	—	—	—	—	—	—	—	—	—	—	—	—	—	—	—
Percentage		36	56	8	—	—	—	—	—	—	—	—	—	—	—	—	—	—	—

Figure 4.2. EDS and XRD results. Gray areas represent horizons without pendants or horizons where pendants were not analyzed. Dashed lines indicate XRD analyses not performed. *Two pendants from horizon were analyzed with SEM

Unit	Depth	Void at contact	Precip. In void	Clast Break-up	Clast inclusions	Displaced Grains	Pellet-like mass	Angular Voids	Grains Dissolved	CaCO3 Consumed	Clay at terminus	Mg rich CaCO3	Sepiolite Fibers
Q1 Backhoe	0-10												
Q1 Backhoe	10-13												
Q1 Backhoe	13-33	X		X			X	X	X			X	
Q1 Backhoe	33-57	X	X	X	X	X	X	X	X			X	
Q1 Backhoe	57-65	X		X	X	X	X						X
Q1 Backhoe	65-82			X	X	X					X		
Q1 Backhoe	82+						X		X				
Q1 Silica	0-10												
Q1 Silica	10-23												
Q1 Silica	23-29												
Q1 Silica	29+	X											X
Q2 Merkler	0-12												
Q2 Merkler	12-40			X	X	X			X				
Q2 Merkler	40-55	X		X	X		X	X	X				
Q2 Merkler	55-72			X			X						
Q2 BLM	0-12												
Q2 BLM	12-40	X	X						X				
Q2 BLM*	40-51	X		X	X		X				X	X	X
Q2 BLM	51-70			X	X	X							X
Q2 BLM*	70-90								X	X			X
Q3 Mystery*	0-11	XZ	X	X					XZ		XZ		
Q3 Mystery	11-38	X	X	X					X		X		
Q3 Mystery	38-73	X									XZ		
Q3 Mystery*	73-100	XZ		X							XZ		
Q3 Mystery	100-118	X							X				
Q3 Last	0-10												
Q3 Last	10-22												
Q3 Last	22-68	X											
Q3 Last	68-100	X											
Q4 Glass	0-2												
Q4 Glass	2-13												
Q4 Glass	13-46												
Q4 Glass	46-89												
Q4 Glass	89-122	X		X									
Total counts		17	4	13	7	5	6	3	11	3	7	3	5
Percentage		68	16	52	28	20	24	12	44	12	28	12	20

Figure 4.3. Information from SEM analyses.
Horizons in gray represent horizons with no pendants or horizons
where pendants were not analyzed. *Two samples analyzed

Unit	Depth	Silica	Large grains	Cupped limestones	Pellets
Q1 Backhoe	0-10				
Q1 Backhoe	10-13				
Q1 Backhoe	13-33				
Q1 Backhoe	33-57	X		X	
Q1 Backhoe	57-65	X		X	X
Q1 Backhoe	65-82	X		X	X
Q1 Backhoe	82+		X		
Q1 Silica	0-10	—	—	—	—
Q1 Silica	10-23	X	X	X	
Q1 Silica	23-29	—	—	—	—
Q1 Silica	29+	X	X		X
Q2 Merkler	0-12				
Q2 Merkler	12-40	X			X
Q2 Merkler	40-55	X			
Q2 Merkler	55-72	X	X		X
Q2 BLM	0-12	—	—	—	—
Q2 BLM	12-40	—	—	—	—
Q2 BLM	40-51	X	X		
Q2 BLM	51-70	X	X		
Q2 BLM	70-90		X		

Unit	Depth	Silica	Large grains	Cupped limestones	Pellets
Q3 Mystery	0-11				
Q3 Mystery	11-38	X			
Q3 Mystery	38-73	X			
Q3 Mystery	73-100	X			
Q3 Mystery	100-118				
Q3 Last	0-10				
Q3 Last	10-22				
Q3 Last	22-68	X			
Q3 Last	68-100				
Q4 Shovel	0-6				
Q4 Shovel	6-28				
Q4 Shovel	28-37	X			
Q4 Shovel	37-90	X			
Q4 Glass	0-2				
Q4 Glass	2-13				
Q4 Glass	13-46				
Q4 Glass	46-89				
Q4 Glass	89-122		X		

Figure 4.4. Results of macroscopic observation. Dashed lines where no pendants are present.
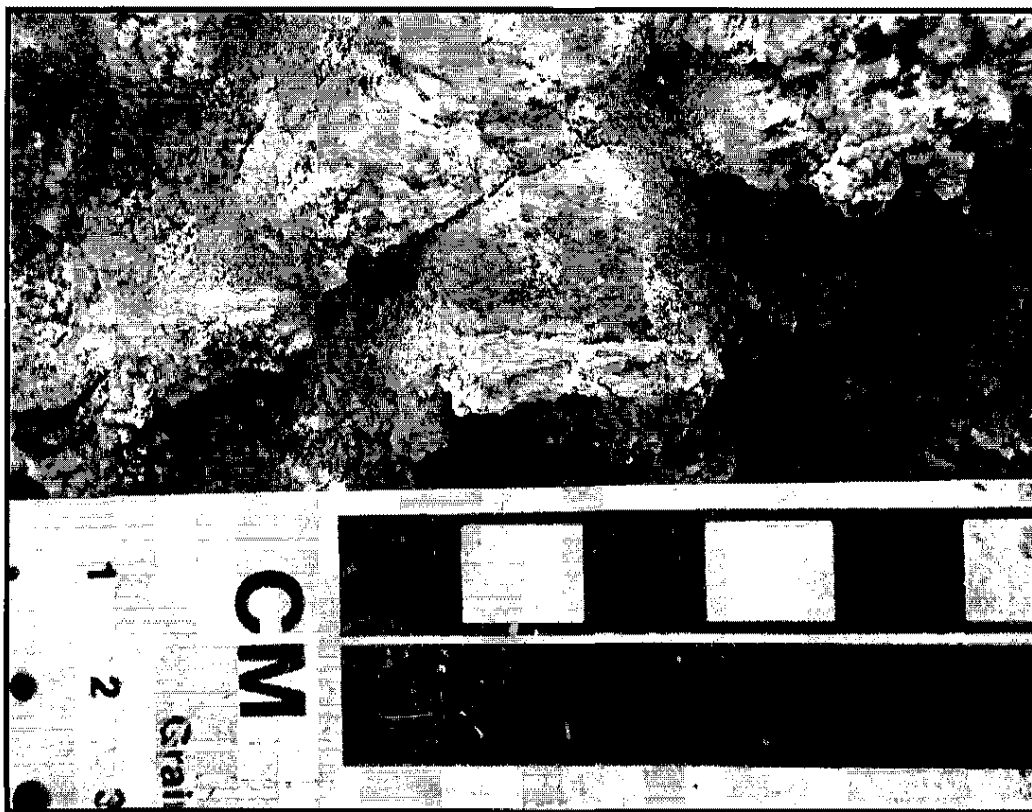
Figure 4.5. Pendants in place in Q1$_D$ Backhoe pit.
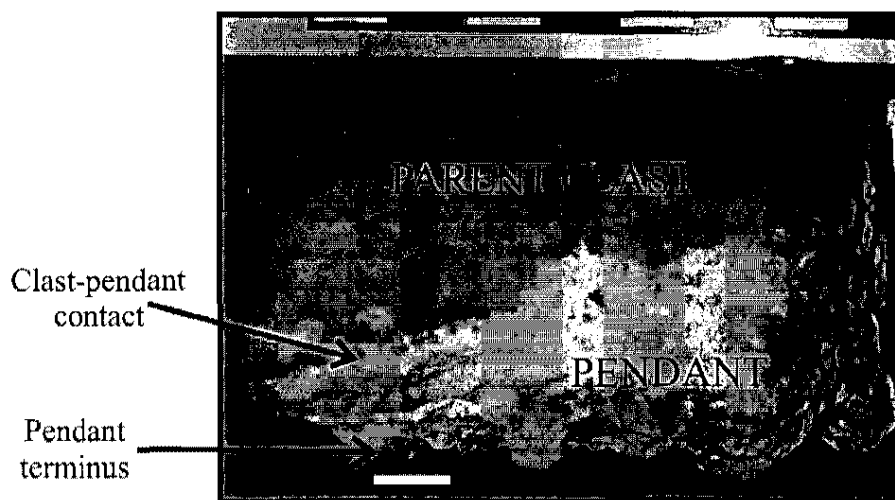

Clast-pendant contact

Pendant terminus

Figure 4.6. Pendant pulled from Q2$_V$ BLM 12-40 cm. Image also shows associated terminology of pendant features. Bar length is 1 cm.

subsurface, underneath which pedogenic materials accumulate creating a pendant. In

some instances, multiple pebble sized parent clasts share one pendant, however, there is

typically one clast per pendant. The clast-pendant contact is the contact between the

parent clast and its pendant. The pendant terminus is the bottom limit to the pendant.

Macromorphology and Micromorphology of Pendants

Pendants were examined in the field as well as in the laboratory with fields of view

ranging from 20 mm to 1 mm. Visual and chemical examinations of pendants were

performed using backscatter electron analyses (BSE) with SEM. The compositional

analyses of BSE greatly assisted in determining pendant-clast differences and

compositional variations throughout the pendant. Figure 4.7 shows an example of a

pendant viewed using this method. Calcium carbonate appears white and darkens with

increasing magnesium and silica. Features such as voids, some crystalline structures,

coatings and grain inclusions can also be viewed using compositional BSE (Figure 4.7

and 4.8). Voids show up as dark, black areas that can exhibit rounded, angular and linear

to sublinear shapes. Crystals are apparent as subhedral, euhedral and anhedral structures.

Silica appears amorphous while sepiolite can occur in either a fibrous or massive form.

Detrital grains have a rounded appearance. In contrast, grains incorporated directly from

the parent clast are angular. The physical relationships between carbonate, silica and clay

can also be seen with BSE and confirmed using EDS.

Pedogenic calcium carbonate

Calcium carbonate is the dominant pedogenic mineral found in all pendants examined

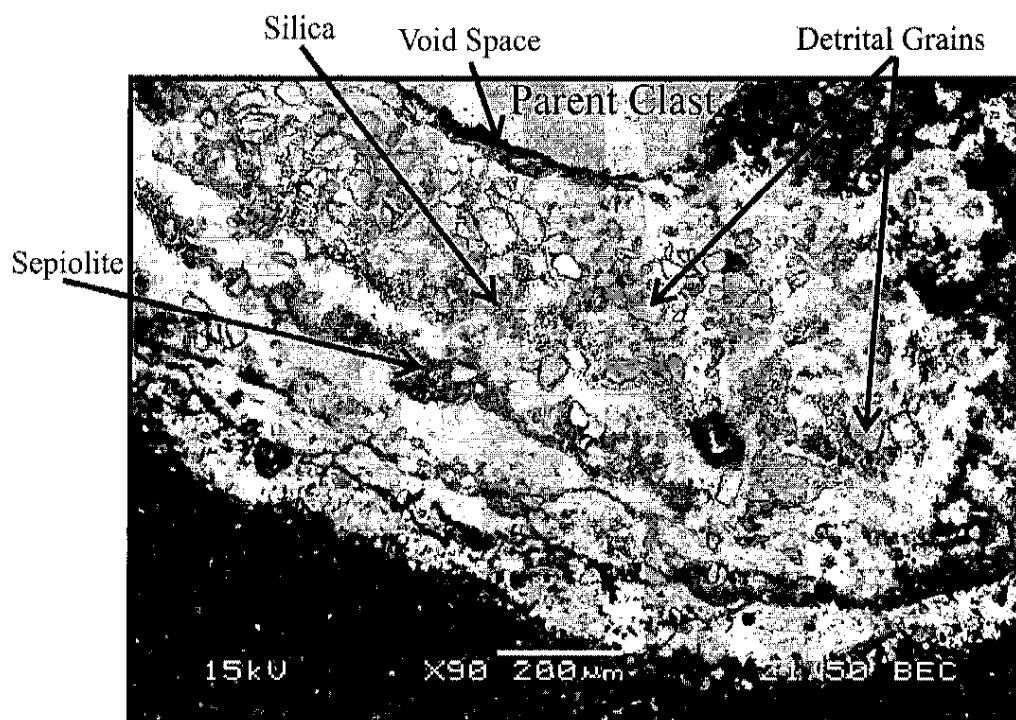in the study area. Carbonate material initially precipitates as a white powdery substance

Figure 4.7. BSE compositional image of a pendant from Q2$_v$ BLM (12-40) cm. This image illustrates common features associated with pendants found in the study area.
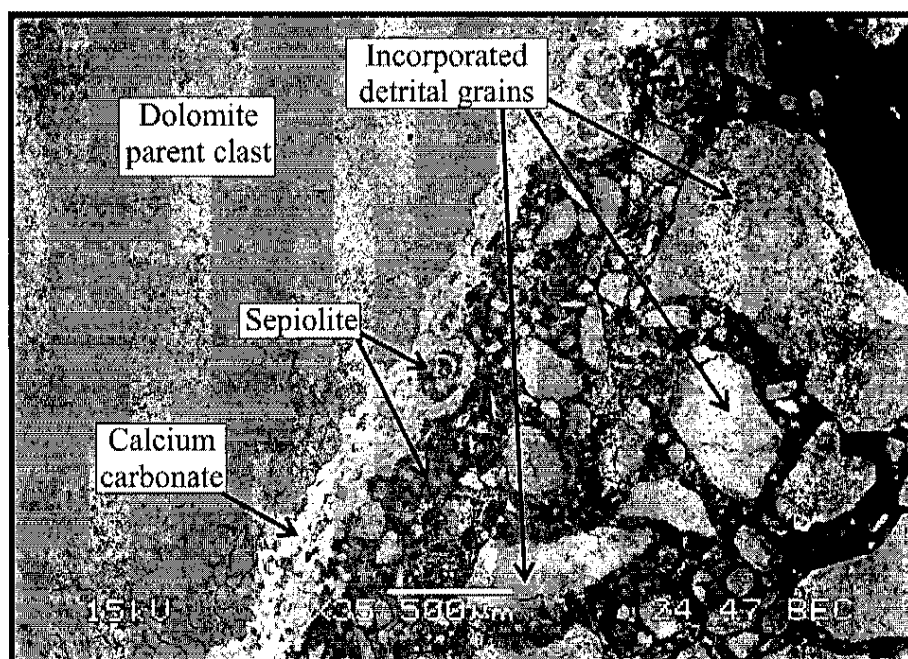

Figure 4.8. BSE compositional image showing pendant from Q2$_v$BLM 40-51 cm. This image also shows common features associated with pendants of the study area.

that coats clast bottoms and increase in thickness from the Q4 to Q1 profiles and with profile depth. When viewed at greater magnification, the powdery material is crystalline and appears to radiate in cavities and cover grains (Figure 4.9).

Diverse chemical characteristics are seen in the calcium carbonate of Pahranagat Valley soil pendants. The amount of calcium carbonate contained in pendants fluctuates with depth in all soil profiles that were sampled. Point counts for carbonate range from 4% to 73%. Greater concentrations of carbonate are seen in samples from Q3-Q5 landforms (38-73%). Pendants from Q1 and Q2 landforms contain lower amounts of carbonate compared to younger samples. EDS analyses indicates pure carbonate exhibits high peaks of calcium, oxygen and carbon. The pedogenic calcite has a variety of crystal habits ranging from massive and anhedral to subhedral crystals (Figures 4.10 and 4.11). Massive carbonate (as seen in thin section) is the dominant form of carbonate found in these pendants. In addition, there are pendants with areas of pure laminar carbonate. However, pendants containing carbonate laminae are not exclusively composed of these layers. The most common laminas consist of subhedral microsparite crystals radiating downward, and in some cases have new laminas adjacent below them. Microsparite crystals (4-50μm) are also seen radiating around grains and in voids between large rounded (transported) grains and pieces of rounded carbonate. Lamina are on average 20μm in thickness and are generally the largest crystalline material found in all pedants examined in this study. Lamina are commonly separated by small voids created from crystalline contacts and may contain linear accumulations of silicate clays (Figure 4.7). Silica lamina are present but rare.
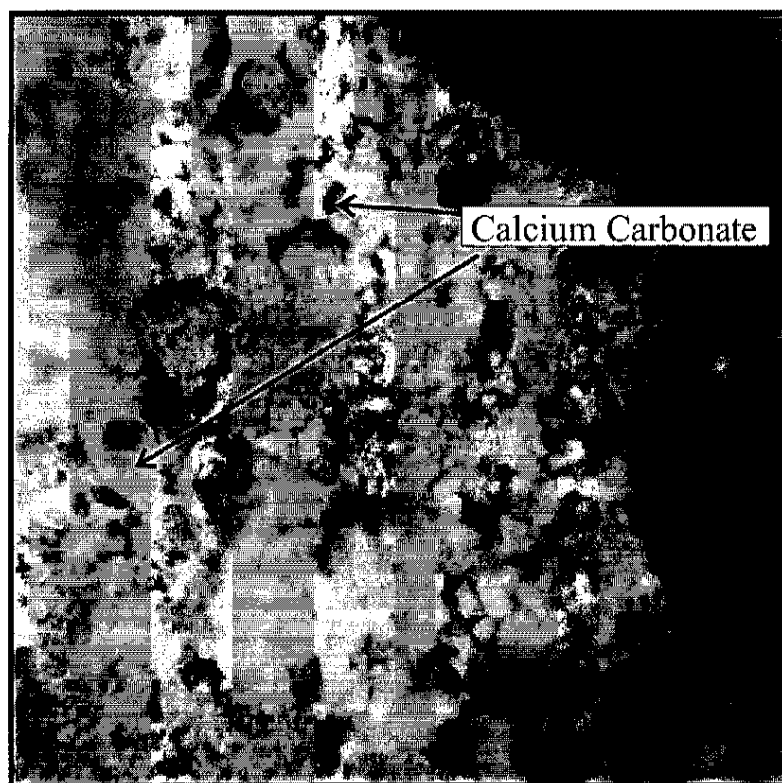
Figure 4.9a. White, crystalline calcite found on the underside of Q3_D Mystery (70-90) cm filling pits and depressions. Field of view is 2mm.
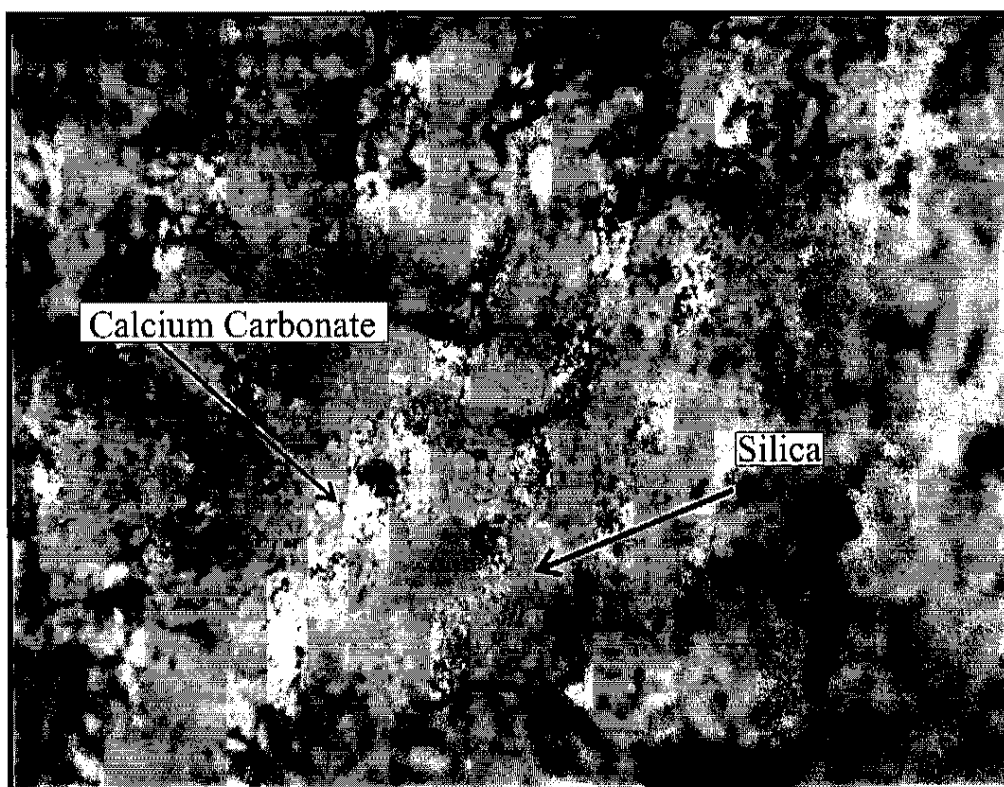

Figure 4.9b. Yellow silica patches on the underside of a pendant pulled from Q2_v BLM (12-40) cm. Field of view is 1.5 cm.
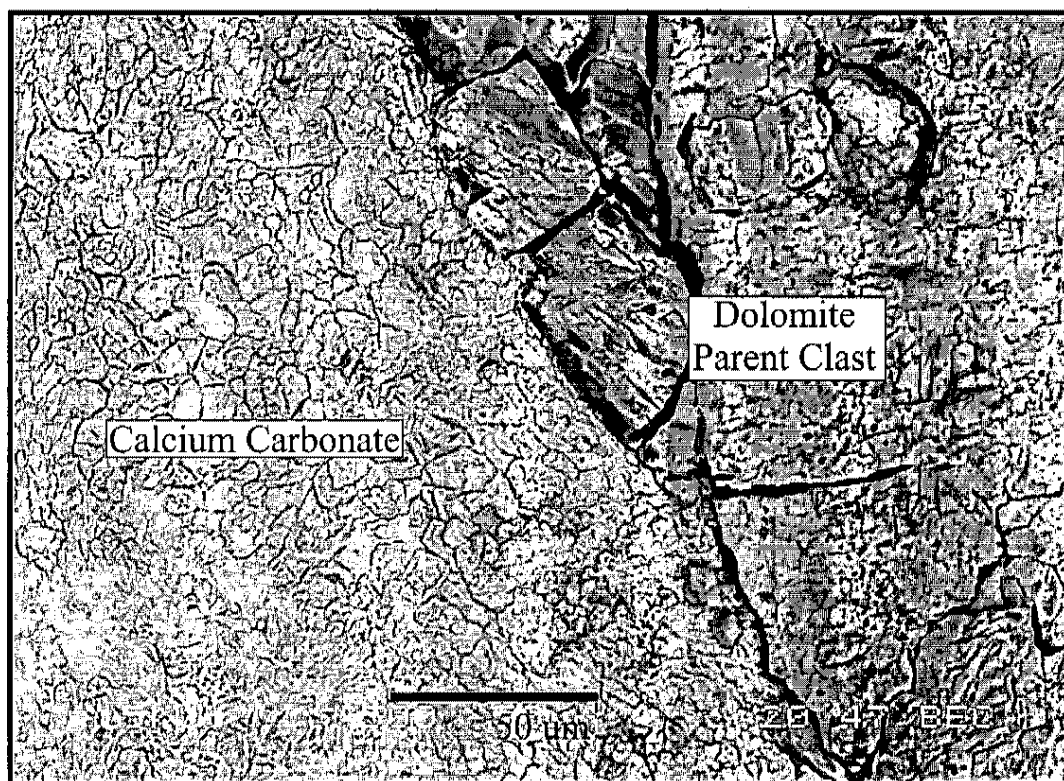
Figure 4.10. Massive carbonate adjacent to parent clast. Image from Q1$_D$ Backhoe (57-65) cm.
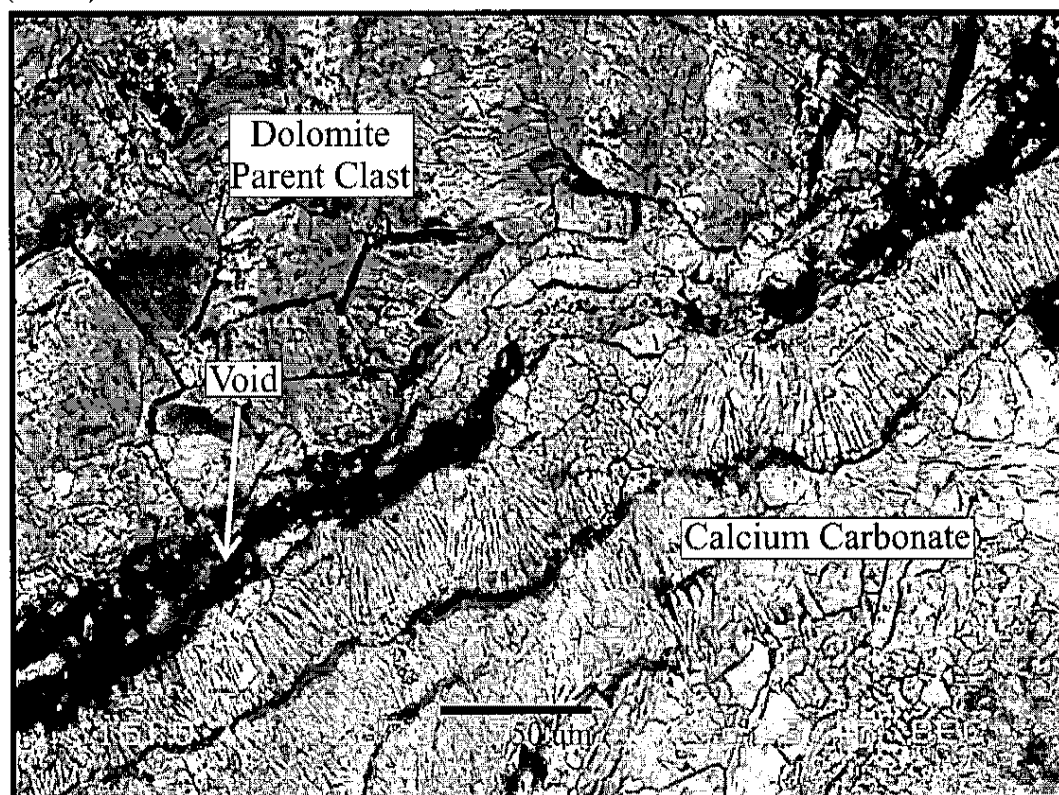

Figure 4.11. BSE image of lamina subhedral calcite radiating adjacent to clast contact from Q3$_D$ Mystery (11-38) cm.

Secondary silica accumulations

Silica is present as yellow, patchy material partially coating the pendant terminus (Figure 4.9). Silica accumulation also appears to increase from Q4 to Q1 and is more common in the BLM fan landforms. Silica was identified in eight of the samples in 3 forms: (1) as rare lamina between adjacent carbonate lamina, (2) on the pendant terminus of one sample and (3) as a coating on incorporated grains. XRD analyses confirmed amorphous silica in two of the eight samples.

Lamina composed of pure silica are rare, and can only be found in three of the 25 samples. They are found in the interiors of pendants and as outer coatings at the pendant terminus (Figures 4.7 and 4.12). Silicious lamina are not continuous across the length of the pendant and vary in thickness. Lamina with pure silica composition are also found alternating with lamina of calcium carbonate, sepiolite and other silicate clays. Silica coatings on pendant termini are only found in the Q3 Last profile. The surface areas of grains incorporated into the pendant matrix from loose soil or by clast inclusions are other areas where silica can be present. Silica coatings surrounding grains are closely associated with grain dissolution and in these conditions, may be closely related (spatially and chemically) to the accumulation of sepiolite (Figure 4.13).

Sepiolite

A variety of clay minerals in pendants were identified using XRD (Figure 4.2). The identified minerals include: kaolinite, montmorillonite, illite, chlorite-montmorillonite, palygorskite and sepiolite. Sepiolite is the only clay mineral present that can be identified using SEM and EDS. Sepiolite has strong peaks of silica and magnesium, with variable concentrations of calcite, depending on the carbonate-sepiolite relationships (Figure
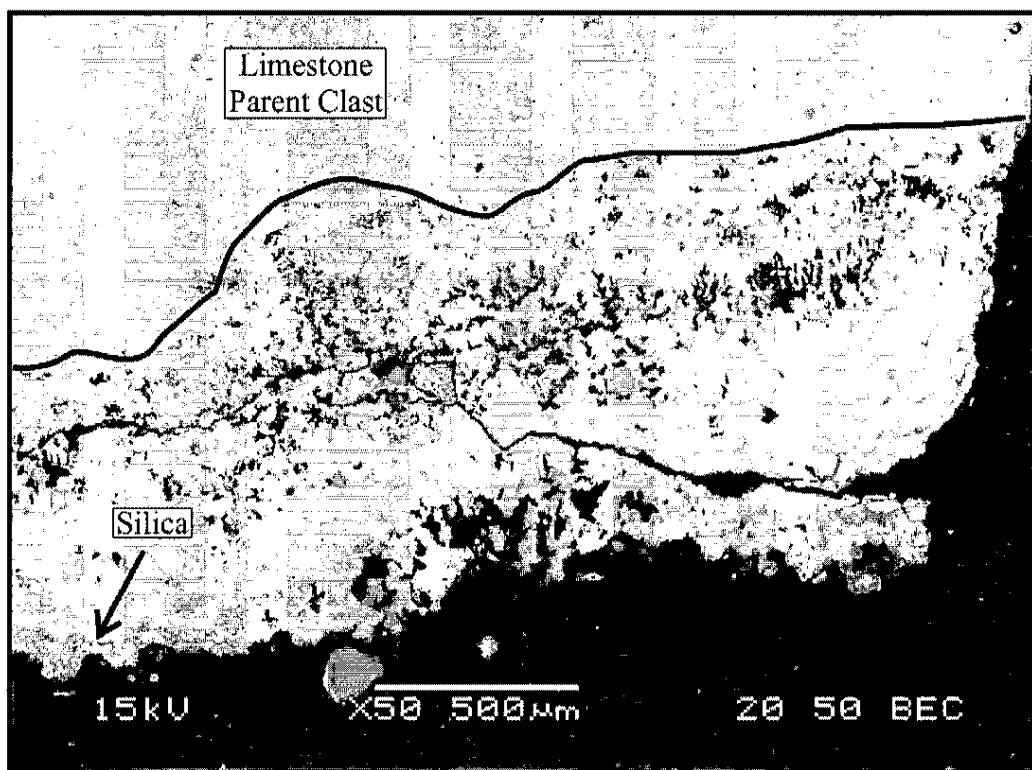
Figure 4.12. Pendant from Q3$_v$ Last (22-68) cm with silica lamina near terminus. Note that parent clast is of limestone composition. Black solid line is approximate area of clast-pendant contact.
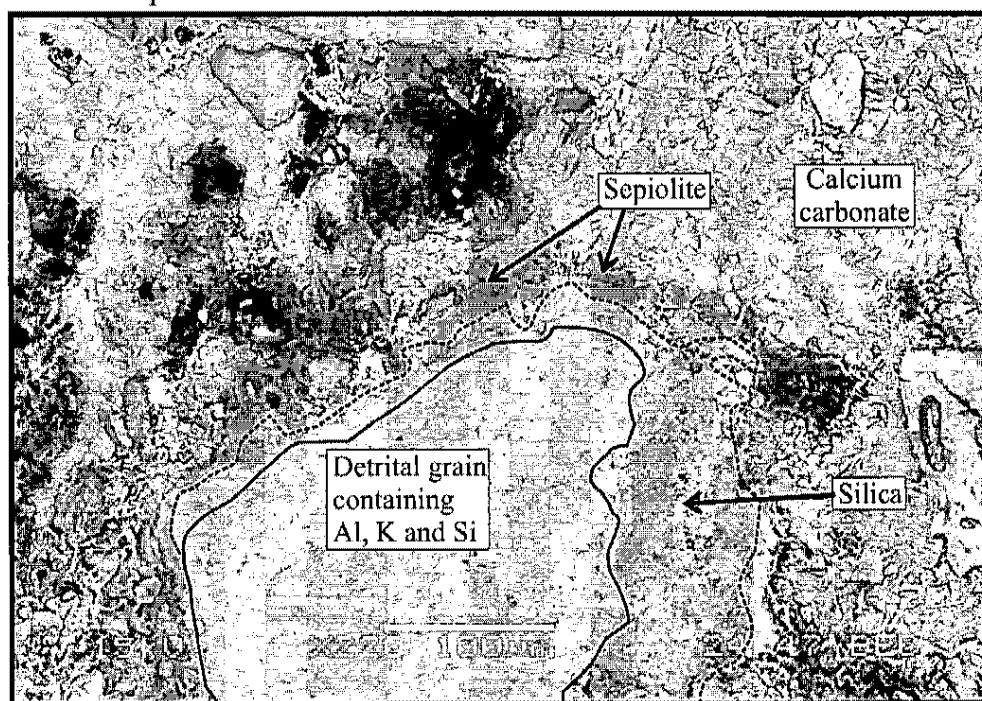

Figure 4.13. Image from Q2$_v$ BLM 70-90 cm showing the common relationships seen between silica and sepiolite in the pendants of the study area. Solid black line shows border of grain and silica. Dotted black line shows contact between silica and sepiolite.

4.14). Sepiolite occurrence is greatest in Q1 and Q2 landforms and some significant amounts of sepiolite are found in the Q3, Mystery and Last pit profiles.

Sepiolite occurs as large masses and more commonly as bands alternating with calcium carbonate (Figures 4.15-4.17). Three samples showed calcium carbonate appearing to be consumed by sepiolite. These areas are present where carbonate with only Ca, C, and O peaks (EDS data) exhibits a visual and chemical transformation into sepiolite (Mg, Si). Figures 4.18-4.22 show a calcium carbonate mass surrounded by material that exhibits EDS peaks of nearly equal Mg, Si, and $CaCO_3$. This transitional material loses calcium and grades into pure sepiolite. This apparent transformation process is seen in three of the 25 samples from Q1 and Q2 landforms.

Distinct sepiolite fibers are not observed in any of the samples probably because of polishing of the thin sections. There are a small number of samples where sepiolite appears to form tunnel-like structures that fill voids and coat grains (Figures 4.23 and 4.24). Circular forms with diameters of approximately 4-5μm are found in layers of sepiolite that alternate between carbonate and may also be a profile view of these fibers. One occurrence of palygorskite (identified with XRD) is found in the Q2 Merkler profile at 12-40 cm but was not be identified using SEM methods.

Soil Pellet Features

Pellets present in the Q1$_D$ Backhoe and Q2$_D$ Merkler profiles were found loosely attached to pendant termini. These features are present in Q1 and Q2 landforms found directly above a stage IV laminar cap. Pellets from these landforms are composed of rounded pieces of carbonate, and rounded detrital grains that were enveloped by sepiolite clay and range in size from 250 μm to 1mm (Figures 4.25-4.27). In thin section,
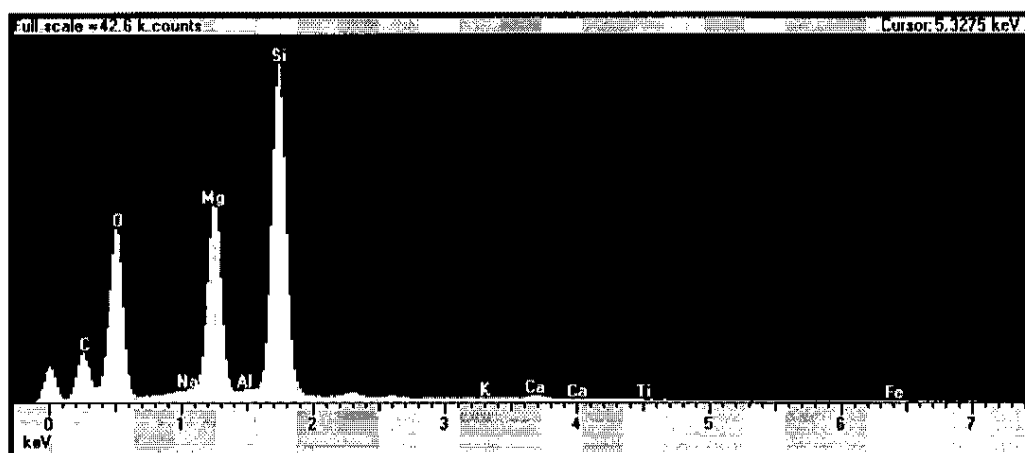
Figure 4.14. Typical EDS peaks associated with the clay mineral sepiolite. Note C peak from carbon coating.
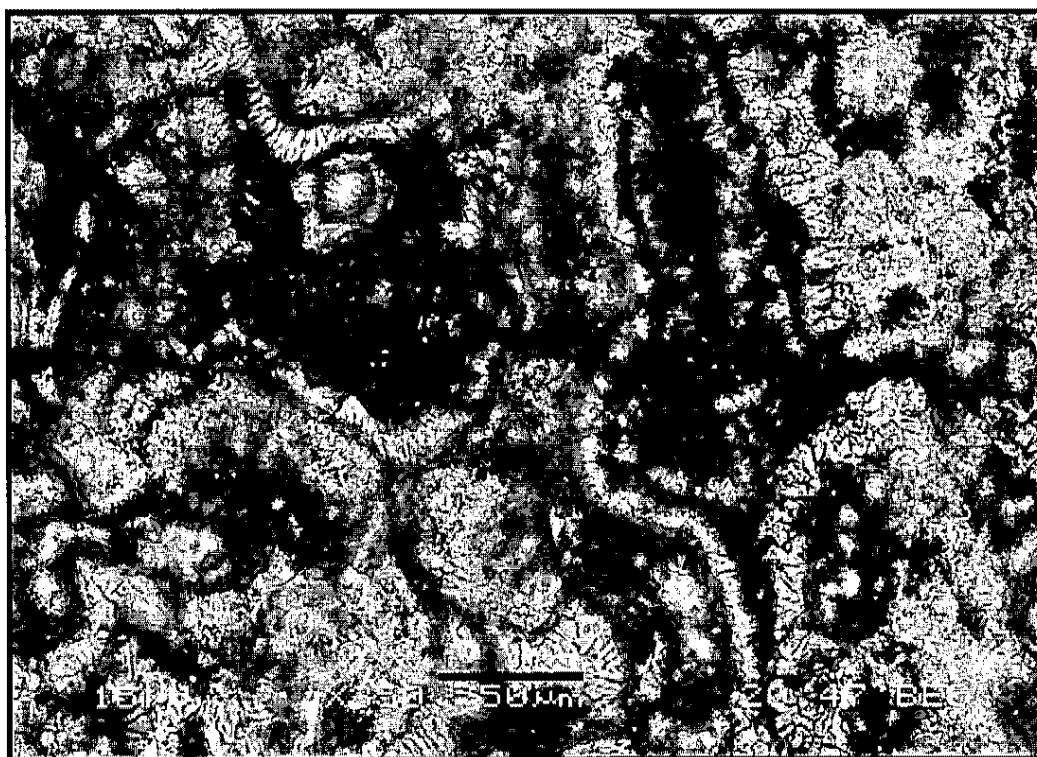
Figure 4.15. Banded sepiolite and carbonate from pendant from $Q1_D$ Backhoe (13-33) cm. The carbonate is white, sepiolite is dark gray and voids are black.
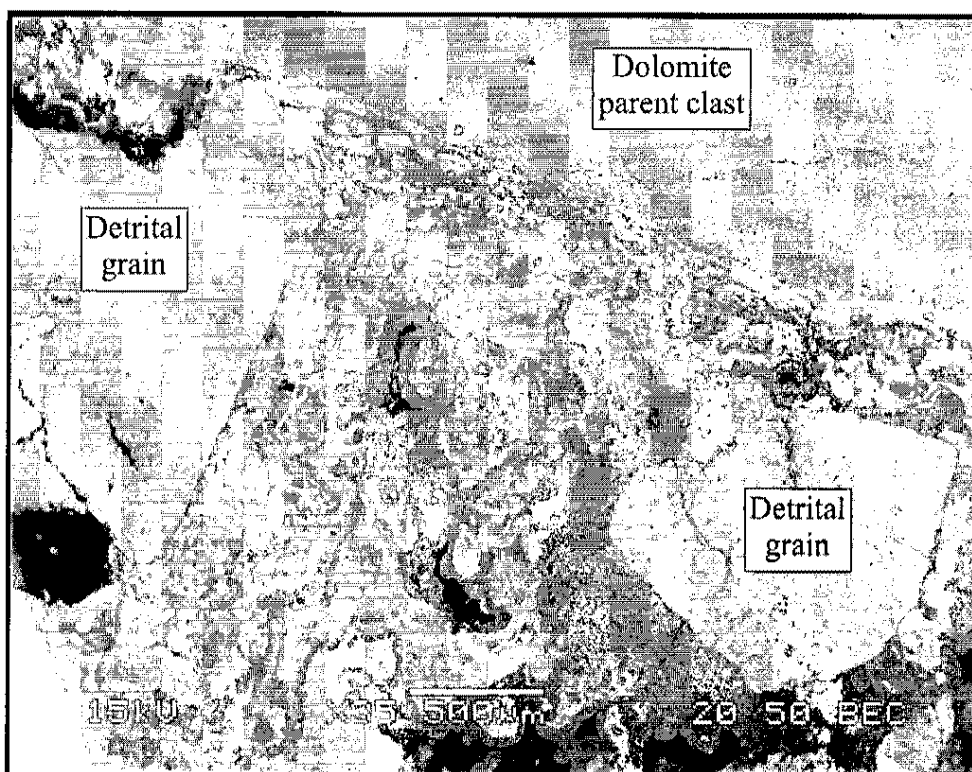
Figure 4.16. Pendant from Q2V BLM 40-51 cm showing calcium carbonate (white) with bands of sepiolite (dark gray).
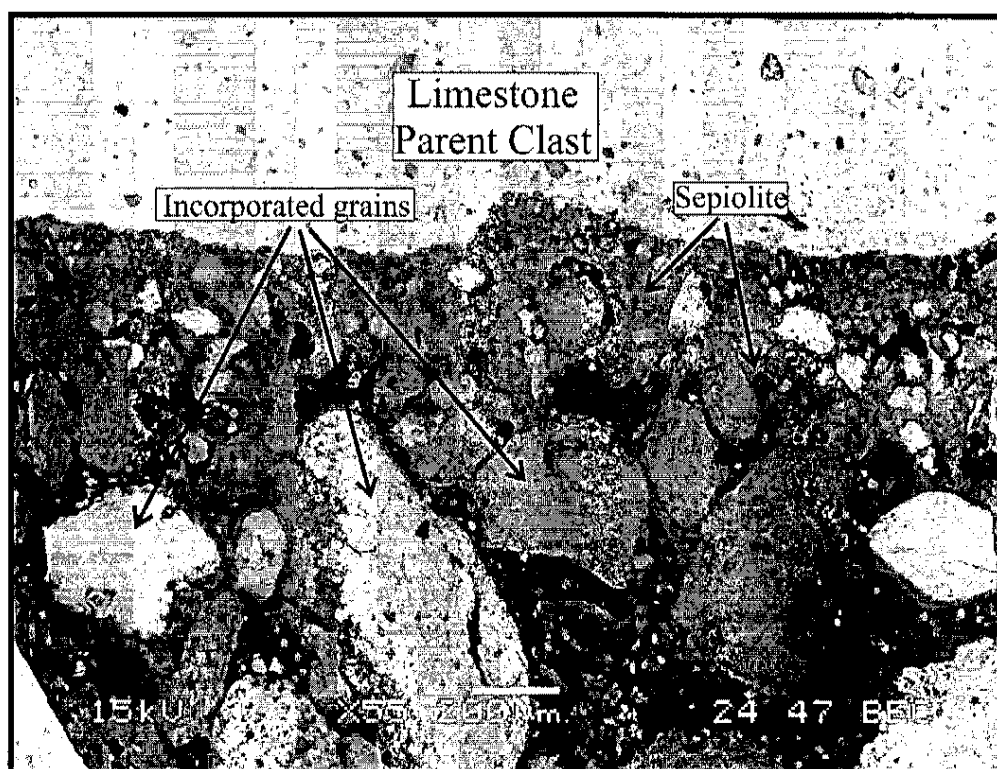
Figure 4.17. Pendant of Q1$_D$ Backhoe (82+). Large rounded detrital grains and chunks of rounded carbonate floating in a sea of sepiolite.
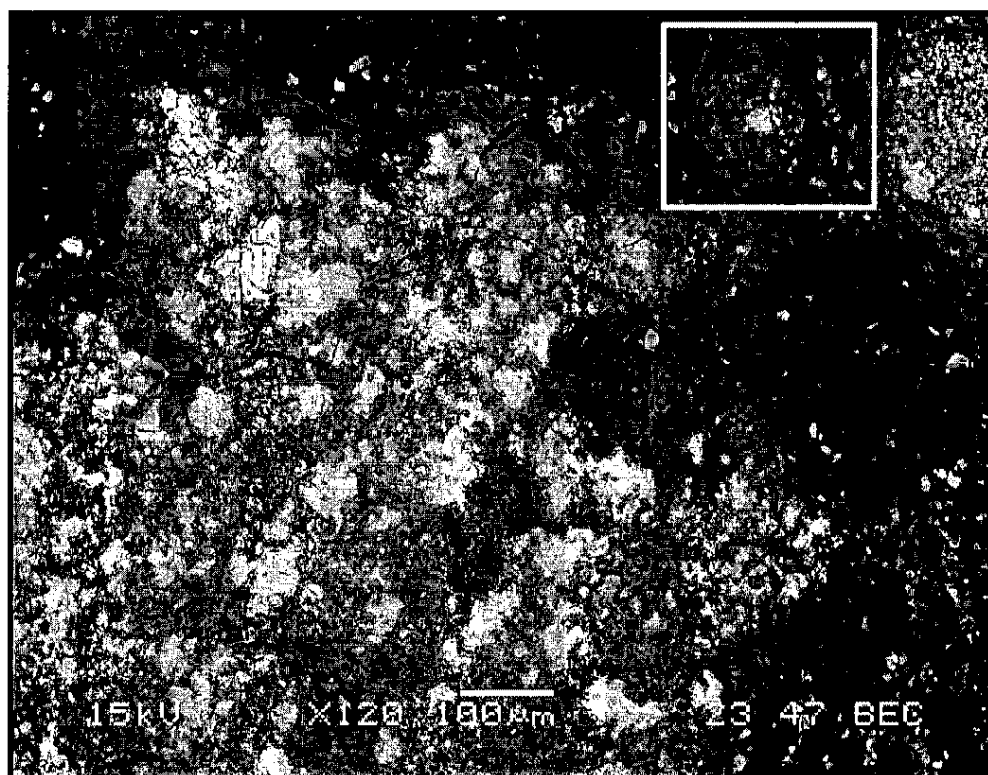
Figure 4.18. Sepiolite occurs with carbonate in a pendant of $Q1_D$ Backhoe (65-82 cm). A close up of the white box is shown in figure 4.19.
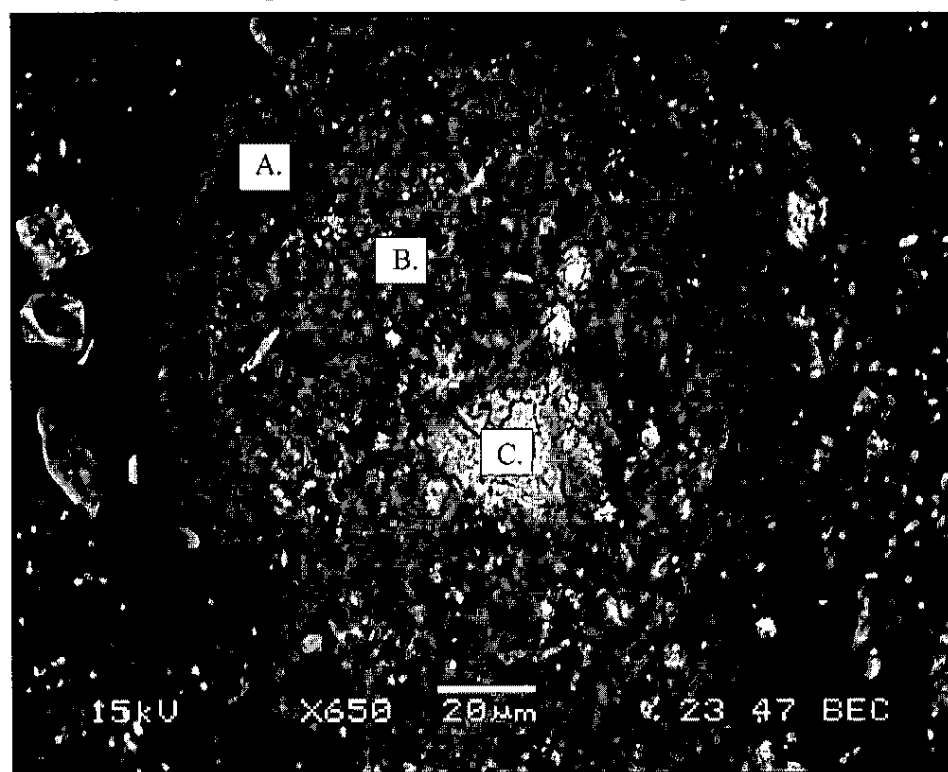
Figure 4.19. Area from 4.18 showing transformation of carbonate into sepiolite. Boxes A-C are areas analyzed by EDS and shown in figures 4.20, 4.21 and 4.22. From $Q1_D$ Backhoe 65-82 cm. (A) is pure sepiolite, (B) has composition of carbonate and sepiolite and (C) is pure carbonate.
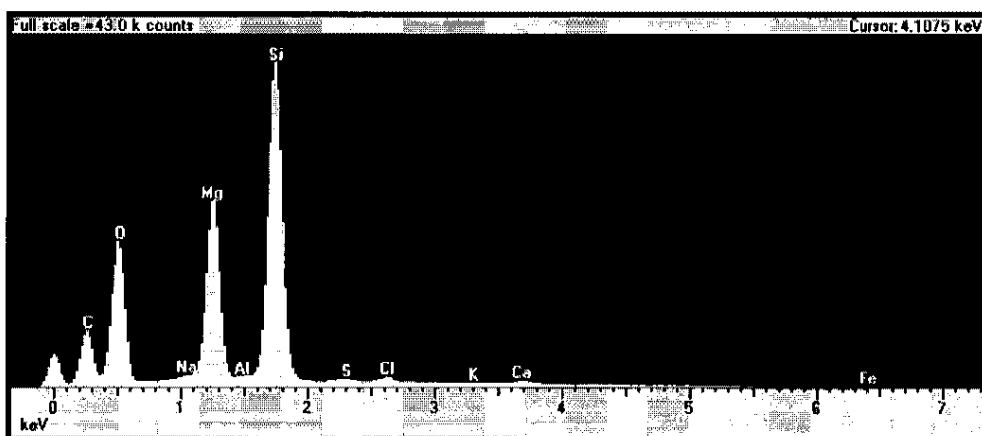
Figure 4.20. EDS of box A from figure 4.19.
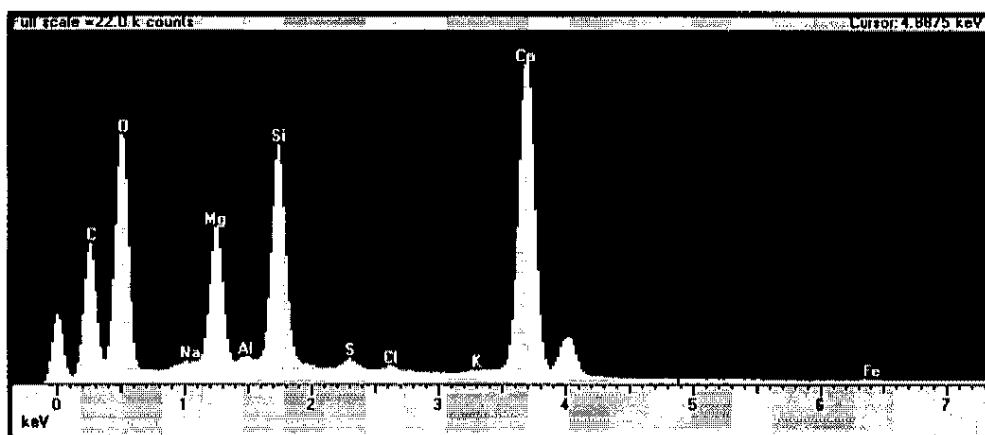
Figure 4.21. EDS of box B from figure 4.19.
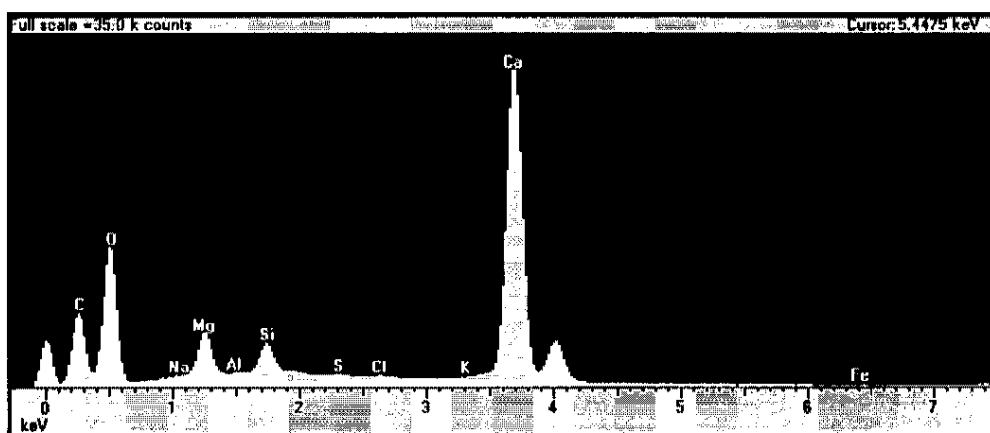
Figure 4.22. EDS of box C from figure 4.19.
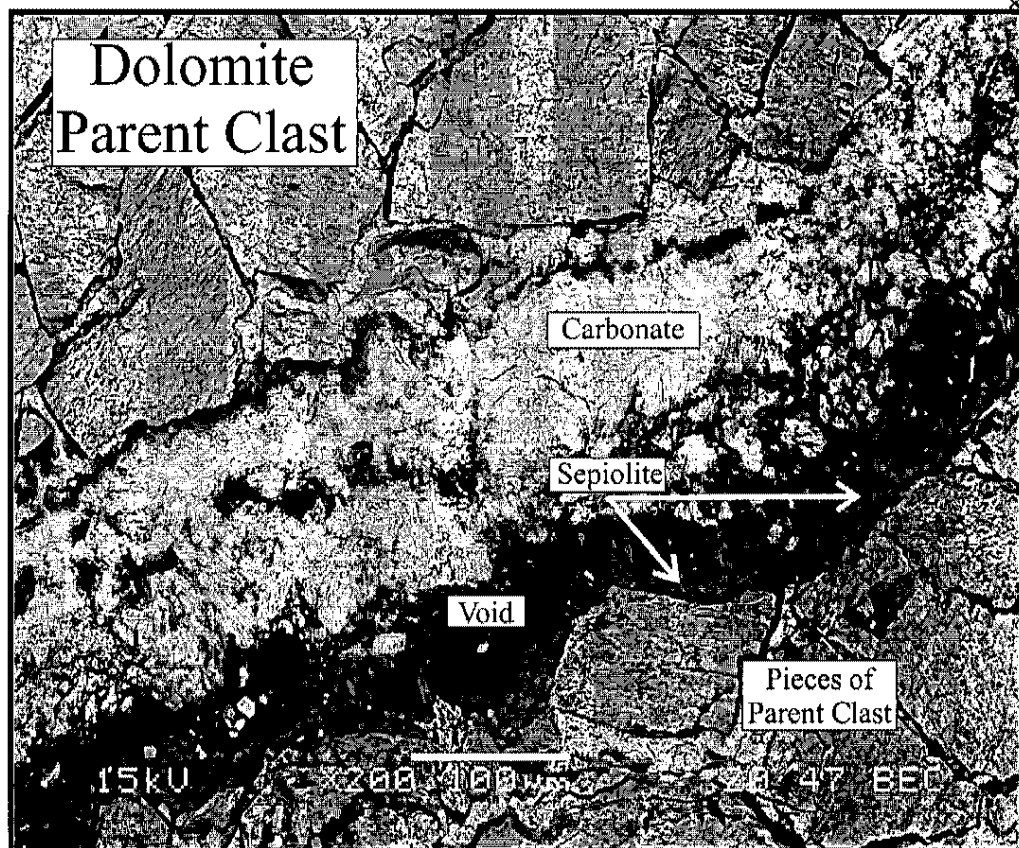
Figure 4.23. BSE image of pendant from Q1$_D$ Backhoe 57-65 cm showing void space with sepiolite and carbonate filling void at clast-pendant contact. Also shown are pieces of parent clast material that has been separated from the clast.
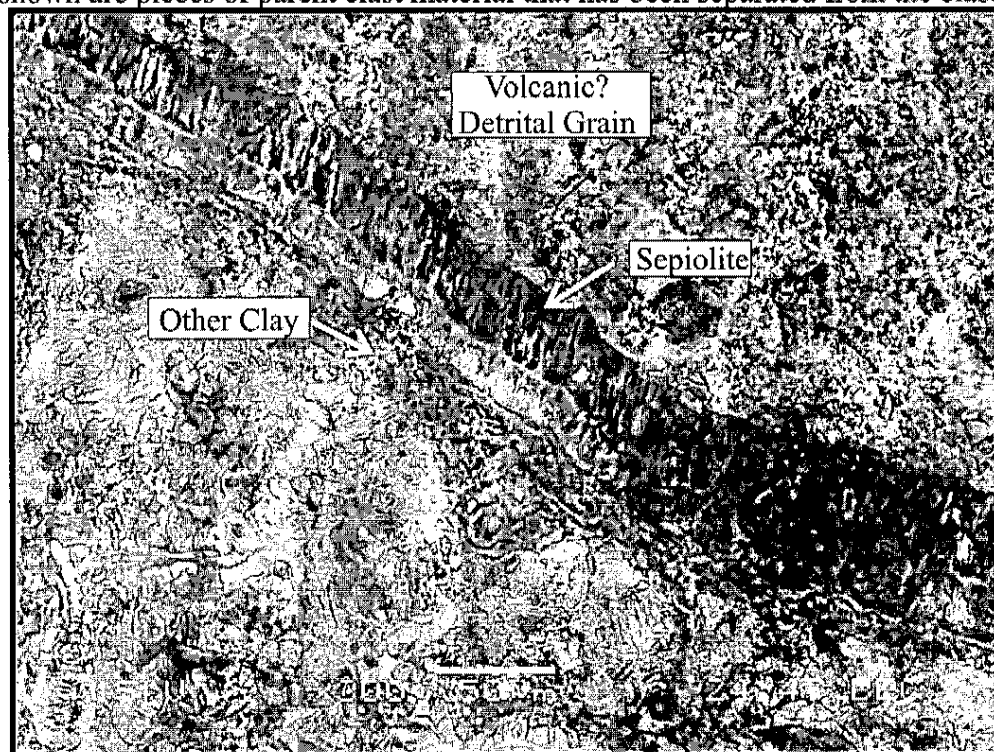
Figure 4.24. Fibrous sepiolite radiating from rounded detrital grain. This image was taken of pendant from Q2$_V$ BLM 51-70 cm.
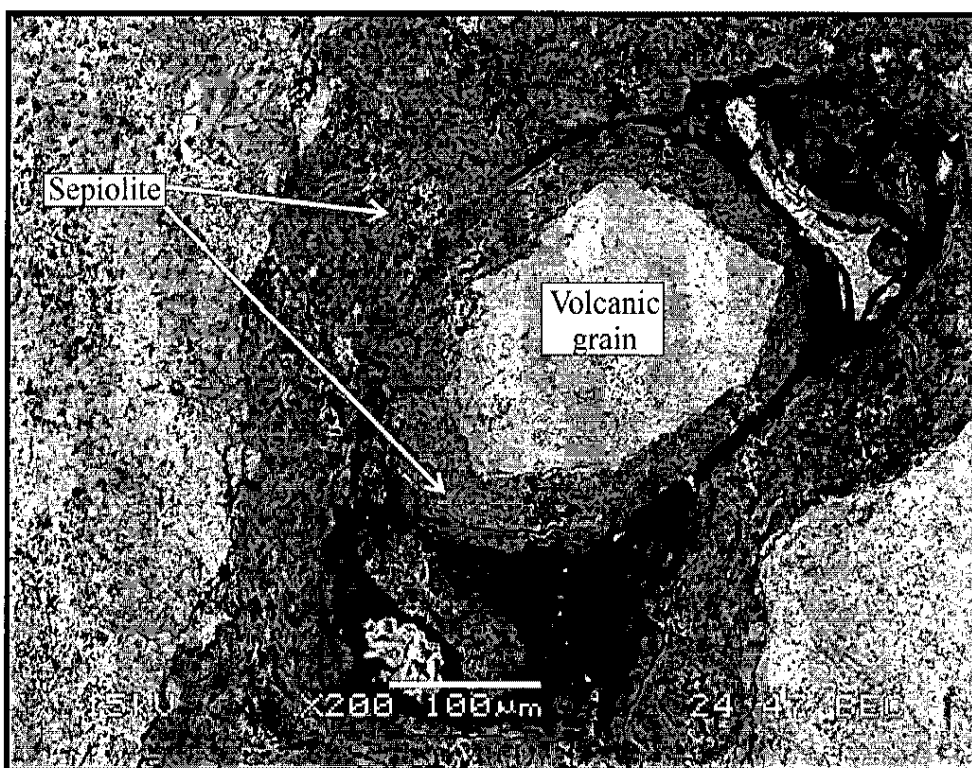
Figure 4.25. Sepiolite encompassing a volcanic grain within a pendant.
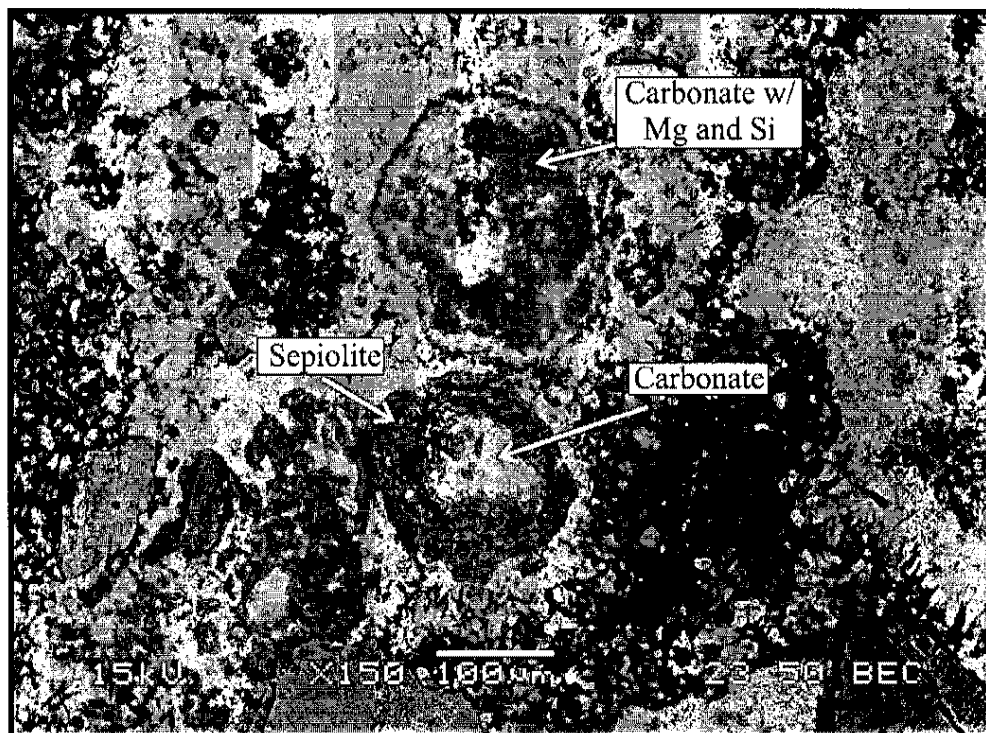
Figure 4.26. Rounded sepiolite features in carbonate matrix. The above feature has carbonate with high Si and Mg and lower feature has pure sepiolite encompassing a rounded piece of carbonate.

Figure 4.27. Pendant from Q2V BLM 40-51 cm showing carbonate near parent clast and sepiolite in a circular form.
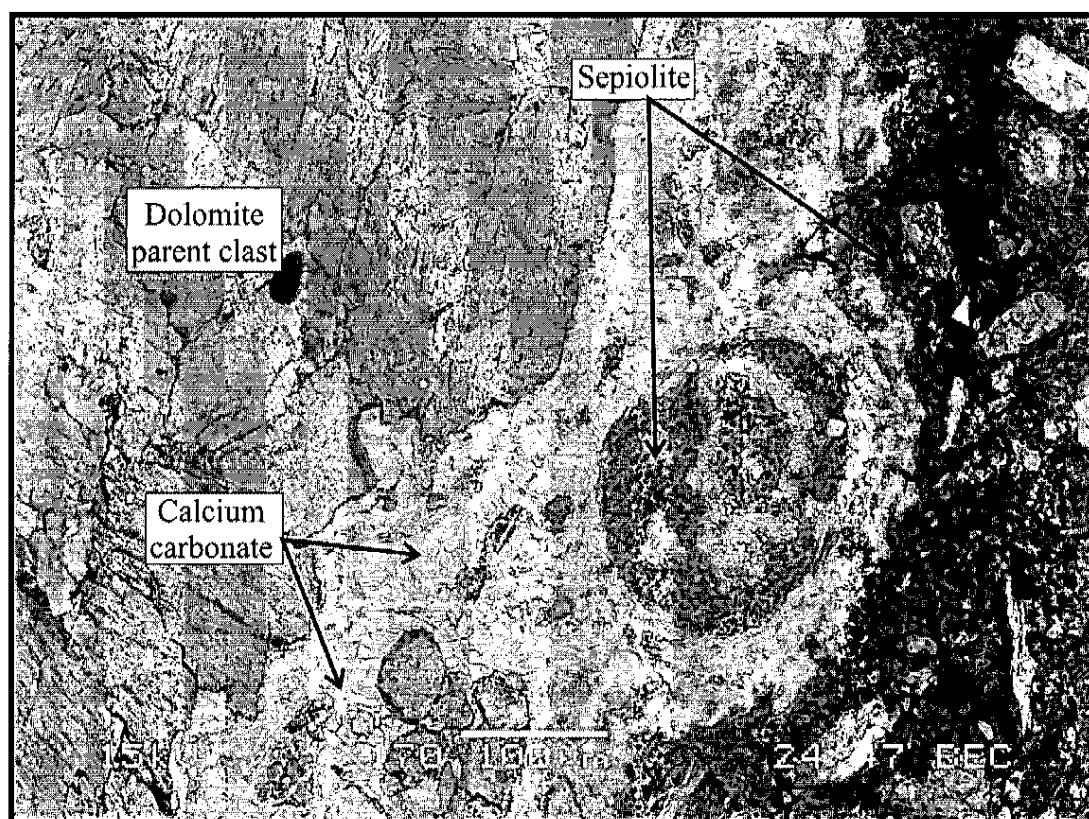
pellets have an ovate or egg shaped appearance. Pellet-like features were found in

pendants and at the pendant terminus of eight samples. These features were only found

in the thin sections of pendants from the Q1 and Q2 landforms. Five out of the five

horizons sampled from Q1$_D$ Backhoe profile contained these features. Two out of three of

the Q2$_D$ Merkler and 1 out of 6 of Q2$_V$ BLM profiles also contained pellet-like features.

Other amorphous materials

Other clays mentioned in the previous segment are found in pendants of the study area

but not to the extent and abundance of sepiolite. Some materials found within pendants

(especially those of the Q3 and younger landforms) display EDS peaks containing Si,

Mg, and Al with minor traces of Fe and K (Figure 4.28). A small sulfur peak is found co-

occurring with other materials in 16 of the 25 samples. These accumulations occur in the

pendant and on the pendant terminus (Figure 4.29 and 4.30). Because of the inability to

associate this set of peaks to exact mineral names, they are all referred to as other clays or

other amorphous precipitates. XRD analyses were conducted on representatives of all

profiles except for Q3 Last and Q4 Glass. Q4 Glass pit coatings were too thin to obtain

enough sample for analysis. Illite is the second most abundant clay mineral (behind

sepiolite) identified through XRD and can be found in 3 out of 10 samples. Kaolinite is

present in pendants from the 55-72 cm horizon of Q2 BLM pit and the 73-100 cm

horizon of Q3 Mystery. Montmorillonite and mixed clay chlorite-montmorillonite are

also found. Pure montmorillonite is found in the 29+ horizon of Q1 Silica pit and the

40-51cm and 70-90 cm horizons of Q2 BLM pit. The mixed clay occurs once in Q3

Mystery at 73-100 cm. Minerals other than carbonate, silica and clay were identified
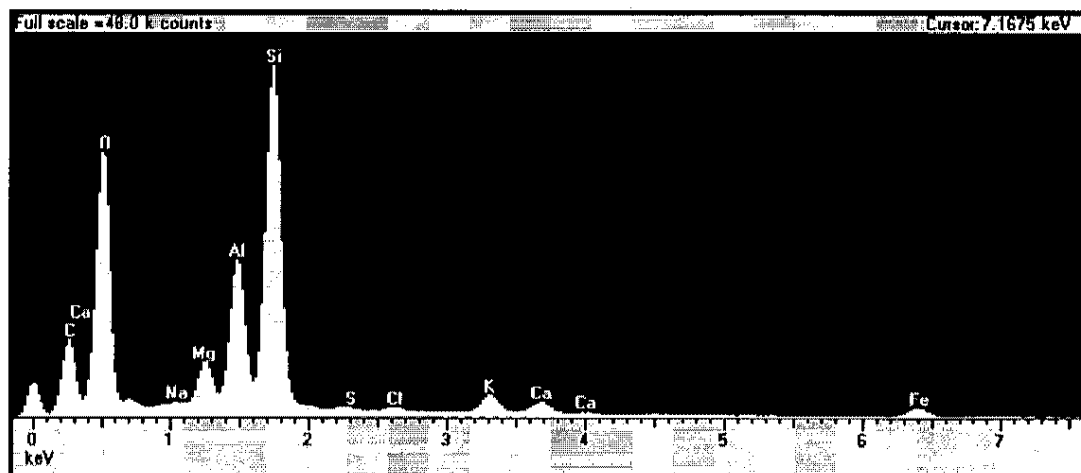
Figure 4.28. EDS peaks of "other clay" mineral. Note the peaks of potassium, iron, and aluminum with little magnesium.
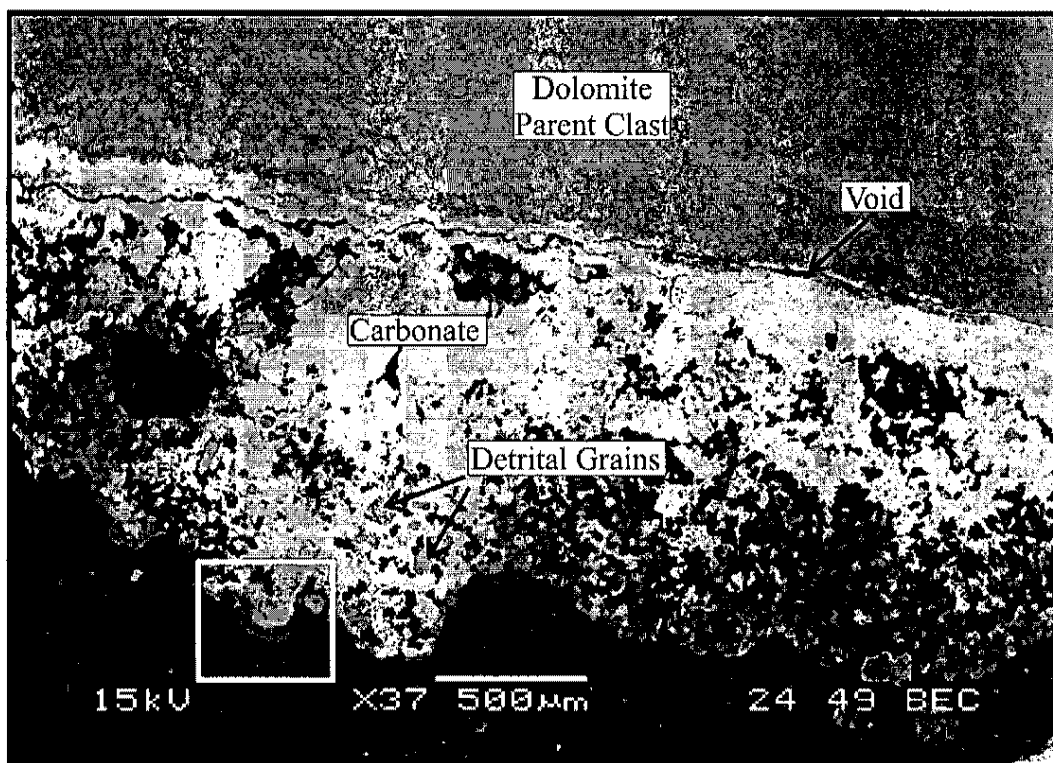
Figure 4.29. BSE image of pendant from Q3$_D$ Mystery 0-11. Terminus of pendant has layer of "other clay". White box outlines area in figure 4.30.
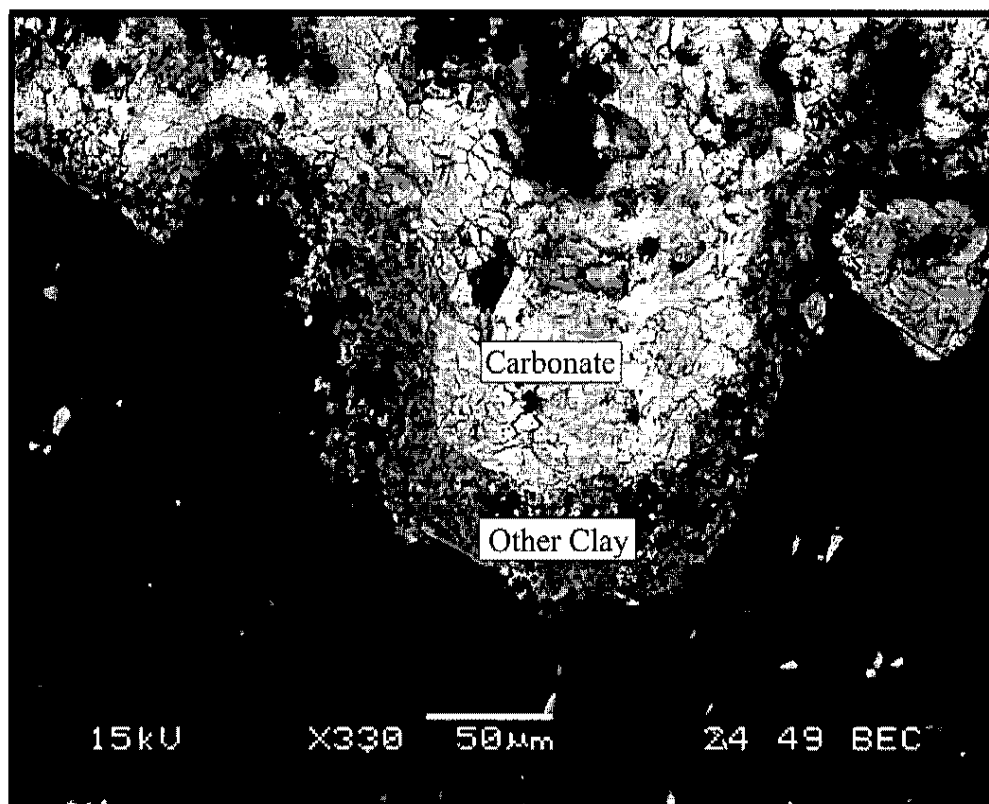
Figure 4.30. Closer view of area in white box of figure 4.29. Notice layer of other clay coating pendant terminus.

through EDS. These minerals were quartz, muscovite, orthoclase and dolomite, all

occurring as detrital grains or crystals and grains derived from the parent clast.

Pendant size

Pendant size is difficult to determine in the field and laboratory because of an

undulating pendant-clast contact and unknown angular or rounded features of the parent

clast. Thicknesses were measured from thin section at the thickest point from clast-

pendant contact to the pendant terminus. Pendants observed in this study range in size

from 1 to 17 mm at their thickest points (Figure 4.1). These measurements may not be

true indicators of pendant thickness due to the thickening and thinning of pendant

material. However, these measurements are assumed to represent the average thickness

of material coating the pendant. Some pendants appear to mimic the topography of the

clast and contain the thickest accumulation of material below the lowest part of the clast

(Figure 4.31).

Pendant-clast contact

Parent clast lithology was recorded using EDS. SEM analyses from thin sections

showed that 14 out of 25 samples were dolomite, 9 out of 25 were limestone and 2 out of

25 were volcanic (Figure 4.2). Volcanic parent material displayed several textures and

chemical compositions. Parent clasts of volcanic lithologies are dark, brittle and have

large fissures creating a rounded appearance to sections of the clast (Figure 4.32).

Limestone parent clasts appeared white or lighter in color (in BSE) because of their high

Ca content (Figures 4.12 and 4.17). The clasts composed of dolomite crystals were easy

to distinguish because of their dark gray appearance (in BSE) caused from increased

magnesium content (Figures 4.34, 4.37 and 4.38). EDS peaks for dolomite were strong
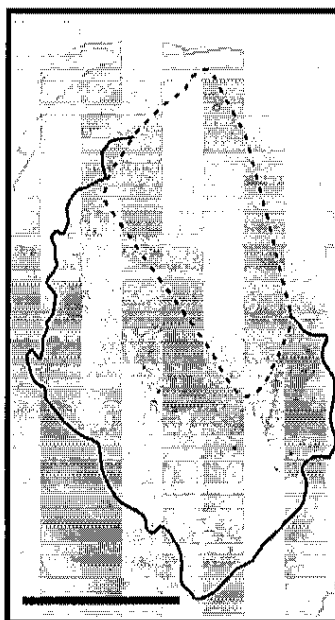
Figure 4.31. Scan of thin section made from $Q2_D$ Merkler 55-72 cm showing pendant mimicking the parent clast form. Parent clast is outlined in dotted line and pendant is outlined in solid line. Red color is from Azilarin-Red stain for carbonate. Bar length is 1.5 cm.
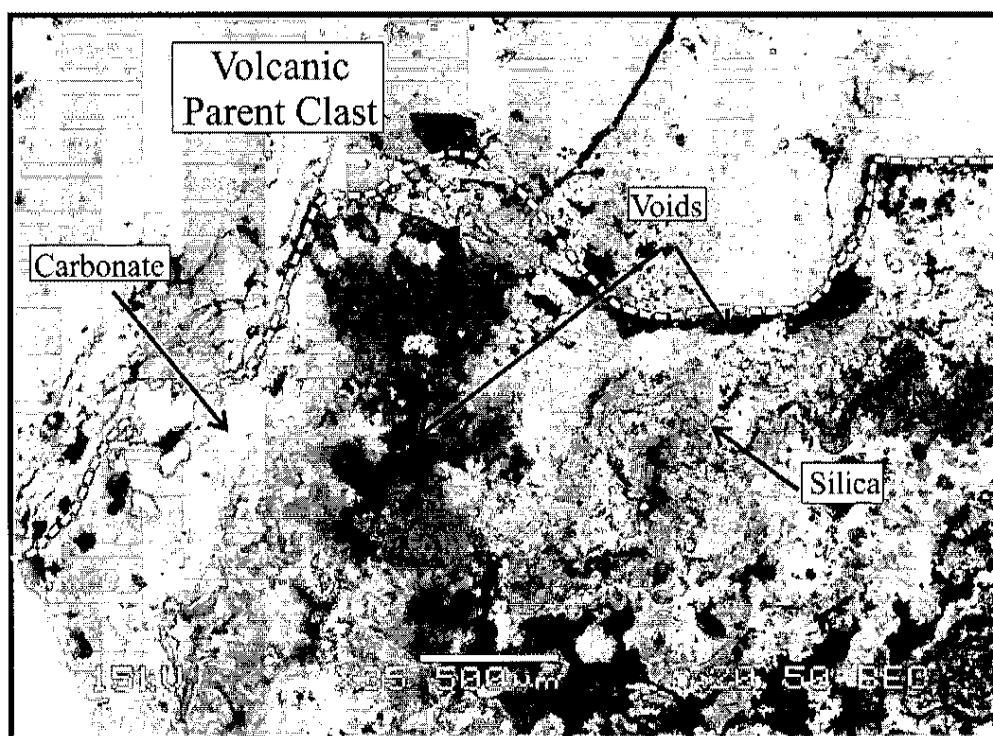
Figure 4.32. Volcanic pendant of $Q1_v$ Silica 29+. Notice rounded, broken appearance of parent clast. White dotted line is approximate location of parent-clast contact.
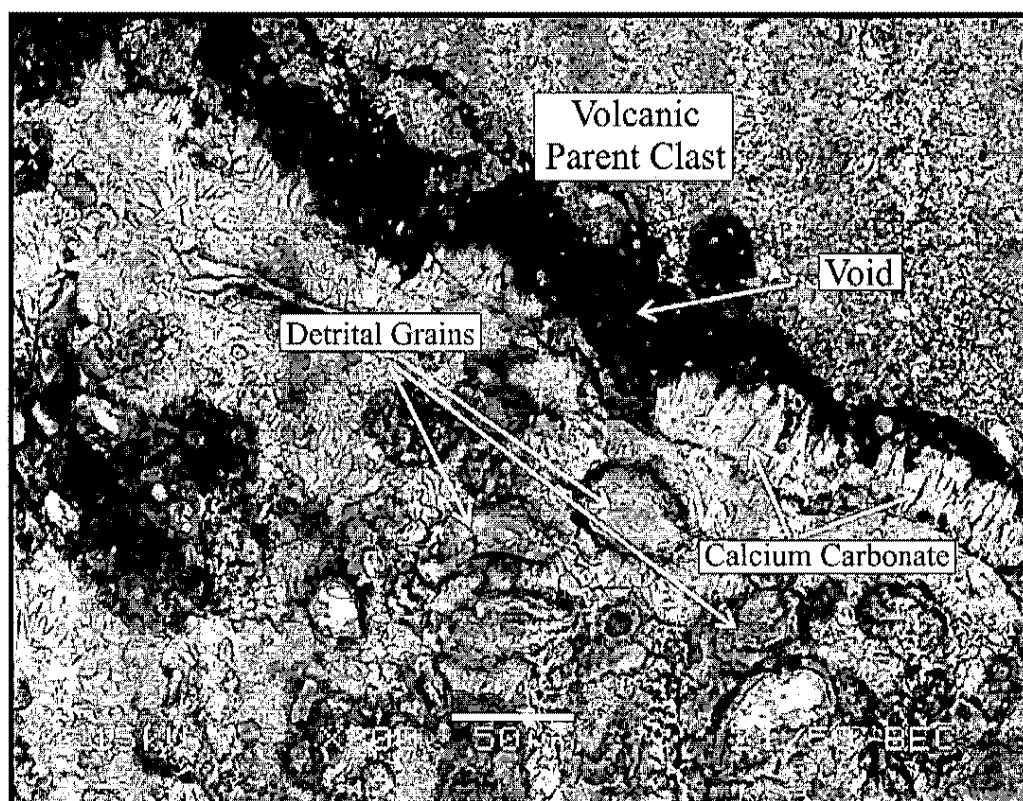
Figure 4.33. Pendant with linear void at clast-pendant contact. This image also shows dissolution of $CaCO_3$ within the void space. From $Q2_v$ BLM 12-40 cm.
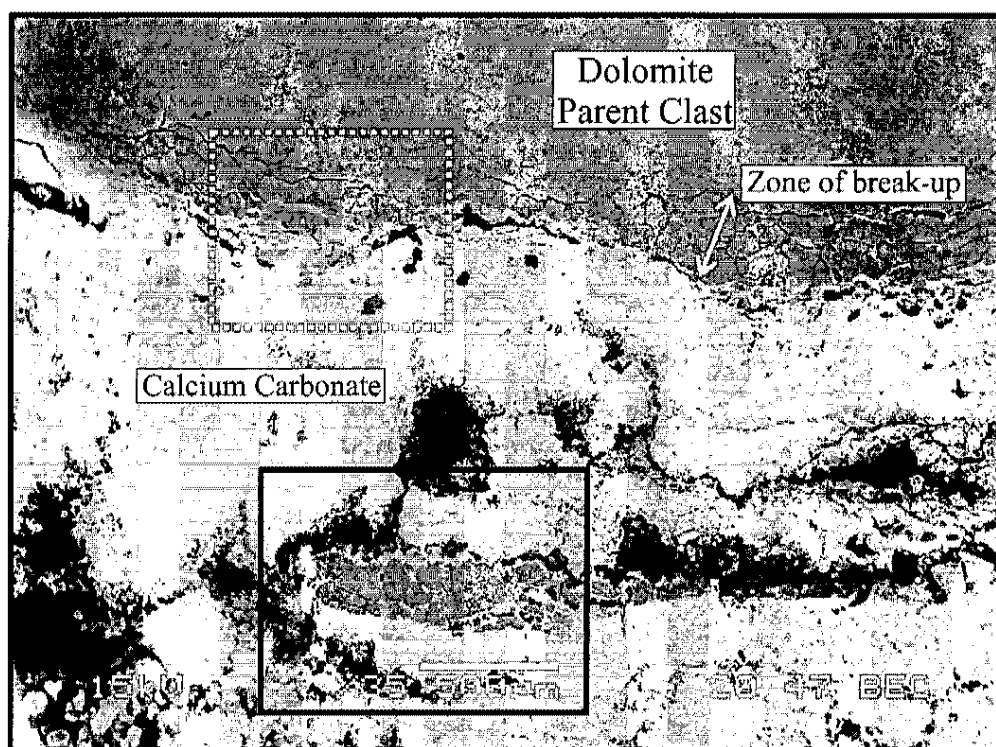
Figure 4.34. Pendant from Q1$_D$ Backhoe 57-65 cm showing zone of break-up and incorporation of parent clast material into pendant. White dotted box shows area covered in figure 4.35. Black box shows area covered in figure 4.36.
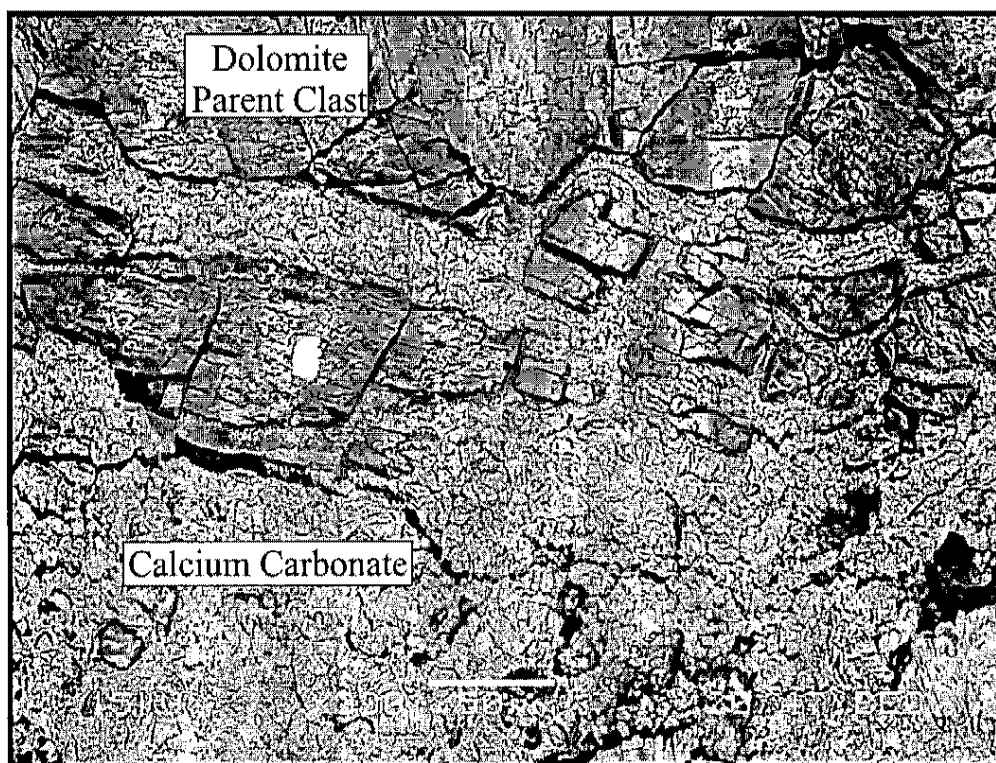
Figure 4.35. Area covered by white box in figure 4.34. Image shows incorporation of parent clast grains into carbonate matrix at clast-pendant contact.
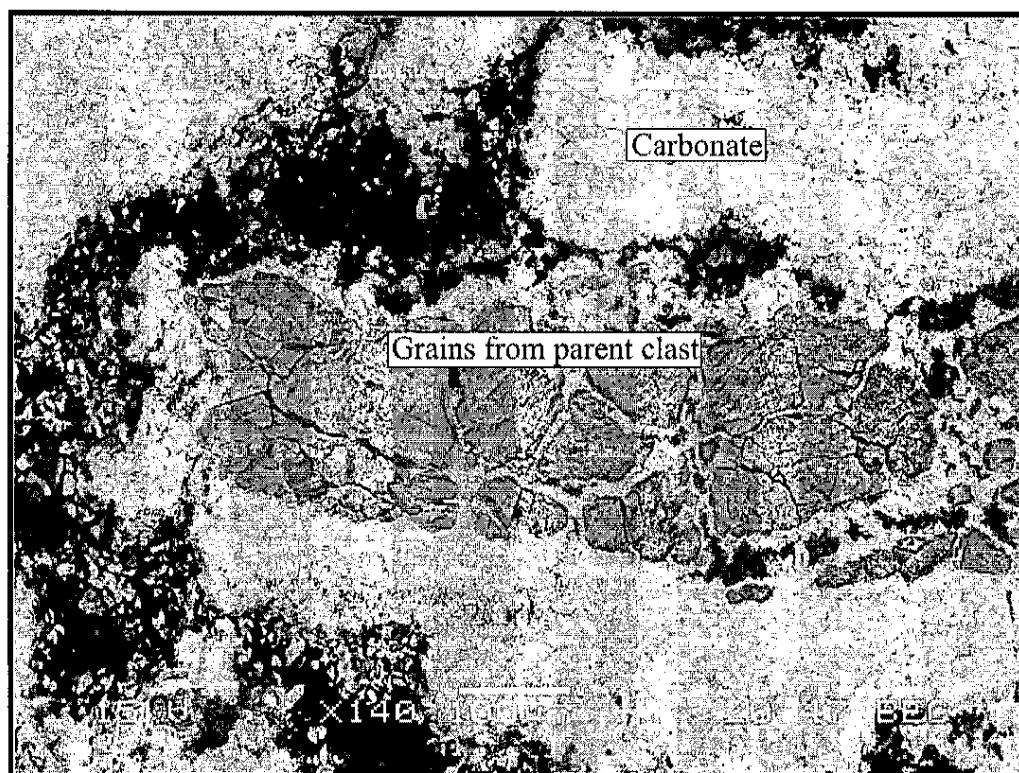
Figure 4.36. Area covered by black box in figure 4.34. Image shows incorporated parent clast grains into carbonate matrix with evidence of displacement.
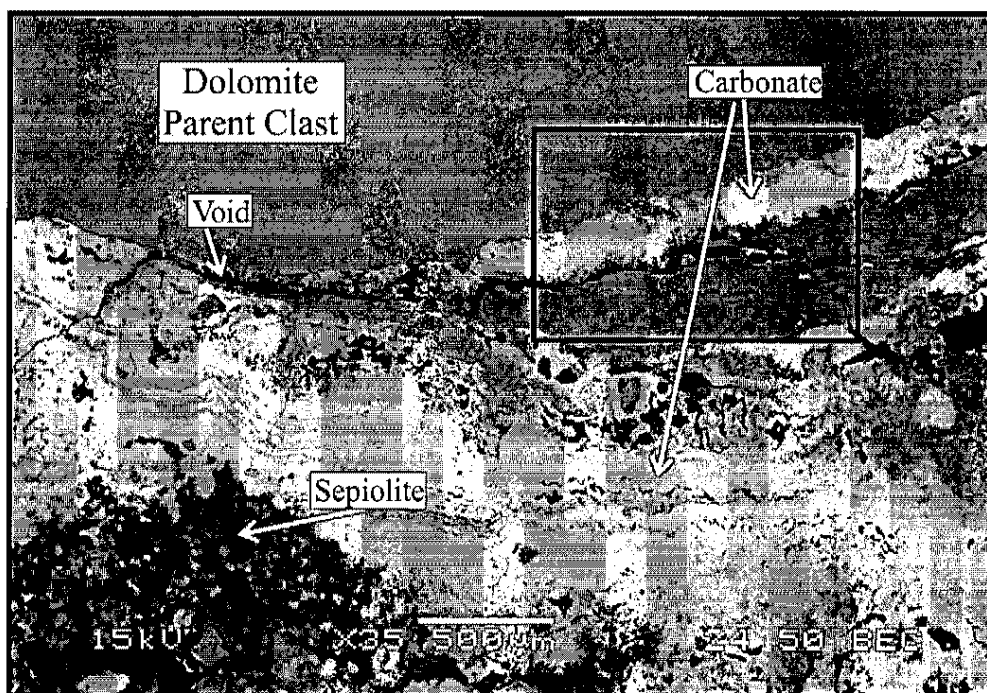
Figure 4.37. Q1$_D$ Backhoe 33-57 cm showing pendant-clast contact
with large portion of clast broken off and incorporated into pendant. Black box
outlines area shown in figure 4.38.
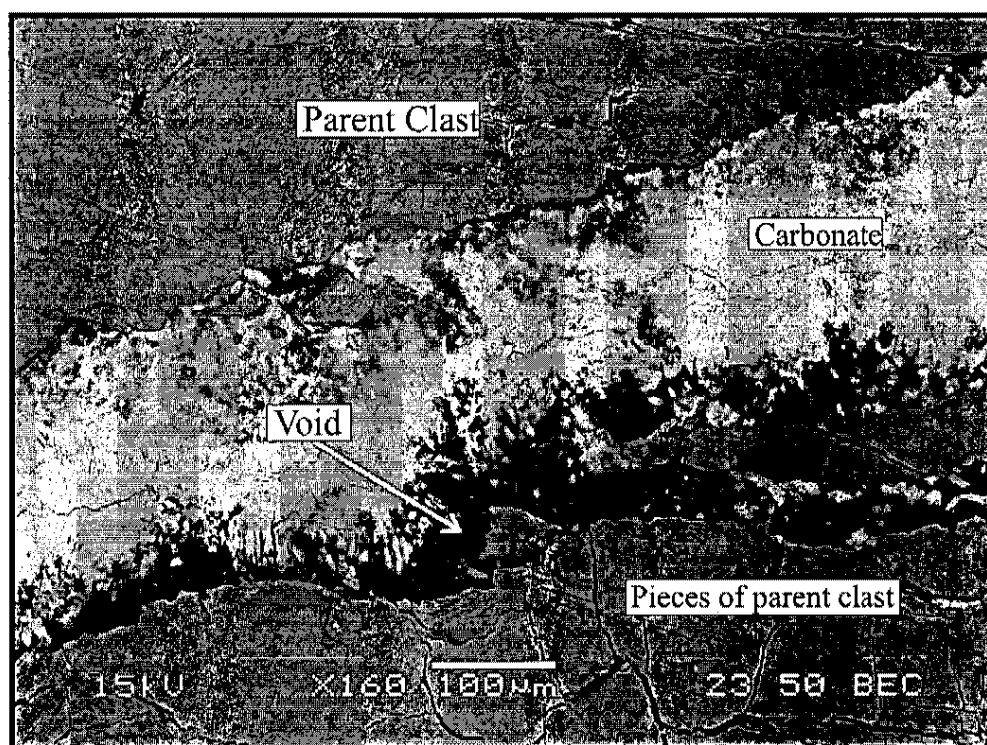
Figure 4.38. Close up of area covered in black box of figure 4.37. Note
the calcium carbonate with acicular crystalline areas radiating downward into
void.

in Mg and Ca. The texture of the dolomite material also facilitated its identification.

Crystalline grains ranging in size from 200μm to 20μm were readily apparent. Crystal

size decreased considerably approaching the pendant-clast contact and in many samples,

the fragments of the parent clast are incorporated into the pendant surrounded by massive

calcium carbonate (Figures 4.34-4.40).

The presence of a linear or sub-linear void between clast and pendant is noticed in

65% of the samples (Figures 4.29, 4.33, 4.37 and 4.38). The linear voids range in

thickness from 10μm to 400μm. These void features do not run the entire length of the

contact but can dominate up to 90% of the contact length. Within this void, evidence for

dissolution and precipitation of calcium carbonate, silica and other clays is evident

(Figures 4.33, 4.37 and 4.38). Five of the seventeen clasts (29%) that contain a

linear/sub-linear void space also contain mineral precipitates in the void. Calcium

carbonate appears as subhedral crystalline material similar to that of carbonate lamina. In

some cases, the carbonate exhibits pure $CaCO_3$ with no evidence of dissolution or other

effects of time and appears undisturbed relative to adjacent carbonate that contains high

Mg and pitted dissolved features.

Grain incorporation from the parent clast occurs in 13 of the 25 (52%) samples.

Usually associated with these features is a "zone of clast break-up" where the clast breaks

along its crystal cleavages. This zone can be up to 200μm with packing of grains

decreasing towards the extremity of the clast (Figure 4.34). Grains dislodged from the

clast are incorporated into the calcium carbonate matrix and can sometimes be found well

into the heart of the pendant (Figures 4.34 and 4.37-4.40). Separation of grains increases
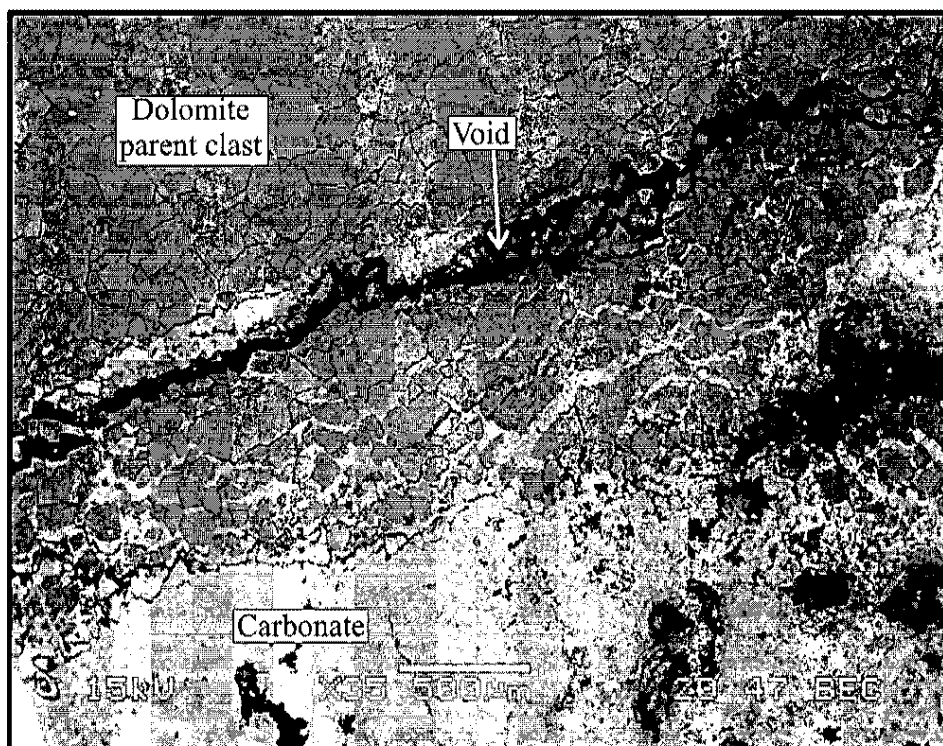
Figure 4.39. Pendant from Q1D Backhoe 57-65 cm with large section of parent clast material that has been incorporated into the pendant.
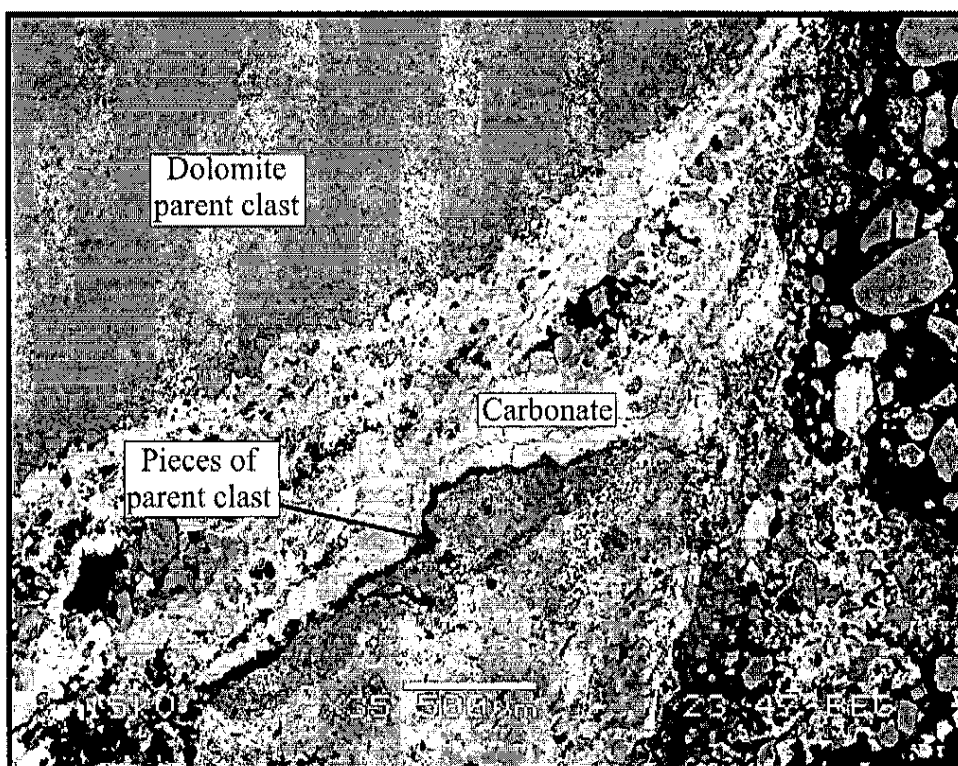
Figure 4.40. Pendant from Q2D Merkler 40-55 cm showing large portions of parent clast material incorporated into pendant.

away from the clast and with depth into the pendant. Seven pendants display "layers" of

incorporated clast grains with large sections of carbonate spanning the area between the

clast and grain layer. The incorporated clast grains may undergo further displacement

and/or dissolution once they have been incorporated into the pendant matrix.

Grain displacement and dissolution

Displacement of detrital and parent clast grains occurs in 20% of the samples, more

commonly in $Q1_D$ Backhoe and $Q2_D$ Merkler profiles. Displaced grains have a "puzzle-

piece" appearance where the grains appear to have once fit together (Figures 4.35-4.40).

These grains are commonly separated by crystalline carbonate. Many grains that have

undergone displacement do not appear to be affected by dissolution although there are

some samples with both processes occurring. Dissolution of incorporated grains occurs

in 44% of the samples and is evident from the pitting and dissolved appearance of grains

that commonly are encircled by clay or silica (Figures 4.41-4.42). There is evidence of

partial and complete dissolution of clasts with the presence of voids in the carbonate

matrix that have an angular shape. Three samples out of 25 had angular void spaces. In

some cases, a remnant grain can be found within this void displaying an obvious

relationship between grain and void (Figure 4.34 and 4.44).

Pendants in Varying Lithologies

Pendants formed in the landforms of the BLM fan (volcanic parent material) have

rough, angular bottoms with pitted surfaces that were once in contact with other grains.

The pendant terminus is commonly coated with yellow silica accumulations (Figure 4.9).

Pendants from the profiles of these landforms have numerous inclusions of coarse sand
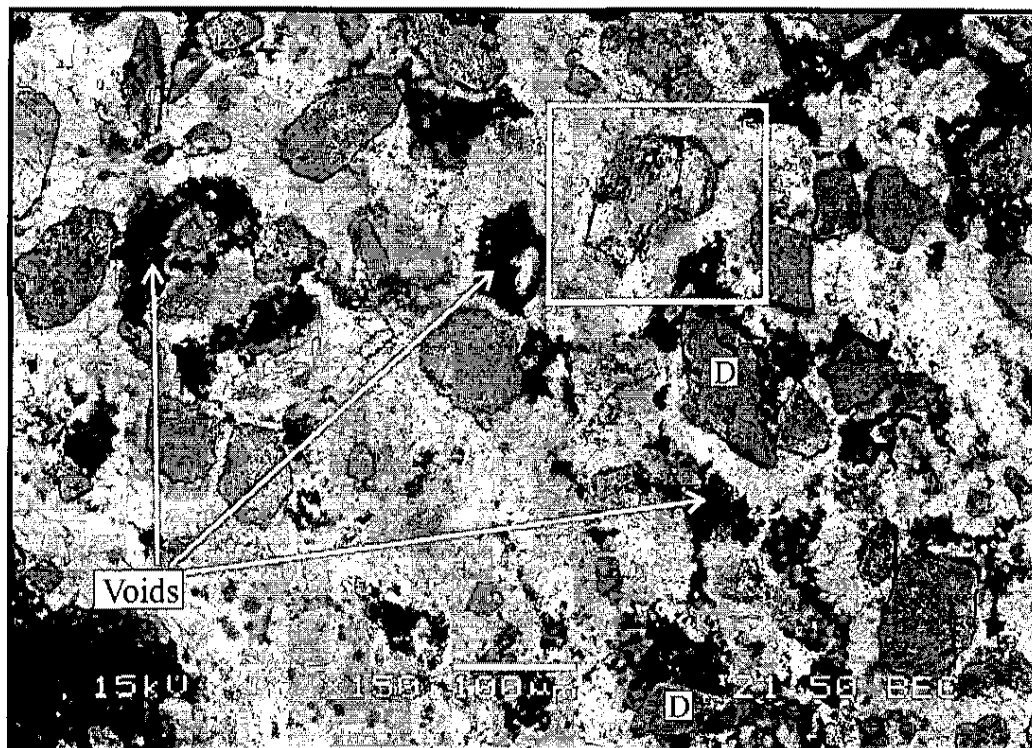
Figure 4.41. Pendant from Q2$_D$ Merkler 13-40 cm with many etched dolomite grains. Area in white box is shown in figure 4.42. D represents dolomite grains. Other grains have high Si and Al chemistries.

Figure 4.42. Heavily etched volcanic grain in carbonate matrix. Area is from area covered in white box from figure 4.41.
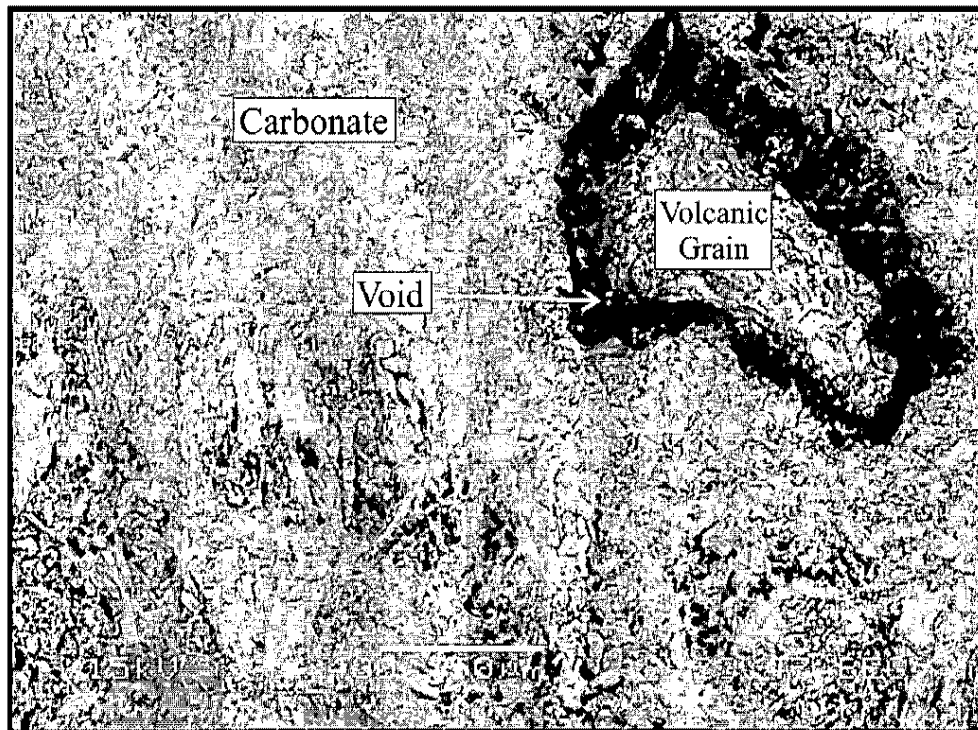
Figure 4.43. Angular void with "matching" grain in carbonate matrix. From Q2$_D$ Merkler 40-55 cm.
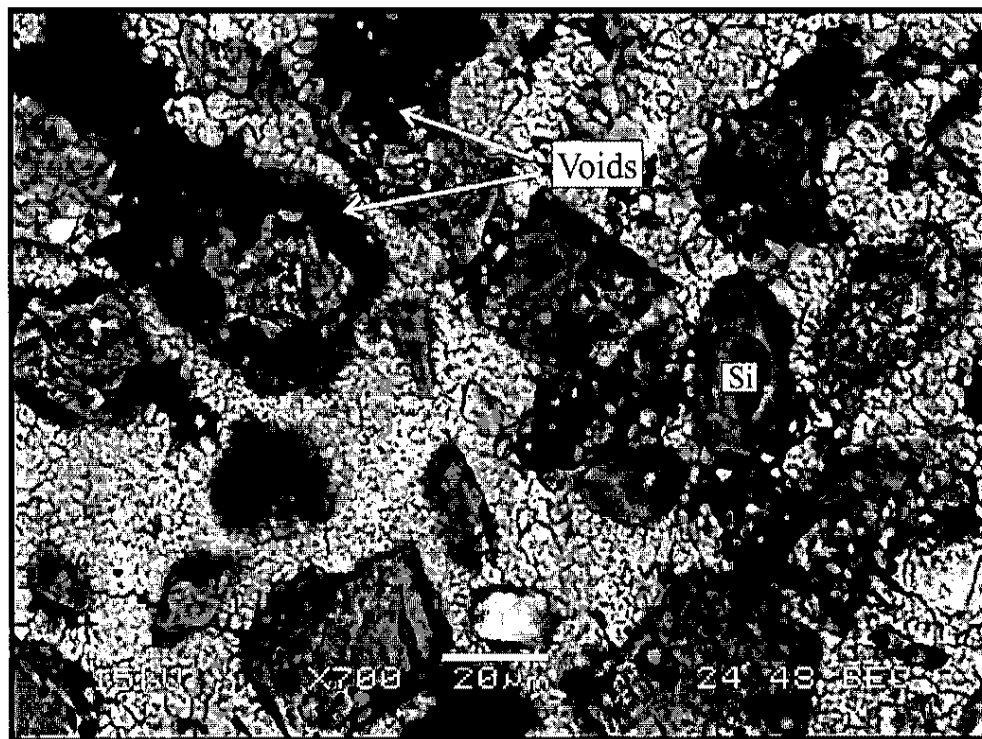
Figure 4.44. Dolomite grains in carbonate matrix with dissolution voids. From Q3$_D$ Mystery 0-11 cm. Grains are dolomite with an occasional quartz grain (Si).

and small gravels that are visible with the naked eye and give the pendant a poorly sorted appearance (Figure 4.45). Pendants from the Mail Summit fan landforms (dolomite parent material) are smoother with less inclusions of sand and gravel than those derived from volcanic lithologies. However, point count data show that there are two pendants from $Q2_D$ Merkler pit and one from $Q1_D$ Backhoe pit that contain significant amounts (>20%) of pendant grains derived from the soil matrix or from the parent clast.

Point counting conducted on 24 samples reveal that 10 pendants have grain percentages above 20%. 70% of these samples were pulled from BLM fan (volcanic parent material) soil profiles (Figure 4.1).

Pendants in Soils of Different Age

Soil pendants associated with the Q1 and Q2 landforms exhibit clast degradation and inclusions of clast material. Q3 soils also exhibit clast break up but not inclusion of clast material. Displaced grains occur in Q1 and Q2 soils and where dissolution features occur in Q1-Q3. Pellet-like masses are only seen in the Q1 and Q2 soils. Sepiolite only occurs in the Q1-Q3 soils and fibers of sepiolite are seen in soils of Q1 and Q2.
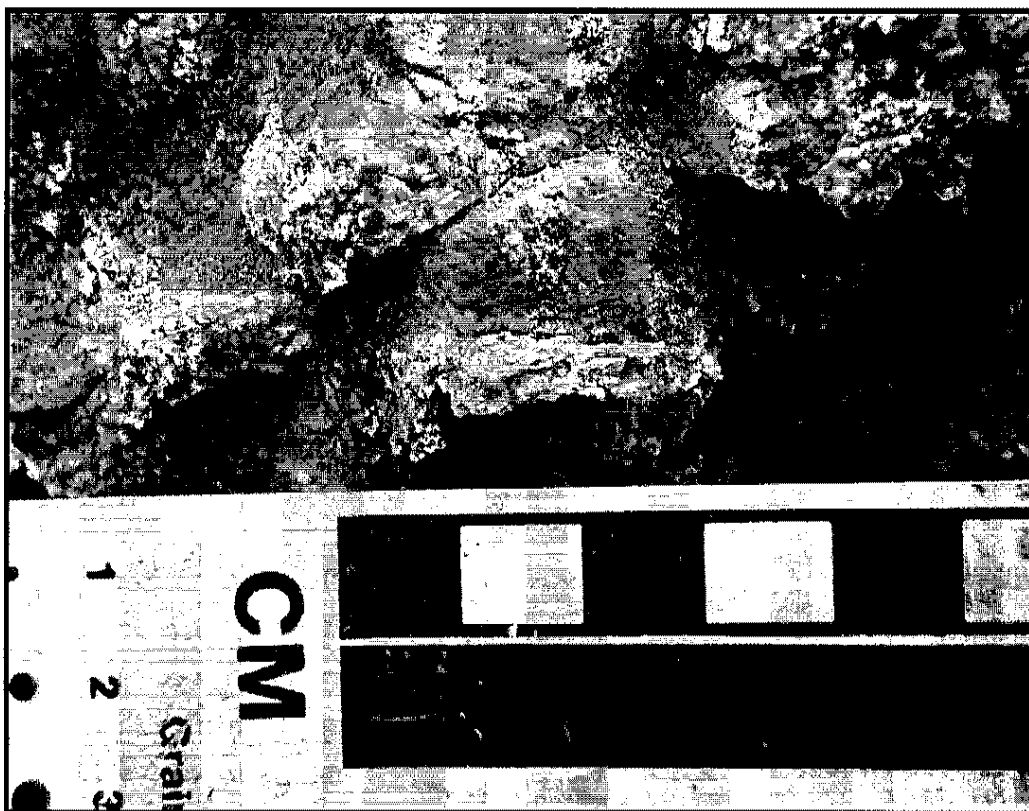
Figure 4.5. Pendants in place in Q1_D Backhoe pit.
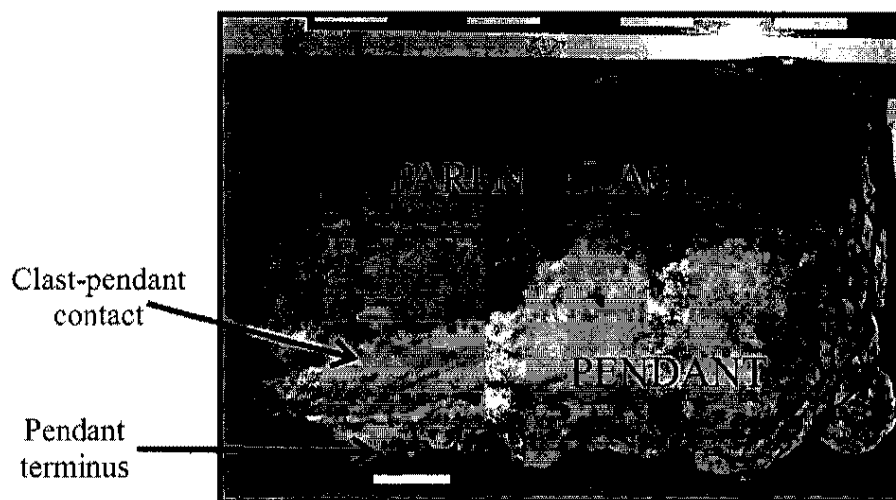
Clast-pendant
contact

Pendant
terminus

Figure 4.6. Pendant pulled from $Q2_V$ BLM 12-40 cm.
Image also shows associated terminology of pendant
features. Bar length is 1 cm.

CHAPTER V

DISCUSSION

Quaternary Landform Relative Ages and Soil Development

Quaternary landforms in the northern Pahranagat Valley developed from several time

dependant alluvial processes with material derived from two different parent lithologies

(Figures 3.1-3.3). These landforms labeled $Q1_D$-$Q5_D$ (dolomite dominant parent material)

and $Q1_V$-$Q5_V$ (volcanic dominant parent material) have distinct characteristics associated

with their temporal development. Surface topography and dissection, degree of desert

pavement, degree of desert varnish, and soil development were used to determine the

relative age constraints of these landforms. Characteristics of the Kyle Canyon fan north

of Las Vegas Nevada (Sowers et al., 1988) and piedmonts of the lower Colorado River

region (Bull, 1991) were compared with the northern Pahranagat Valley landforms.

Stages of carbonate morphology constructed by Gile et al. (1966) and Bachman and

Machette (1977) were used to better constrain the ages of these surfaces according to

carbonate development. Landform topography, elevation and spatial relationships with

other landforms were used for relative dating based on Peterson's (1981) descriptions for

landforms of the Basin and Range Province (1981) (Figure 5.1). Temporal terms for the

Quaternary are used and provided by Bull (1991) (Figure 5.2).

107

Landform Unit	Unit Description*	Taxonomic Classification[&]	Dominant Vegetation	Slope Percent	Relative Age
$Q1_L$ $Q1_V$	Ballena	Calcic Petrocalcid Calcic Petrocalcid	Blackrush	3	Early Pleistocene
$Q2_L$ $Q2_V$	Fan Remnant	Calcic Petrocalcid Calcic Petrocalcid	Blackbrush NV. Effedra	3-6	Middle Pleistocene
$Q3_L$ $Q3_V$	Fan Remnant	Typic Haplocalcid Durinodic Haplocalcid	Blackbrush NV. Effedra	3	Late Pleistocene
$Q4_L$ $Q4_V$	Inset Fan	Typic Haplocalcid Durinodic Haplocalcid	Blackbrush NV. Effedra Rabbit Br. Cholla	6	Early Holocene
$Q5$	Active Drainage	Typic Torriorthent	Blackbrush NV. Effedra Rabbit Br. Cholla	6	Modern

Figure 5.1. Characteristics of Q1-Q5 landforms with varying lithologies. *-Peterson, 1981 &-Qualitative taxonomic classification.

Age	Ka
Holocene	
Late	0-4
Mid	4-8
Early	8-10
Pleistocene	
Latest	10-20
Late	10-125
Middle	125-790
Early	790-1650

Figure 5.2. Assigned ages of Quaternary temporal terms, in thousands of years before present (ka) (Bull, 1991).

Q1 Landforms

Q1 landforms represent the oldest remnants of the Mail Summit and BLM fans and are interpreted to be Early Pleistocene in age. Q1 surfaces are found as ballenas that have undergone significant weathering and removal of an unknown amount of soil. Evidence for weathering and removal of upper horizons is indicated by an exhumed petrocalcic horizon with pieces of stage IV laminar cap at the surface. Gravels containing pendants are also present upturned and on their sides. Desert pavement is well developed with moderate sorting of clasts. Surface clast counts reveal 99% of the clasts recorded and measured on the $Q1_D$ surface were either limestone or dolomite (Figure 3.3). In contrast, $Q1_V$ surface clasts were dominantly volcanic (71%). However, sixty percent of the larger (>32 mm) clasts found on the $Q1_V$ surface were dolomite or limestone. The Av horizons vary between 10 cm ($Q1_V$) and 13 cm ($Q1_D$) which are roughly equivalent to the Q2 landforms, but are much thicker and well developed than the Q3-Q5 landforms (Figures 3.7, 3.9, 3.12 and 3.13). The sandy loam textures of the Bk, Bkqm1, Bkqm2 and Bkqm3 horizons of $Q1_D$ Backhoe (Figure 3.8) give no evidence for significant clay accumulation in the fine soil fraction (<2 mm), although significant clay accumulation would have been predicted to develop during the Pleistocene with increased moisture allowing the development of argillic horizons. This suggests that erosion has removed argillic horizons or carbonate has either masked and/or inhibited clay accumulation in these soils which has been suggested to have happened in other studies conducted in the southwestern U.S. (Gile and Grossman, 1968; Allen, 1985; Monger et al., 1991).

The EC data for $Q1_D$ Backhoe shows a relative increase with depth suggesting a possible increase in salts. pH values for $Q1_D$ Backhoe remain fairly consistent at 8.22 to

8.28 for the upper 5 horizons but decrease to 8.11 and 7.92 in the lower two horizons.

These two lower horizons also show an increase in EC values from 362µs/cm in the

Bkqm2 horizon to 819 µs/cm in Bkqm3 and 4121µs/cm in Bkqm4. This increase in EC

and corresponding decrease in pH suggests a possible increase in sulfate minerals such as

gypsum. Shallow lakes throughout the valley could provide an eolian source for this

material. Gypsum is more soluble than carbonate so it is possible that it would be found

deeper in the profile (below sampled horizons). If deeper horizons within the profile had

been excavated and analyzed, an increased accumulation of gypsum might have been

found. The possible accumulation of gypsum below the top of the carbonate

accumulation depth concurs with studies conducted by Harden et al. (1991) where the

highest percentage of gypsum in the profile was located below the top of the carbonate

horizon in a simple leaching regime. Q1$_V$ Silica profile provides no information about

texture, structure, EC or pH because they were not measured for this profile.

Soil development, erosional features and the classic ballena form correlate to those of

the oldest landforms of the lower Colorado River region (~790 ka) as well as the Surface

1 landforms of the Kyle Canyon fan that were dated at ~800ka using paleomagnetism.

Soil development is similar to Surface 1 of the Kyle Canyon fan with shallow carbonate

horizons exhibiting exhumed petrocalcic pieces on the surface and in upper horizons. In

Kyle Canyon fan, Stage IV carbonate occurs at 32 cm with an incipient stage IV at 8 cm

in the Surface I soils (Sowers et al. 1988). Q1$_D$ Backhoe pit has similar changes in

morphology with a stage IV carbonate horizon found at 82 cm with an incipient stage IV

at 57 cm. The complicated and advanced carbonate morphology found on this landform

suggests an early Pleistocene age and may indicate a paleo-wetting depth influenced by

past glacial climates (Gile et al. 1966; McFadden and Tinsley, 1985). McFadden and

Tinsley (1985) attributed two "bulges" of carbonate of Pleistocene soils to the Holocene

(upper bulge) and Pleistocene (lower bulge) maximum depths of wetting in soils near

Vidal Junction, California. However, Q1 soils of the study area and Surface 1 soils of

Kyle Canyon fan display two laminar stages of development implying that multiple

glacial climates over 100's of thousands of years have contributed to their development

(Gile et al. 1966; Bachmann and Machette, 1977). The inferred decrease in effective

precipitation suggested by the carbonate morphology could be caused by seasonal or

large-scale climatic changes associated with glacial/interglacial cycles. The presence of

two laminar caps could be explained by (1) high rates of sedimentation increasing the

profile depth during the Pleistocene in turn pushing the cap deeper and allowing the

formation of a second laminar cap above and/or (2) an increase in aridity (less

precipitation or a change in seasonality of precipitation) which would decrease the depth

of wetting. This change could result in the upper laminar cap forming at a shallower

depth than the lower one. Relating the formation of the upper laminar cap to increased

aridity at the onset of the the Holocene is unlikely because of the extensive amount of

time that it would take to form a stage IV horizon as seen in the $Q1_D$ Backhoe profile

which well exceeds the length of time within the Holocene (Gile et al. 1966). The

Holocene carbonate accumulations would be predicted to be only weakly developed as

stage I, or less likely, stage II accumulations (Gile et al. 1966) similar to those found in

the Q4 profiles.

Pendants of $Q1_D$ Backhoe profile that were measured in thin section had an average

thickness of 10.2 mm. One sample from $Q1_V$ Silica profile had a thickness of 4 mm

which may not represent the true average thickness of all pendants in that profile.

Silica patches increase with depth in both $Q1_D$ Backhoe and $Q1_V$ Silica profiles. The increase in silica accumulation throughout both of these profiles can be attributed to an increase in solubility of silica from pressure dissolution within petrocalcic horizons and/or from Pleistocene wetting that would have flushed silica deeper into the profile before later and shallower carbonate accumulation.

The soils associated with Q1 landforms are Aridisols because they have an aridic soil moisture regime, an ochric epipedon (dry with no significant organic components) and contain calcic and petrocalcic horizons. Although specific calcium carbonate percentages were not measured, these soils were observed to contain a petrocalcic horizon with an upper boundary within 100 cm of the surface and an associated calcic horizon above. Therefore, these soils are qualitatively classified as Calcic Petrocalcids.

Q2 Landforms

Q2 landforms do not exhibit the rounded ballena style of the Q1 landforms and instead have planar topographies similar to inset fans. They are found at lower elevations than the Q1 ballena surfaces (Figures 3.4 and 3.5). Pedogenic carbonate stages of the Q2 landforms are similar to that of Q1 containing incipient stage IV calcium carbonate in the $Q1_V$ BLM and full stage IV carbonate in $Q2_D$ Merker both at 40 cm depth (Figures 3.12 and 3.13). The increased development of a stage IV laminar cap (compared to the incipient stage IV of $Q2_V$ BLM) in the dolomite material may be a function dissolution and reprecipitation of $CaCO_3$ in parent material (Rabenhorst and Wilding 1986; Sowers et al. 1988; Levine and Hendricks, 1990).

Surface characteristics are similar to those of the Q1 landforms with no evidence of

bar and swale topography and a well developed desert pavement. However, they are not

ballenas and the erosion and exhumation of petrocalcic horizons present on the Q1

surfaces are not as prevalent as seen in the Q2 profiles. The $Q2_D$ surface had 99%

carbonate lithologies. Fifty-nine percent of the surface clasts recorded for the $Q2_V$ surface

were volcanic and 83% of the clasts larger than 32 mm were calcareous. This evidence

again suggests that preferential weathering of volcanic material into smaller clasts leaves

the more resistant calcareous material at the surface. The Av horizons of the Q2

landforms remain thick (13 cm for $Q2_D$ Merkler and 12 cm for $Q2_V$ BLM) similar to

those of the Q1 landforms (Figures 3.12 and 3.13). Silica accumulations on the

undersides of clasts and pendants are present as faint to distinct in $Q2_D$ Merkler profile

and faint to prominent in $Q2_V$ BLM profile. The increase in visible silica in the $Q2_V$

BLM profile could result from parent material with volcanic glass and other silicious

sources more readily available for dissolution and reprecipitation into the soil. Pendant

thicknesses average 12.3 mm for $Q2_D$ Merkler and 10.2 mm for $Q2_V$ BLM. These

thicknesses appear to be similar to the $Q1_D$ Backhoe profile average and represent the

highest averages of all pendants measured throughout all landforms (Q1-Q4).

EC values for $Q2_D$ Merkler remain consistent with readings from 310.9μs/cm to

352.5μs/cm throughout the profile. pH values steadily increase with depth from 8.13 to

8.28. For $Q2_V$ BLM profile, EC values vary at depth from 288.5 μs/cm (lowest) to 412.0

μs/cm (highest). The highest EC reading was found at the lowest horizon but occurs with

the highest pH (8.9) suggesting that perhaps salts other than sulfates could be present.

The soils associated with Q2 landforms are aridisols that also have a petrocalcic horizon with an upper boundary within 100 cm of the surface and have a calcic horizon above the petrocalcic horizon. Because of these features, the soils associated with Q2 landforms are given a qualitative taxonomic classification of of Calcic Petrocalcid similar to Q1.

Soil development with an incipient stage IV petrocalcic horizon in Q2$_V$ BLM profile suggests a Mid Pleistocene age, younger than the Q1 landforms. These landforms do not exhibit the rounded, erosional ballena forms of Q1. Q2 landforms are that interpreted to be Middle Pleistocene in age consistent with those of Surface 2 of Kyle Canyon fan ranging from ~730-130ka. This landform was dated using paleomagnetism and $^{230}Th/^{234}U$ ages of inner lamina of pendants (Reheis, 1988). Other similar surfaces in the region are the Q2 surfaces of the lower Colorado River. These surfaces range in age from 730-130ka and have normal polarity and age constrains based on K/A ages of a basalt flow in Q2 alluvium and $^{230}Th/^{234}U$ ages of carbonate pendants (Bull, 1991).

Q3 Landforms

Q3 landforms are inset fan remnants located stratigraphically below Q1 and Q2 landforms and considerably higher than Q4 and Q5 landforms. These surfaces contain no petrocalcic horizons and have no desert pavement development. Bar and swale topography is present, yet poorly preserved, suggesting leveling of the surface consistent with initial stages of carbonate development (McFadden et al., 1987). On the Q3$_D$ surface, 100% of clasts were carbonate in lithology. Conversely, surface clasts of the Q3$_V$ landform were 65% volcanic. Av horizons are not present and the profiles reach a maximum stage II carbonate development at 100 cm depth in the Q3$_D$ Mystery profile

and 68 cm depth in Q3$_V$ Last profile. Texture varies between sandy loam and loamy sand throughout both profiles showing no significant accumulation of clays in the fine grained material. Visual accumulation of silica was not seen in the Q3$_D$ Mystery profile but are present as faint patches on the undersides of gravel in the Q3$_V$ Last profile. In addition, durinodes were found in the 68-100 cm horizon of Q3$_V$ Last profile. The presence of durinodes and faint patches of silica in this profile contrasted with the lack of them in Q3$_D$ Mystery supports the hypothesis that silica accumulation in the volcanic material is greater than in the dolomite material because of its availability to be taken into solution and reprecipitated. Pendant thicknesses average 2.7 mm for Q3$_D$ Mystery and 1.5 mm for the two pendants measured from Q3$_V$ Last profile. These measurements are significantly less than the older Q1 and Q2 averages suggesting pendant thickness increases with age.

EC and pH values for Q3$_D$ Mystery profile show an increased salinity in the A (upper) and Bk4 (lower) horizons. Corresponding pH values are 8.15 for the A and 8.21 for Bk4. Both pH readings are the lowest of those recorded in the profile. Again, increased EC and decreased pH values may be explained by the presence of sulfate minerals. Salts accumulated in the upper (A) horizon could be a product of Holocene eolian material accumulated at the surface. Salt accumulations present deeper in the profile could result from increased wetting depths during the Pleistocene (Harden et al., 1991). Q3$_V$ Last readings show highest EC values in the top horizons (A-481.5, Bk1-409.3) similar to Q3$_D$. pH values are difficult to interpret because they range from 6.6 to 7.23, considerably lower than the readings of any other horizons in this study. pH and EC analyses for this profile were conducted at a later date than the other profiles analyzed in

the study. Factors such as distilled water pH and instrument error could be a factor in these unique readings. However, the upper horizon EC readings of 481.5µs/cm and 409.3µs/cm suggest increased salt accumulations when compared with the lower horizons of the profile consistent with Holocene eolian input.

The soils associated with Q3$_D$ landforms are Aridisols that also have a calcic horizon with an upper boundary within 100 cm of the surface and do not have a petrocalcic horizon. These soils also do not have aquic conditions, natric horizons, xeric or ustic moisture regimes, argillic or a significant calcic horizon above, shallow depth, or xeric and ustic soil moisture regimes. A qualitative taxononomic classification of Typic Haplocalcid is given to the soil of the Q3$_D$ Mystery profile. Soils associated with the Q3$_V$ landforms are similar in carbonate and other soil development factors to the Q3$_V$ landform soils. However, the presence of durinodes found at the 68-100 cm horizon places this soil qualitatively into the classification of Durinodic Haplocalcid for the Q3$_V$ soils. These landforms are interpreted to be Late Pleistocene in age consistent with those of the 12-2ka Q3 deposits of the lower Colorado River region and 15-10ka Surface 3 deposits of the Kyle Canyon fan (Sowers et al. 1988; Bull, 1991). In Kyle Canyon fan, Surface 3 carbonate development reaches a stage II at 61 cm depth similar to the stage II depths of the Q3$_D$ Mystery profile. The lower Colorado River region Q3 landforms were dated using desert varnish development and ^{14}C of plant fossils (Bull, 1991). Surface 3 of Kyle Canyon fan was dated using ^{14}C and uranium-series analyses of soil pendants (Sowers et al. 1988).

Q4 Landforms

Q4 landforms are inset fan remnants located significantly below the Q1-Q3 landforms

and approximately 1 meter above the Q5 active drainage. There is no desert pavement or

desert varnish development and bar and swale topography is well preserved. Carbonate

development is limited to stage I in both $Q4_D$ Shovel and $Q4_V$ Glass profiles. No visual

accumulation of silica is apparent in $Q4_D$ Shovel but $Q4_V$ Glass displays distinct

accumulations in all horizons excluding A and Bw. Durinodes are present in the 89-122

cm horizon of $Q4_V$ Glass. Silica accumulation in the volcanic material and not the

dolomite parent material again implies that silica is more readily available in the volcanic

parent material. Pendant thickness recorded from one pendant from the $Q4_V$ Glass

profile was 4 mm. This sample was preferentially selected because of its size and may not

be a true representative of the average pendant thicknesses of this profile.

The fine grained fraction of soil has textures that vary from sandy loam to loamy sand

in the $Q4_D$ Shovel profile and loamy sand to sandy loam and sand in the $Q4_V$ Glass

profile (Figures 3.20-3.21). Again, no distinct development of clay is seen in either

profile probably due to the lack of time needed for the development of significant argillic

horizons. Also, calcite crystal growth from carbonate accumulation may be inhibiting the

development of clay in these profiles. pH and EC values for $Q4_D$ Shovel show a high EC

reading of 972.4 μs/cm in the Av horizon correlating with a low 7.91 pH. $Q4_V$ Glass

profile exhibits the same pattern with an EC reading of 1103 μs/cm and pH of 8.01 in the

A horizon. These high salinity and low pH readings of the surface horizons suggest an

accumulation of sulfate salts (i.e. gypsum) that could be a product of Holocene aridity

and transport from nearby pluvial sources.

Soils associated with the $Q4_D$ Shovel profile are similar to those of $Q4_V$ but do not have the calcic horizon development seen in Q3 and older soils so they are qualitatively classified as Typic Haplocalcids. $Q4_V$ Glass profile contains durinodes in the 89-122 cm horizon and is qualitatively classified as Durinodic Haplocalcid. Soil development and surface characteristics of the Q4 landforms suggest an Early Holocene age for these deposits. Similar deposits from the lower Colorado River region are interpreted to be 4 ka based on light desert varnish. The Kyle Canyon deposits were not dated. The presence of stage I coatings in the Q4 landforms suggests an age of approximately ~8 ka correlated to similar carbonate development in the Las Cruces, NM area (Gile, et. al. 1966). Precipitation differences between the study area and Las Cruces would suggest a slightly older age estimate for the Q4 soils in the study area. Less precipitation in the study area would decrease the rate of calcium carbonate accumulation in the soils. Thus, older soils of the Pahranagat Valley may contain carbonate accumulations equivalent to younger soils of southern New Mexico (Machette, 1985).

Q5 Landforms

The Q5 landforms of the study are the modern drainages located 1 meter below Q4 surfaces. They have active bar and swale topography and contain no vegetation. They are frequently subjected to flowing water in rainstorm events. One soil profile ($Q5_V$ Wash) was sampled and analyzed and yielded four poorly developed horizons of sand. No carbonate or silica accumulations are present. EC measurements decrease with depth from 510.4 µs/cm to 302.6 µs/cm. pH values range from 8.2 to 8.6 with a value of 9.0 in the C3 horizon. $Q5_V$ Wash profile is an Entisol (little soil development) with an aridic moisture regime that does not fit into any other subgroup and therefore is classified as

Typic Torriorthents. This classification is believed to be the same for $Q5_D$ landforms.

The Q5 landforms are modern in age.

Q1-Q5 landforms show increased elevation with age. Q1 is highest and oldest

followed by Q2, Q3, Q4 and the modern, active Q5 channels occur at the lowest

topographic position. Landform surfaces display an increase in weathering through time

with both limestone/dolomite and volcanic parent material. However, volcanic material

appears to weather faster. This interpretation is supported by the abundance of volcanic

clasts weathered to 2mm and smaller grains. In contrast, calcareous material remains as

larger clasts on the surface of both $Q1_V$ and $Q2_V$ landforms. Disappearance of bar and

swale topography with increased age and increased desert pavement development with a

corresponding increase in Av thicknesses supports McFadden et al's (1987) interpretation

of desert pavement formation whereby eolian input uplifts gravel to smooth the

microtopography associated with bar and swale. The similarity in Av thickness between

Q1 and Q2 indicates that pavement development significantly contributes to the

formation of the Av (McFadden et. al. 1987). Q3-Q5 landforms have no desert pavement

and thus do not contain significant Av's.

Soil development increases with increasing age with stage IV carbonate development

in the Q1 and Q2 landforms. A slight difference in development between soils of the

same age with different lithologies ($Q2_D$ Merkler and $Q2_V$ BLM) could be the product of

increased calcium carbonate in the calcareous lithologies (Sowers et. al. 1988; Levine and

Hendricks, 1990; Rabenhorst and Wilding 1986). Although not as readily seen in the

younger landforms, this effect may become more important with increasing age. Perhaps

the differences between $Q2_D$ Merkler and $Q2_V$ BLM are from local variations of the

surfaces with micro-topography or by natural variations within the soil profile. Soil

pendants in the study area appear to increase in thickness with increasing age which is

consistent with observations from other studies (Pierce and Scott, 1982; Pierce, 1985;

Chadwick et. al. 1988; Bull and Vincent, 1994; Treadwell-Steitz and McFadden, 2000).

This may result from the selection process and difficulty of measuring pendants without

cutting them. Q3 and Q4 pendants are significantly thinner than those of Q1 and Q2

pendants. Figure 5.3 shows the overall characteristics and soil development on each

surface.

Pendant Genesis

Soil pendants found in the Quaternary landforms of northern Pahranagat Valley

provide a unique look into the characteristics and processes of their formation. Pendants

have become the focus of many recent studies to determine absolute ages of soil profile

development related to landform stability. The current, accepted method of pendant

genesis is similar to the formation of stalactites, in which successive precipitation events

occur at the base of the pendant forming lamina in successive ages from youngest (most

recent precipitates at or near pendant terminus) to oldest towards the interior of the

pendant (Figures 5.4 and 5.5) (Pierce and Scott, 1982; Pierce, 1985; Chadwick et al.

1988; Sowers et al. 1988; Amundson et al. 1989; McFadden et al. 1991; Reheis et al.

1992; Amundson et al. 1994; Courtey et al. 1994; Birkeland, 1999; Treadwell-Steitz and

McFadden, 2000; Wang and Anderson, 1998; Ludwig and Paces, 2002). These lamina

form as the result of multiple episodes of precipitation in which successive episodes of

accumulation occur at the pendant terminus. All studies that have been conducted on soil
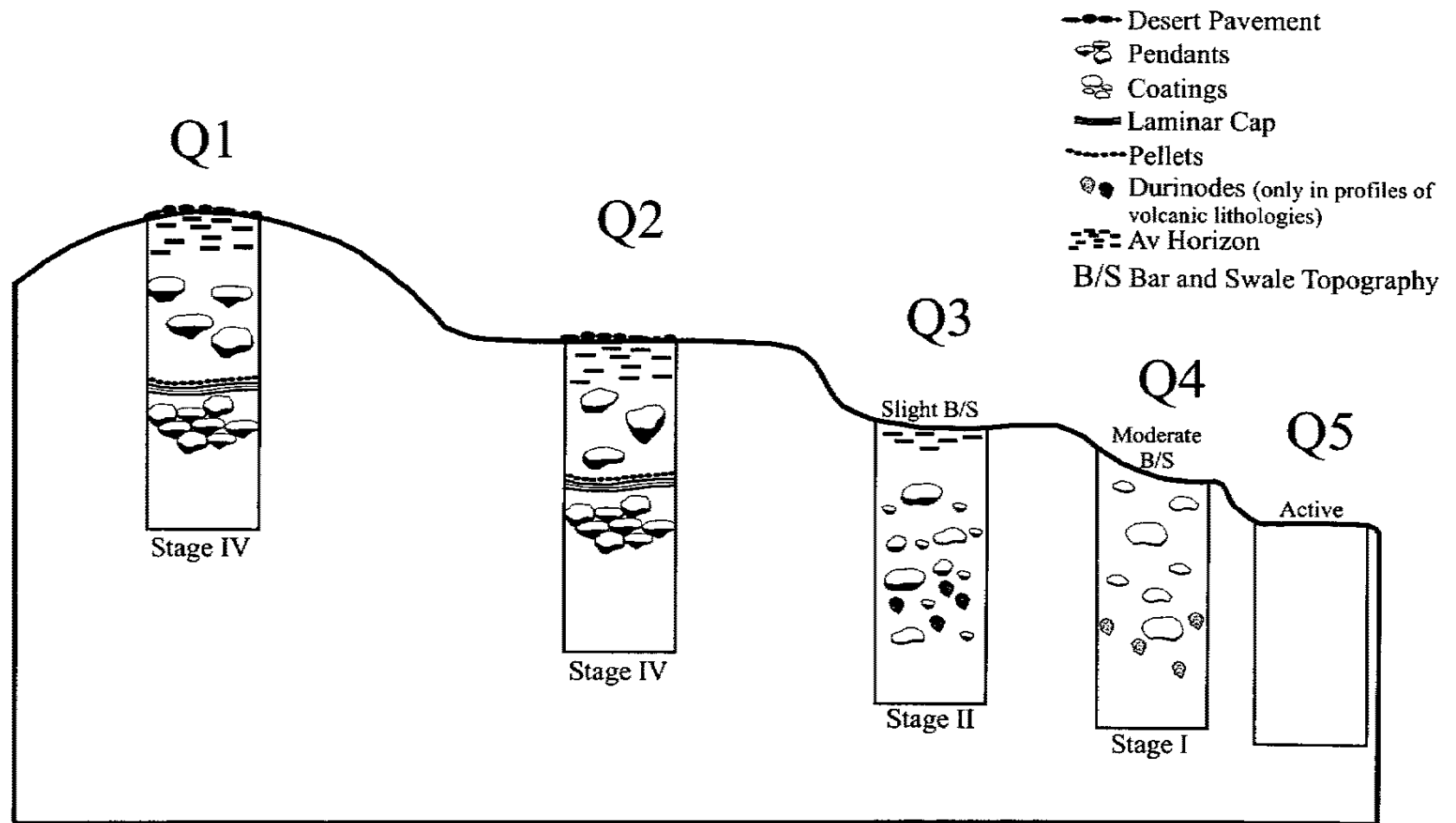
Figure 5.3. Development of certain soil features of landforms of the northern Pahranagat Valley.

Stalactite-Style Formation

Ia.

Ib.

Ic.

Oldest

Youngest

Mixed Stalactite-Style and Clast-Contact Formation

IIa.

IIb.

Meteoric
Water

IIc.

IId.

Youngest ⟶

Also possible youngest ⟶
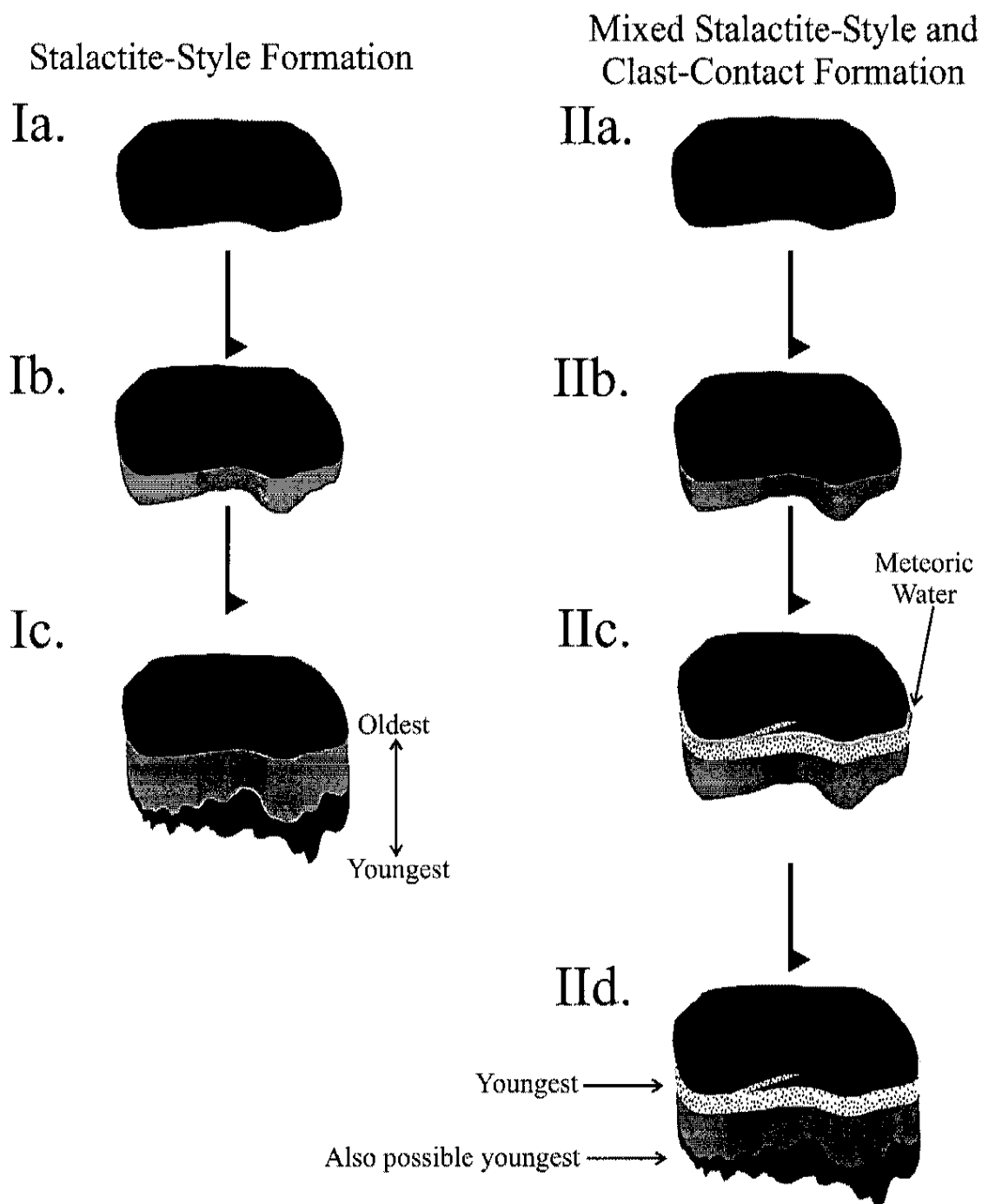
Figure 5.4. Stalactite-style formation process commonly accepted as pendant formation (Ia-Ic), and the proposed formation style where material is precipitated out at the clast-pendant contact. Note that both styles of development can co-occur. A chart describing both styles of formation is given in figure 5.3.

I. Stalactite-Style Formation Stages	II. Mixed Stalactite-Style and Clast-Contact Formation Stages
A. Clean, newly deposited clast.	A. Clean, newly deposited clast.
B. No void space between clast and pendant. Initial accumulation forms on bottom of clast.	B. Initial accumulation forms on bottom of clast.
C. Accumulation continues in a stalagtite-style deposition with youngest lamilla at bottom of pendant.	C. Void space between clast and pendant allows meteoric water to precipitate $CaCO_3$ and incorporate clast grains into the pendant. Younger deposits are now at clast/pendant contact.
	D. Precipitation can continue as well as laminar formation. Ages vary throughout pendant.

Figure 5.5. Description of Stalactite-style and Clast-contact formation processes for soil pendants of the study area.

pendants have assumed that pendants form in this manner (Chadwick et. al. 1988; Sowers et. al. 1988; Amundson et. al., 1989; Duclous and Laouina, 1989; Blank and Fosberg, 1990; Levine and Hendricks, 1990; Munk and Southard, 1993; Vincent et. al. 1994; Treadwell-Steitz and McFadden, 2000). However, this study has found that only a few pendants of the Pahranagat Valley exhibit this style of development.

Macroscopic and microscopic techniques reveal that pendants of the Pahranagat Valley are similar to those observed by Treadwell-Steitz and McFadden (2000) but dissimilar to other calcic pendants that are discussed in the literature. Most studies conducted on pendants describe them as being composed only of laminar calcium carbonate with minor amounts of other materials (Gile et al. 1966; Chadwick et al. 1989). Similarities to pendants observed by Treadwell-Steitz and McFadden (2000) include the presence of clay, abundant silicate grains and the absence of clearly laminated structure. They also found disrupted lamina attributed to a void located at the parent-clast contact. Pahranagat pendants are composed primarily of calcium carbonate but also contain significant amounts of other materials. Many of these layers contain high amounts of grains included in the pendant matrix that were originally pieces of the parent clast or detrital grains. Pendants that were point counted have grain inclusions that range from 0-53%. In thin section, some pendants contain large, rounded grains (up to 2mm in size) that were incorporated from the soil matrix as well as apparent fragments of the parent clast incorporated near the clast pendant contact (Figure 4.1).

Only 5 of the 25 samples analyzed had evidence for the previously inferred method of stalactite-style formation. The remaining 20 samples had evidence contradicting the accepted method of pendant genesis. Many features found in the pendants that were

examined in this study provide evidence for a new formation process for pendants of

the study area (Figure 5.6). These features include dissolution and precipitation into a

void at the clast-pendant contact, a clast "break-up" zone, inclusions of parent clast

material in the pendant, and the formation of sepiolite and pellet-like features (Figures

4.3, 4.7, 4.8, 4.10-4.44). Sixty-eight percent of the total samples observed had clast-

pendant contact voids. Twenty-eight percent had parent clast fragments included into the

carbonate matrix suggesting precipitation of carbonate either into fractures of the parent

clast or a significant amount of precipitates that pushed grains of the parent clast down

into the pendant. The position of these fragments within the pendant indicate that the void

at the clast/pendant contact has remained open through time allowing successive

generations of precipitation of calcium carbonate, silica and silicate clays (Figures 5.4

and 5.5). The youngest material is now at the pendant-clast contact. This process will

continue as long as there is a void at the contact where water can infiltrate and precipitate

minerals. Continued precipitation at the void or at the pendant terminus causes ages to be

mixed throughout the pendant. It is likely that pendants displaying this formation process

contain the oldest lamina toward the middle of the pendants.

The proposed genesis through time for pendants in this study is detailed and described

as follows. (1) A void develops at the clast pendant contact and remains open to soil

water through time (Figures 4.11, 4.23, 4.29, 4.33) (2) Evaporation within this void leads

to the supersaturation and eventual precipitation of materials such as carbonate, salts

other than carbonate, silica or silicate clays. However, the precipitation of materials

within this void does not result in the void closing. The contact between the pendant and

parent clast remains open to soil fluids. This appears to be a physical process possibly
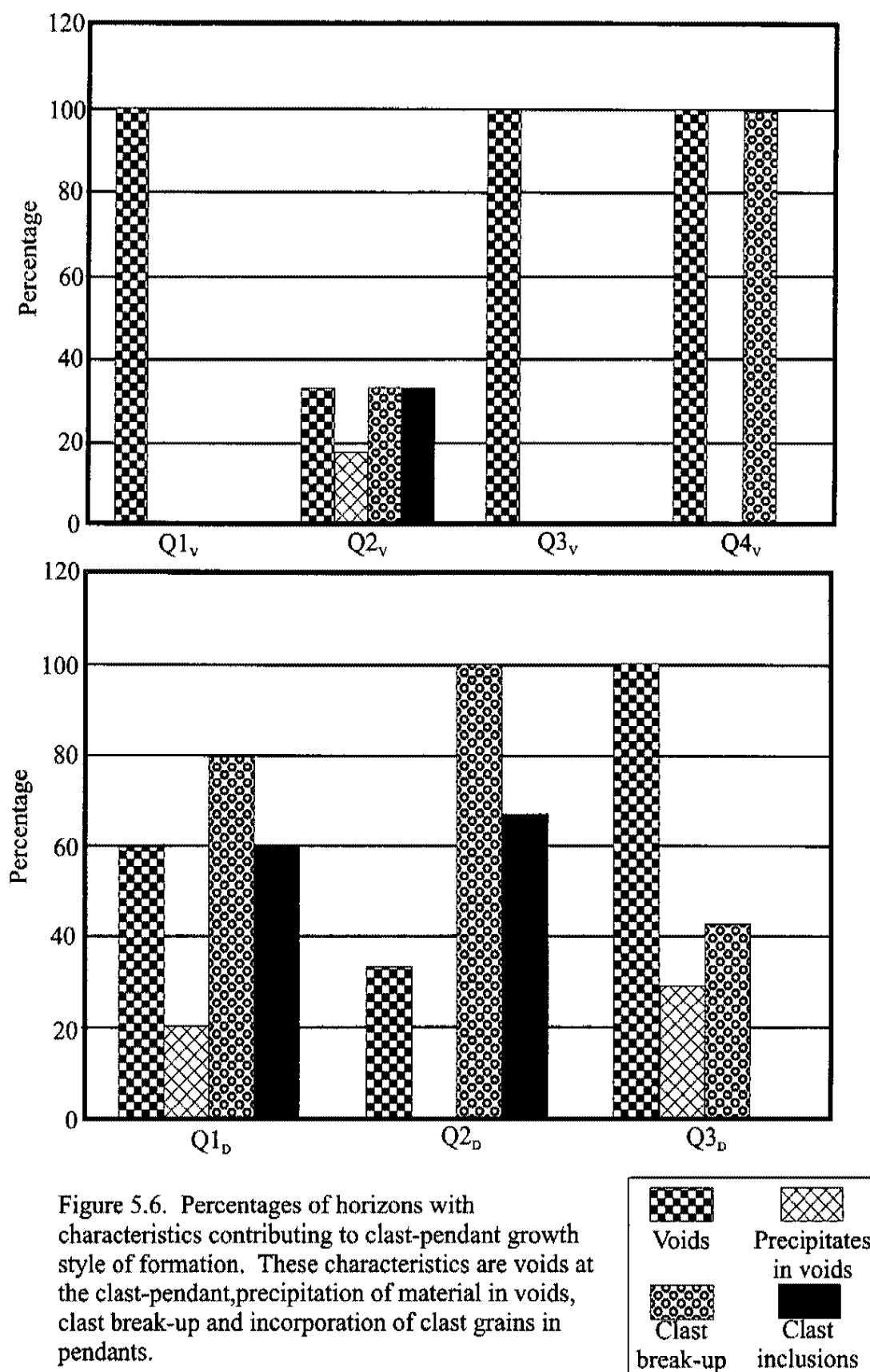
Figure 5.6. Percentages of horizons with characteristics contributing to clast-pendant growth style of formation. These characteristics are voids at the clast-pendant,precipitation of material in voids, clast break-up and incorporation of clast grains in pendants.

caused by different degrees of thermal expansion and or freeze-thaw processes

between the soil pendant and the parent clast. Thus, each successive precipitation event

results in the pendant growing from the clast contact outward (Figures 4.11, 4.23, 4.33).

(3) In some cases the pendant-clast contact contains a break-up zone where crystalline or

amorphous minerals can infiltrate into microfractures within the clast, precipitate, and

displace fragments of the parent clast down into the pendant (Figures 4.34-4.40). (4) The

precipitated material displaces parent clast fragments downward into the pendant as

continued precipitation of materials continues in the void through time. (5) The process

of precipitation in the void can alternate or occur simultaneously with precipitation at the

pendant terminus. At the terminus, detrital grains within the surrounding soil can become

incorporated into the pendant as well (Figures 4.17 and 4.29). (6) Dissolution of

incorporated grains occurs from either the force of carbonate crystallization or by

undersaturation of ions in the soil solution (Figures 4.41-4.44). (7) The products from the

dissolution of grains contribute to the pore water chemistry which may cause repeated

dissolution and/or reprecipitation of secondary products including the mineral sepiolite.

(8) Pore water chemistry can change through time so that alternating episodes of

dissolution and precipitation could occur affecting the presence and relationship of

different pendant constituents. (9) The formation of sepiolite either as the product of

dissolution around grains or by neoformation within the pendant occurs. (10) Rounded

forms of sepiolite develop and form pellet-like features in the carbonate matrix (Figures

4.25-4.27). The resulting morphology of pendants is similar to that of petrocalcic

horizons possibly up to stage V. The developmental process described above was

formulated from specific features seen in pendants of the study area. They are discussed below.

The primary mineral present in soil pendants of the study area is micro-sparite masses of calcium carbonate (Figures 4.10 and 4.11). Some calcite crystal structure is seen as lenticular crystals radiating as lamina, however these are rare (Figure 4.11). Pendants consisting wholly of laminar calcium carbonate were not seen in this study. Instead, pendants are heterogeneous, composed of high amounts of magnesium calcites, silica, silicate clays and incorporated detrital grains and grains derived from the parent clast. Carbonate and other materials can be precipitated at the pendant terminus or inside voids within the pendant itself. Voids at the pendant-clast contact contain evidence for the dissolution and reprecipitation of these minerals.

<u>Voids at clast pendant contact</u>

Sixty-eight percent of the pendants examined in this study had linear voids at the clast pendant contact. Similar voids have been found in other studies. Courtey et. al. (1994) noticed a "thin fissure" at the clast-pendant contact that was interpreted to have no affect on pendant formation. Treadwell-Steitz and McFadden (2000) also noticed an area where the pendant had "separated" from the clast and into which calcite had precipitated. However, these studies report that this clast-pendant contact feature is not a significant player in pendant development. Voids found in samples from the study area can cover up to 80-90% of the length of the contact (viewed in thin section) and range in vertical thickness from $10\mu m$ to $400\mu m$. Four of the samples with voids had precipitates of calcium carbonate, silica and/or silicate clays within these voids.

Void development through time

Linear voids at the clast-pendant contact are present in pendants from all landforms

sampled: 67% of pendants sampled from Q1, 43% of pendants from Q2 and 100% of

pendants from Q3 and Q4 profiles (Figure 5.6). Because they are found in all ages of

landforms, these void features do not appear to be time dependant features. Their

presence is necessary for the clast-pendant contact growth throughout pendant

development. Since they are found in all ages, this supports the newly proposed

formation process.

Void development with different lithologies

Of the 17 pendants that had voids at the parent-clast contact, 41% of the parent clasts

were limestone, 47% were dolomite and 11% were volcanic (Figure 5.7). Only two

volcanic parent clasts were analyzed. The small percentage of volcanic parent clasts with

voids reflects this sampling bias. However, it is important to note that both volcanic

samples had voids at the contact. Treadwell-Steitz and McFadden (2000) reported voids

on metamorphic clasts, therefore voids have been found to occur in several major

lithologies. To fully understand whether lithology affects void formation, more

observations need to be made on pendants in other lithologies.

Clasts of dolomite lithologies show increased weathering and separation of grains near

the clast-pendant contact (Figure 5.7). The development and stability through time of

linear voids at the clast-pendant contact might be attributed to differences in thermal

expansion characteristics between the pedogenic carbonate material of the pendant and

the lithified dolomite or volcanic lithology of the parent clast. Treadwell-Steitz and

McFadden (2000) suggested that weathering of the biotite in metamorphic clasts

Clast-contact void*

Grain displacement&

Clast Lithologies

Clast break-up@
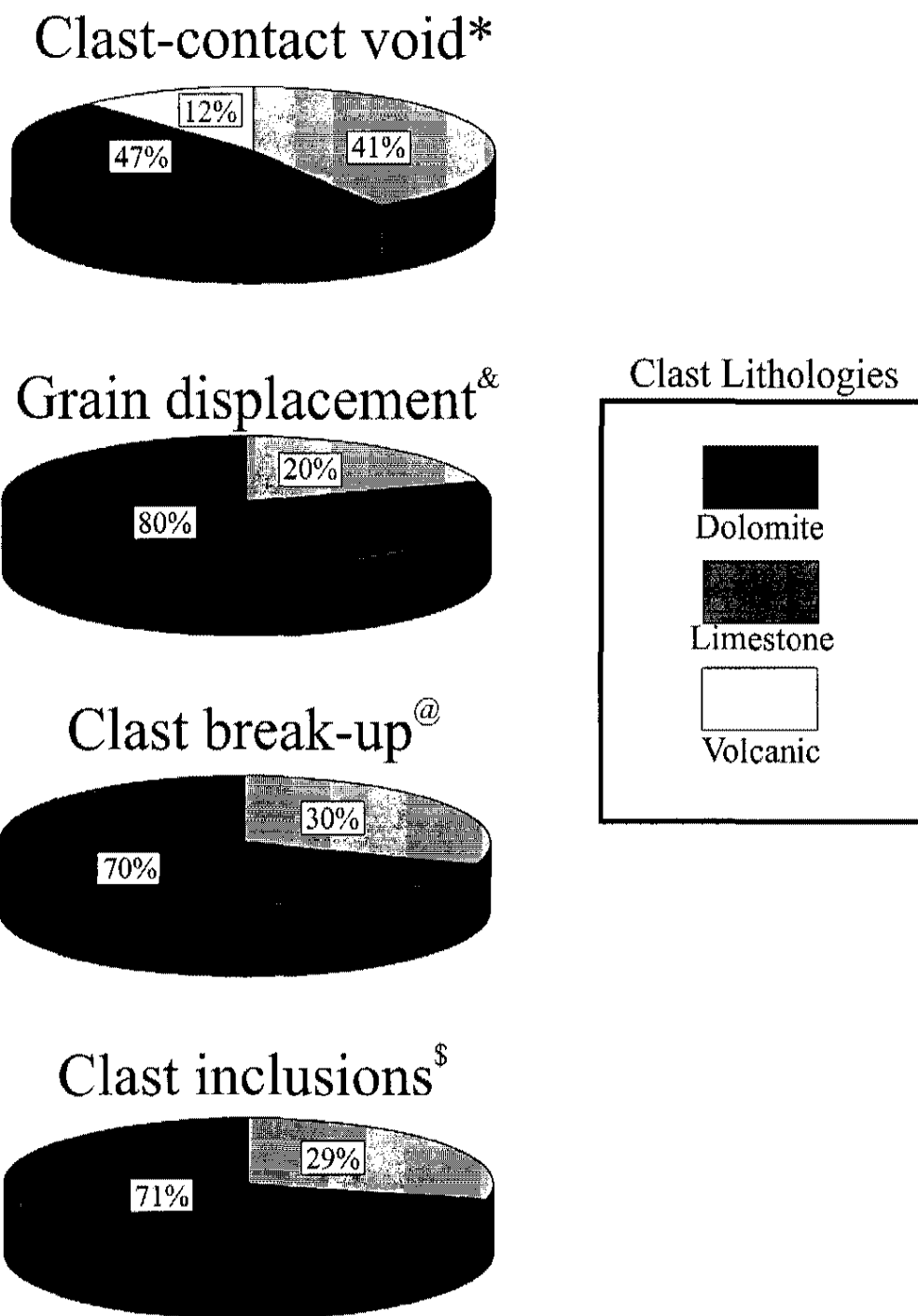
Clast inclusions$

Figure 5.7.Percentage of dolomite, limestone and volcanic parent clasts containing voids at pendant-clast contact, grain displacement, clast break-up and clast inclusions. *Percentages out of 17 occurrences, &Percentages out of 6 occurrences, @Percentages out of 13 occurrences, $Percentages out of 7 occurrences

contributes to the separation between the clast and pendant contact. Weathering is attributed to cycles of wetting and drying (Treadwell-Steitz and McFadden, 2000). Physical weathering of the clast prior to deposition can also a key factor in the development of pendants. The loose grains in the clast break-up zone provide areas that calcite can precipitate and grow forcing grains further apart and into the carbonate matrix (see discussion on 'break up zone' below). However, this clast break up zone only helps to explain how fragments of the clast are found within the pendant. Another explanation is needed to understand why this clast/pendant void remains open despite precipitation of carbonate and other compounds. A possible explanation is the difference in thermal expansion between pedogenic minerals in pendants and the more dense parent clasts. A slight difference in thermal expansion between the pendant and the clast could cause the voids seen in this study as well as allow those voids to remain open through time. More work should be conducted on the differences in thermal expansion between pedogenic carbonate and lithified materials and the importance of the clast break-up zone to fully understand the causes of the void space at the clast-pendant contact.

Clast inclusions and the "break-up" zone

The presence of grains and large fragments of parent clast that have been included into the carbonate matrix of the pendant suggest that clast-pendant voids are an important mechanism for pendant formation. Material derived from the parent clast is commonly associated with a zone located at the outermost edges of the parent clast that is breaking into smaller pieces. This zone is referred to as the "zone of break-up" and is observed in 52% of the samples (Figure 4.34). This zone is marked by a decrease in grain size toward the clast edges. A hypothesis for the formation of this zone is that it initially begins as a

zone of weakened crystals or grains at the exterior edges of the parent-clast. This weathering is possibly initiated by collision with other cobbles and grains during transport before deposition. Microfractures caused by this weathering allow water to infiltrate, precipitate carbonate, and force apart fragments of the parent clasts. However, some process, perhaps thermal expansion, is needed to keep the void open at this contact as it is seen to be a dominant feature in all ages of pendants in this study. Seven out of 13 samples that exhibited a clast break-up zone also had pendants with grains and pieces of parent clast that were incorporated into the pendants indicating previous break-up and incorporation. Also, 9 out of 25 samples containing clast break-up zones also contained voids. For example, weakened dolomite material at the clast-pendant contact allows crystalline calcite to grow and perhaps contribute to the separation and displacement of grains by force of crystallization (Weyl, 1959; Winkler and Singer, 1972; Watts, 1978; Allen, 1985; Maliva and Siever, 1988; Monger et al. 1991). Many parent clast inclusions can be seen incorporated well into the heart of the pendant (Figures 4.34-4.40). Grains that are incorporated from the parent clast undergo displacement with carbonate crystallization forcing grains apart and down into the pendant. Evidence for this is the presence of large chunks of parent material that would fit together similar to pieces in a puzzle. XRD data shows the presence of dolomite and/or quartz material in 8 out of the 8 samples analyzed (Figure 4.2). This material is probably from detrital (especially quartz) and parent clast (most likely dolomites) grains that were incorporated from either the "plucking" of grains from the parent clast or included from the soil matrix in the lamina during stalactite-style formation.

It is important to note that pendants could appear to have a stalactite style formation process and show no evidence for growth at the clast-contact void. Clast inclusions are a positive sign that this process is occurring, however, with parent clasts of lithologies other than dolomite, it may be difficult to discern.

Clast inclusions and the "break-up" zone with age

The presence of a clast break-up zone in all ages (Figure 5.6) supports the hypothesis that the clast-pendant void remains open through time and precipitation within microfractures in the parent clast result in fragments being broken off of the clast and incorporated into the pendant . This data suggests that it occurs throughout the development of the pendant and is seemingly not dependent upon time. Clast inclusions are only seen in the Q1 and Q2 soils implying that development of these features may depend upon age. The amount of time that it would take to include significant portions of the parent clast into the heart of the pendants may be on the order of 100,000+ years.

Clast inclusions and the "break-up" zone with different lithologies

Clast "break-up" zones are seen in predominantly dolomite parent-clasts (70%) (Figure 5.7). Thirty-one percent of the recorded break-up zones were in limestone material. The two samples with volcanic parent clasts did not contain a break-up zone but did have a clast-pendant contact void. This evidence suggests that the crystalline material of dolomite is more apt to break apart and form the break-up zone. However, not enough samples with lithologies other than dolomite were observed to make a definite interpretation. In this study dolomite grains are the most prevalent lithology found incorporated in the pendant matrix. Seventy-one percent of pendants with clast inclusions have dolomite parent clasts. The remaining 29% are limestone in lithology.

This study was unable to assess the importance of volcanic parent clasts due to the low number of samples of this lithology.

Grain displacement

Grains incorporated into the carbonate matrix either by detrital processes or from the zone of break-up can appear to undergo displacement by force of crystallization (Figures 4.35-4.37 and 4.39) (Bachman and Machette, 1977; Allen, 1985; Machette, 1985; Reheis, 1988; Monger et. al. 1991). Grain displacement is a physical process that does not dissolve the material involved. The portions of material that are incorporated are separated by calcium carbonate and would readily fit together similar to pieces of a puzzle. The edges of these displaced grains are sharp and may appear to have not undergone dissolution. Grain displacement is seen in 20% of the pendants sampled.

Grain displacement with age

Grain displacement is seen only in profiles of the Q1 and Q2 landforms suggesting that this process occurs in pendants Mid-Pleistocene or older in age (Figure 5.6). This is consistent with the findings of Bachman and Machette (1977) who found grains to be dispersed throughout the carbonate matrix of stage IV through VI petrocalcic horizons. Monger et al. (1991) described displaced framework grains in the stage IV laminar zone of the lower La Mesa surface in southern New Mexico. They also attribute a layer of framework grains incorporated into the lamina of the stage IV carbonate to an exclusionary process where soil particles are pushed ahead of a micrite crystallization front.

Grain displacement with differences in lithology

Grain displacement tends to be a greater factor in pendants with parent clasts of dolomite lithologies (compared to limestones) (Figure 5.7). Eighty percent of pendants that had evidence for displacement had dolomite parent clasts and only 10% (1 out of 5) were limestone. Only two volcanic clasts were studied and may not provide a true look at the relationship between grain displacement and volcanic lithologies. Inclusions of detrital and parent material grains in the pendant that are observed to undergo displacement are also found to undergo dissolution.

Grain dissolution

Grain dissolution occurs in the Q1-Q3 landforms and is represented by (1) grains that are surrounded by a large void with matching angular shape where the grain appears to have been completely or partially dissolved (Figures 4.41-4.44), (2) grains that are surrounded by amorphous silica exhibiting an indistinct boundary between grain and surrounding material (Figures 4.13 and 4.33) and/or (3) grains that are etched (Figures 4.41-4.32). Grain dissolution is probably the result of pressure applied to grain edges from calcite crystal growth (Watts, 1978; Reheis, 1988; Maliva and Siever, 1988; Levine and Hendricks, 1990; Allen, 1985). Grain dissolution is a common characteristic of petrocalcic horizons (stage III and higher).

Large, angular voids are present in 3 of the 25 samples. These features are most likely the result of partial or complete dissolution of grains. Monger et al. (1991) and Allen (1985) both described displaced and partially dissolved grains in petrocalcic horizons. These voids were also commonly associated with partial dissolution and even replacement of quartz and silicate grains (Allen, 1985). Halitim et al. (1981) also

described large angular voids surrounding small dissolved quartz grains in calcareous accumulations from the high steppes in Algeria.

In this study, amorphous coatings of silica are also observed surrounding grains (Figures 4.13 and 4.33). The dissolution of silica and other silicate minerals can contribute large amounts of silica into the soil solution that eventually precipitates as amorphous silica or silicate clays. Wang et al. (1994) attributes the dissolution of silicate grains to the formation of sepiolite. The incorporation of dissolved silica into the sepiolite crystal structure causes the surrounding soil solution to become undersaturated in silica. Wang et al. (1994) state that this process leads to enhanced dissolution of silica-containing detrital grains in the petrocalcic horizon. The minerals dissolve and release cations of Si, K, Na, Ca, Al dependant upon the grain mineralogy (Singer, 1981; Boettinger and Southard, 1990). Once in solution, the cations may be flushed through the profile, taken up by plants or join with other cations to form amorphous silica or silicate clays.

Grain dissolution with age

Grain dissolution occurs in the Q1-Q3 landform soils. However, no evidence for dissolution is seen in the Q1$_V$ Silica and Q3$_V$ Last profiles possibly due to the small number of samples observed. Grain dissolution is a time dependant process relating to stage III and greater soils. Other factors, including the formation of silicate clays in a petrocalcic horizon (Wang et al. 1994) or a well developed pendant can control the amount of dissolution in a pendant or petrocalcic horizon.

Grain dissolution with change in lithology

Grains of dolomite, quartz and feldspar were all observed to be dissolved in the

carbonate matrix of pendants. No one type of grain was observed to dissolve more

readily than the others. However, dependent upon the specific chemistries of soil pore

solutions, it is possible that specific lithologies could be more readily dissolved

Amorphous silica in pendants

Amorphous silica was found with XRD analyses in two of the samples from $Q1_D$

Backhoe and $Q2_V$ BLM profiles. Silica was also observed encompassing grains and as

lamina of pendants. Silica was observed in 8 out of 25 samples. Other studies have

reported and reviewed the occurrence of amorphous silica in arid and semi-arid soils

(Jones and Uehara, 1973; Halitim et al. 1981; Allen, 1985; Chadwick et al. 1989; Drees

et al. 1989; Boettinger and Southard, 1990; Harden et al. 1991; Eghbal and Southard,

1993; Birkeland, 1999)

Amorphous silica in pendants with age

EDS analyses show amorphous silica occurring in pendants of Q1-Q4 profiles (Figure

4.2). Macroscopic observations also show that silica is present on the undersides of clasts

in all landforms except for Q5 landforms (Figure 4.4). There is no evidence to suggest

that only older or younger surfaces contain amorphous silica. Reheis (1988) suggests that

the solubility of aluminosilicate and detrital silicate grains increases with increasing

aridity where silica and carbonate would precipitate out simultaneously. In addition, the

solubility of silica increases with increasing pH. This is also indicated in models

produced by Wang et al. (1994) where an increase in aridity is predicted to increase the

concentration of magnesium in soil pore water. This increase in dissolved magnesium

could drive the chemical precipitation of sepiolite. As explained previously, this would

deplete soil pore waters in dissolved silica that could enhance silica dissolution. Increased

evaporation would concentrate magnesium in the profile. This magnesium would "take

up" free silica (the product of grain dissolution) and combine to form sepiolite. As

sepiolite formation increases, an undersaturation of silica forces more silica to dissolve

and be added to the soil solution. Amorphous silica precipitating without sepiolite

involves complicated chemistries associated with the over and undersaturation of ions in

the soil solution. These chemical processes all take place with respect to the amount of

magnesium in the soil solution. If magnesium is not available to capture silica, then

sepiolite will not develop. It is possible that the silica seen in the samples could be an

intermediate stage before the formation of sepiolite. Perhaps local variations in silica

concentration allows amorphous silica to precipitate where in other sections it must be

used to make sepiolite.

Amorphous silica in pendants with changes in lithology

No amorphous silica was identified with EDS in $Q1_D$ and $Q2_D$ profiles and in only one

sample of $Q3_D$. However, silica was found in pendants from $Q1_V$, $Q2_V$ and $Q4_V$,

implying that pendants derived from volcanic materials have more access to soluble silica

or quartz for dissolution and reprecipitation. This evidence supports the interpretation

that silica accumulation in soils is heavily controlled by parent material composition

(Chadwick et al. 1989; Harden et al. 1991; Reheis et al. 1995). Additionally, the

contribution of volcanic ash during the Quaternary could play a significant roll in the

production of silica in Holocene aged soils. For example, ash falls such as the one

produced by Mt. Mazama approximately 6900 years ago has contributed to the Holocene

development of silicious soils in the southwest (Chadwick et al. 1989). The study area is

located on the southernmost border of the area where Mazama ash fell. An increase in magnesium from the atmosphere or parent material could cause significant dissolution of quartz then subsequent precipitation as sepiolite (Halitim et al. 1983; Wang, et al. 1994). In the soils of the study area, magnesium is believed to be available from the dissolution of dolomite parent material. The oversaturation of magnesium in these soils contributes to processes similar to those expressed by Wang et al. (1994) and Halitim et al. (1983) where the availability of magnesium combined with silica causes sepiolite to precipitate.

Sepiolite in carbonate pendants

Sepiolite has been only moderately evaluated in pedogenic environments, far less than palygorskite (Rogers et al. 1956; Bachmann and Machette, 1977; Bigham, 1980; Hay and Wiggens, 1980; Velde, 1985). However, similar developmental processes are proposed for the occurrence of both of these minerals in soils. Both palygorskite and sepiolite may form in identical pedogenic environments. The prime difference between the two is the availability of aluminum. In soils with high magnesium, silica and aluminum, the formation of palygorskite is preferred over sepiolite (Abtahi, 1980; Jones, 1983; Singer, 1984; Guzel and Wilson, 1985; Ducloux and Laouina, 1989; Monger and Daugherty, 1991). In environments where there is little or no aluminum available, sepiolite is favored to form (Abtahi, 1980; Hay and Wiggins, 1980; Jones, 1983). In the remaining discussion, the formation of sepiolite and palygorskite is assumed to be similar with differences due only to soil water chemistry.

Sepiolite can be found in several environments including arid soils. In marine environments, sepiolite forms by precipitation from solution or by transformation. Lacustrine sepiolite forms in arid and semi-arid regions in aquatic conditions containing

high magnesium and silica. Sepiolite can also form by the replacement of minerals in
rocks by the other minerals. The marine, lacustrine and rock-replacement forms of
sepiolite can be ruled out for the soils of the study area because they are formed on
alluvial sediments far from these environments.

Sepiolite is the dominant clay present in pendants of the Q1-Q3 landforms of the study
area. Pedogenic sepiolite found in these soils can be associated with with either: (1)
rising groundwater or hydrothermal alterations (Singer, 1989), (2) inheritance from
marine parent material containing these clays (Singer, 1989), (3) translocation of
materials from brought in from eolian processes from playas (Guzel and Wilson, 1983;
Jones, 1983), or (4) neoformation within the pendant or within the petrocalcic horizon as
a product of available ions from dissolution and reprecipitation of grains or other
magnesium and silica containing materials (Vanden Heuvel, 1966; Abtahi, 1980; Hay
and Wiggins, 1980; Monger and Daugherty, 1991).

Carbonate micromorphology and morphological characteristics of the soils of the study
area indicate that groundwater or hydrothermal alteration has not contributed to the
development of sepiolite in these profiles. Sepiolite as a marine product is also not
considered because XRD results do not report sepiolite or any other clays in the dolomite
clasts of the soils. However, their influence cannot be completely excluded because only
three clasts were analyzed and they may not represent the overall compositions of all
dolomites in the profiles.

Translocation of sepiolite into the soils of the study area could be plausible because
(1) nearby sources of sepiolite deposits that may have blown in, (2) the majority of
sepiolite in the study area appears to have massive form (Figure 4.17), and (3) the

occurrence of sepiolite in older landforms could be attributed to past wetter climates

that would be conducive to the formation of argillic horizons formed by translocation.

The massive appearance of the sepiolite in the study area may be attributed to the thin

sectioning of samples that would obscure the fibrous nature of this clay. However, this

does not rule out the possible translocation of these clays into the profile. A regional

source of sepiolite that could support a translocated origin includes deposits recorded by

Papke (1972) who found 4 meter thick deposits of sepiolite in the Amargosa Flat playa of

southern Nevada. Sepiolite blown from this source was noted to be a possible contributor

to the occurrence of sepiolite found in Nevada Test Site (NTS) soils. Southerly summer

winds crossing Amargosa Flat could carry the sepiolite deposits to the NTS. This process

could also happen in soils of the study area because they are in close proximity (roughly

100km) to the NTS and approximately 250km northeast of the Amargosa deposits.

However, the close proximity of these deposits to the study area cannot explain the

presence of sepiolite found within pendants of this study. Texture analyses reveal no

distinct horizons of clay accumulations suggesting that translocation of these materials

into profile does not occur to form an argillic horizon. Additionally, no sepiolite was

found in pendants younger than Late Pleistocene in age supporting that recent transport

of significant amounts of Amargosa or similar deposits has not occurred during this time.

It is important to note that only pendants were analyzed with the XRD. It is possible that

the fine grained fraction could contain some sepiolite in soils of all ages that were not

observed suggesting that translocation of sepiolite into the profile could have occurred

during the Pleistocene and even up to modern day. However, the sepiolite found within

this study occurs within the pendants and therefore it is extremely unlikely that it

accumulated there through translocation. There are no connecting pore spaces within the soil pendants except for the clast/pendant void. It is more plausible that the sepiolite found in this study is a result of neoformation. Evidence for neoformation includes instances where fibrous forms are present that appear to have formed in place. Also, the necessary ions needed for its formation are available from the magnesium rich parent material and silica from dissolved grains within the pendant. Monger and Daugherty (1991) found palygorskite fibers radiating into pore spaces and interpreted their shape and arrangement to be a product of neoformation. Fibers found parallel to grains and showing no displacement or disturbance would also provide evidence for neoformation (Monger and Daugherty, 1991). Five samples of the study area appear to have a fibrous form in void spaces and radiating perpendicular to grains (Figures 4.23, 4.24) supporting the hypothesis of neoformation.

High concentrations of silica and magnesium are needed for the formation of sepiolite in a pedogenic environment. In the study area, these materials can be provided from high magnesium parent material (dolomite) and silica found in the Tertiary volcanic rocks and from other silica-rich detrital materials (Jones, 1983; Chadwick et. al. 1989; Harden et. al. 1991; Reheis et. al. 1995). Dissolution of dolomite clasts (cupped limestones) seen in the profiles could be a source of magnesium needed for sepiolite formation (Jones, 1983; Singer, 1989). Magnesium input from eolean sources and brought into profile is another source that could be concentrated in evaporitic environments of soil poor spaces (Jones, 1983; Wang et al., 1994). Free silica is present as the result of dissolution of silicate grains and volcanic material with high glass content (Chadwick et. al. 1989; Harden et. al. 1991; Reheis et. al. 1995). The volcanic material that makes up the BLM fan and

associated surfaces provides ample silicate material that is seen eroded out as $\leq$2mm

grains at the surface. Once incorporated into the profile, it is possible that they will

undergo dissolution producing the needed silica in solution for sepiolite formation.

Samples from two horizons of Q4 Glass profile contained 20 and 19% glass in the very

fine fraction and 18 and 17% glass in the fine fraction. These grains are likely a huge

factor in the production of silica in the volcanic dominant soil profiles.

It is important to note the observation of calcium carbonate appearing to be

consumed by sepiolite in some areas of the pendants (Figures 4.18-4.19). These

relationships suggest soil pore waters that are or have been undersaturated with respect to

calcium carbonate, and possibly over saturated with silica and magnesium. This situation

may explain the relationships seen in this study in which sepiolite appears to be replacing

calcite. More research is needed to understand the specific controls and chemical

relationships between the calcium carbonate and sepiolite.

Sepiolite material as bands with carbonate appear to be formed by an "exclusionary

process" where clay is physically forced outward by the growth of calcite crystals (Allen,

1985). The appearance of carbonate being consumed (chemically) by sepiolite is noticed

in 3 of the 25 samples analyzed (Figures 4.15 and 4.16). Most often fibrous clays are

seen being consumed by carbonate in petrocalcic environments. However, those findings

do not support Bachman and Machette's (1977) proposal that sepiolite is formed in

carbonates of Mid-Pleistocene or older. Instead, sepiolite appearing to consume the

carbonate through its dissolution and the increase in silica and magnesium due to their

oversaturation seems to support these observation. Point counts conducted on the

pendants of the study area reveal an increase in clay concentration with increased time.

This data is consistent with the idea that sepiolite forms in the petrocalcic horizons with time (Figure 5.8). This data also supports the newly proposed pendant genesis where increased calcium carbonate causes pressure dissolution. This is the key to sepiolite precipitation. Overall, if the clay was being consumed through time, a decrease in accumulation with age should be noticed. Perhaps with additional time and a change in the chemical environment, sepiolite will be consumed by calcium carbonate or other minerals.

Sepiolite in pendants with age

Sepiolite is found in pendants of the Q1-Q3 landforms. Sepiolite was also identified with XRD in the $Q1_D$ Backhoe and $Q2_V$ BLM profiles. The presence of sepiolite clay in these landforms is consistent with studies conducted by Bachman and Machette (1977) and Vanden Heuvel (1966) where sepiolite and palygorskite are shown to form in petrocalcic horizons of Middle Pleistocene or older age. $Q3_D$ Mystery profile is an exception because development of the profile is determined to be only Late Pleistocene in age. An increase of sepiolite formation in older soils with little formation in younger soils supports the interpretation of pendant genesis in which sepiolite forms in petrocalcic horizons of the study area (Figure 5.8).

Sepiolite in pendants with changes in lithology

Sepiolite is found in profiles of both dolomite and volcanic parent materials. $Q3_V$ Last is the only soil profile from Q1-Q3 landforms (Pleistocene in age) where sepiolite is not found. The amount of sepiolite material was not determined in this study. However, point counts combining all clays and silica give an idea of the amount of these types of material seen in pendants of the study area. Understanding all effects of parent lithology
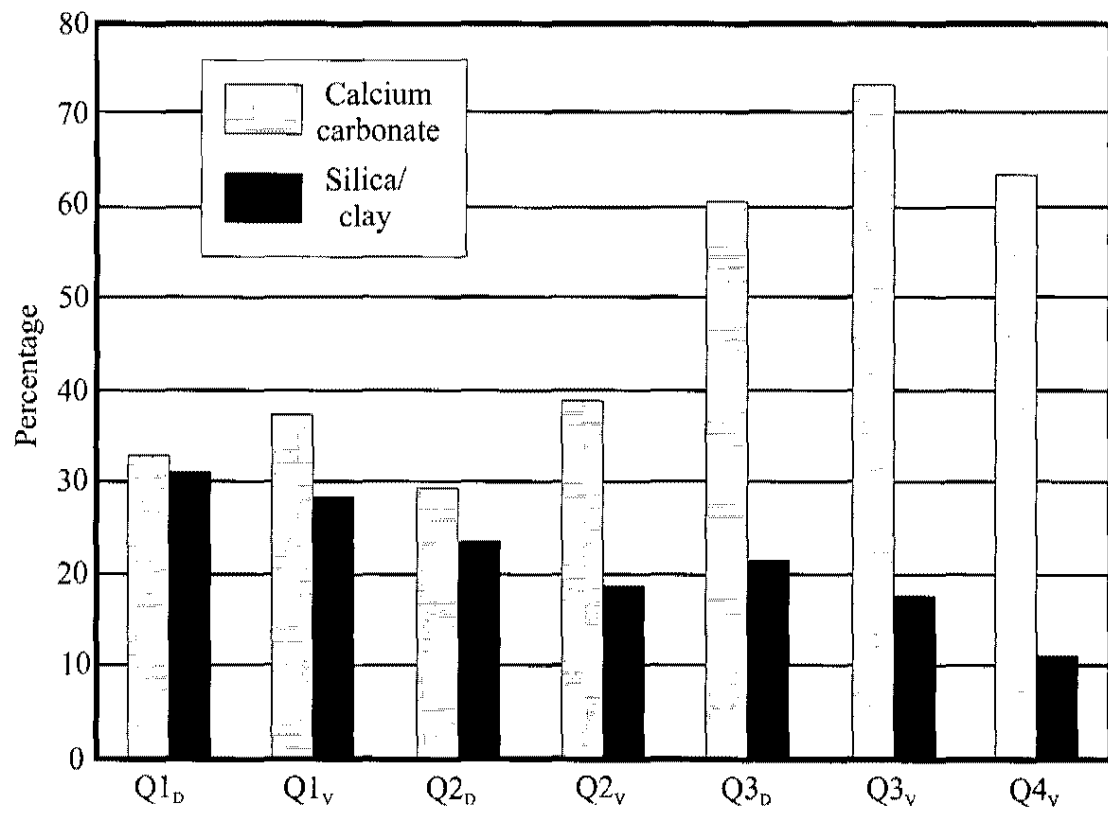
Figure 5.8.Point count data of percentage of carbonate vs. silicate amorphous material.

in soil pendants is not possible in this study. However, it is likely that parent material

may play a large role in sepiolite development. Wang et al. (1994) noted that more silica

compared to magnesium is needed for the neoformation of sepiolite. If the abundance of

dolomite within the study area soils provides significant magnesium, then the limiting

factor in the genesis of sepiolite would be silica.

Pendants as an Environment for Pellet Formation

Sepiolite in pendants of the study area appears to play an important role in the

development of pelletal material in the Q1 and Q2 landforms. In the pendants, sepiolite

appears to preferentially "roll up" and encompass grains and pieces of carbonate and

other pendant material as seen in soils studied by Hay and Wiggins (1980). The

appearance of sepiolite surrounding grains and other rounded materials could be

produced by the following mechanisms: (1) coatings of sepiolite deposited around the

grains before incorporation into the pendant, (2) dissolution of grains within the pendant

and precipitation of sepiolite as a result of pressure from calcium carbonate

crystallization and/or (3) translocation or neoformation of sepiolite to encompass grains

already existing in the pendant. Micromorphic identification of pellet-like features as

well as ovoid shaped sepiolite in Q1-Q3 pendants provides evidence for the inital

formation of pellets in pendants of the Pahranagat Valley. Sepiolite has been shown in

previous studies to preferentially encompass grains and form round masses (Hay and

Wiggens, 1980). Hay and Wiggens (1980) found pellets in fractures of petrocalcic

horizons and as inclusions within lamina at the bottoms of pendants. Grains and

carbonate surrounded by sepiolite, as well as circular masses of sepiolite found in the

carbonate matrix of pendants, are proposed to be the initial formation stages of pellets.

A proposed development for pellets in soils of the study area is as follows. (1) Detrital or

clast grains incorporated into the pendant undergo pressure dissolution to form silica

and/or the grain is surrounded by sepiolite with no dissoluion processes occuring (either

by translocation or preferential surrounding of sepiolite to grains). (2) For those grains

that have undergone partial or complete dissolution, silica released through dissolution

combines with magnesium available from the dominant dolomite material to form the

mineral sepiolite. (3) Increased precipitation with climate change and/or increased

erosion increasing the depth of wetting, dissolves the laminar carbonate of the pendants

holding these circular features allowing them to be released into the soil matrix. (4) In

time, the pellets are slowly transported down through the profile in fissures and

abandoned plant roots to be eventually deposited on the laminar cap. Hay and Wiggens

(1989) report "pustulose" mamillary appearances of the petrocalcic material. This

supports the idea that pellets are released into the profile from the dissolution of the

carbonate matrix that holds them in place. The dissolution of the carbonate matrix from

increased wetting of past glacial climates supports the presence of pellets in the Q1 and

Q2 landforms. Both of these landforms have undergone multiple episodes of glacial

climates that would contribute to the dissolution of carbonate in the soil profile. Pellets

formed in pendants would be released during these episodes and accumulate through time

in fissures (Hay and Wiggins, 1980) and on tops of laminar caps deeper in the profile.

Pellet-like forms are found in the carbonate of pendants above and below the laminar

caps. However, the pellets above the laminar cap would be subject to more wetting

episodes releasing the pellets into the soil. Because pendants have such similar

characteristics and processes that take place in the carbonate matrix, it is very likely that they are also developed in petrocalcic (stage III and greater) horizons.

Pendants as Petrocalcic Equivalents

In soil profiles, pendants are associated with stage I and stage II carbonate morphology because they coat the bottoms of clasts and/or begin to cement adjacent clasts together (Gile et al. 1966). However, at the micromorphic scale, characteristics and processes seen the pendants of the study area suggest that they are more similar in morphology to the stage III and greater carbonate horizons. Grain dissolution and sepiolite neoformation are recorded to occur in arid and semi-arid pedogenic environments with petrocalcic horizons (stage III or greater) that are interpreted to be Mid-Pleistocene or older in age (Bachman and Machette, 1977). In these soils, grains incorporated by the carbonate matrix undergo significant changes resulting from the force of crystallization by calcite crystals. This process can force silica and other ions into solution to be picked up by plant roots, or flushed through the profile. Silica in solution can combine with magnesium, aluminum and other cations to form silicate clays or precipitate out as amorphous silica. Evidence for dissolution and reprecipitation, displacement of grains and the formation of sepiolite in pendants of the Q1, Q2 and Q3 profiles of the study area suggest that these pendants are comparable to petrocalcic (stage III and greater) horizons (Bachman and Machette, 1977; Allen, 1985; Monger et al. 1991). More work must be conducted on the processes taking place in carbonate pendants to fully understand their relationship with petrocalcic horizons.

Application of Contact-Formation Style to Dating Laminae

As mentioned above, pendants have recently become important as absolute dating

tools for timing of soil development on surfaces throughout the southwestern United

States. Numerous studies have attempted to use ^{14}C and U-series methods to date inner

and outer lamina of soil pendants. Unfortunately, these techniques have not proven to be

entirely successful. Several studies have had problems with lamina dates not producing

expected values (Sowers et al 1988; Pierce, 1985). For example, work done on the Kyle

Canyon fan in southern Nevada (Sowers et al. 1988) and King Canyon fan along the Arco

fault in central Idaho (Pierce, 1985) found pendants that had inner lamina younger than

outer lamina. It is difficult to determine if pendants dated in the Kyle Canyon fan had

problematic dates because inner and outer lamina were not sampled from the same

pendant. However, Pierce (1995) recorded reversed ages for two samples where inner

and outer lamina were dated from the same pendant. In one questionable sample, inner

lamina provided $^{230}Th/^{234}U$ ages of 30±5 ka and outer lamina were 98±25ka. Another

sample had inner lamina dated at 23±ka and outer lamina of 42±8ka. These dates do not

conform to the previously assumed method of development for pendants. However, the

suggested method of pendant genesis described herein can explain these discrepancies.

Several methods are involved when evaluating the ages of pendant lamina: (1) whole

pendants are ground and dated to represent the average age of the pendant (Amundson et

al.,1989; Courtey et al. 1994; Wang and Anderson, 1998), (2) outer lamina are removed

and inner lamina are dated to reveal the approximate age for the beginning of soil

formation (Amundson et al. 1989; Amundson et al. 1994; Courtey et al. 1994; Ludwig

and Paces, 2002) and (3) both inner, outer and occasionally middle lamina are dated to

look at the stratigraphic sequence of ages within the pendant for the comparison of development through time (Pierce, 1985).

The first method described is not affected by this study because the pendant is examined as a whole. However, the application of this study to the second and third methods mentioned is critical. Without close observation of the micromorphology and relationships between lamina of pendants, the ages of lamina could be skewed. Inner lamina revealing much younger ages than the outer may not be the result of errors of the dating technique and instead may reveal true ages of a pendant that has formed by the clast-pendant contact process.

Observations of pendants on dolomite in this study area show inclusions resulting from input at the clast-pendant void. Other lithologies may not be as foretelling about their formation process. The occurrence of voids at metamorphic parent material in the study conducted by Treadwell-Steitz and McFadden (2000) implies that this formation process may occur in all lithologies so caution is recommended when dealing with any pendant from any lithology.

This study does not suggest that all pendants form in the newly proposed way. This study does however, suggest a thorough evaluation of each pendant before dating to help interpret what those dates mean to the age and/or genesis of the landform.

CHAPTER VI

CONCLUSIONS AND FUTURE WORK

Five Quaternary landforms in the northern Pahranagat Valley range in age from Early-

Pleistocene to modern (Q1-Q5) and are derived from two different lithologies of parent

material. $Q1_D$-$Q5_D$ landforms in dolomite material exhibit similar development according

to surface characteristics and soil evolution through time as the equivalent aged

landforms that were derived from volcanic material ($Q1_V$-$Q5_V$). Q1 (ballenas) are

topographically highest and oldest followed by Q2, Q3, Q4 and the lowest, modern,

active Q5 channels. Bar and swale is a common feature of the Q3-Q5 landforms in

contrast to Q1 and Q2 that contains significant Av horizons and well developed desert

pavement. Q1 landforms have undergone significant soil erosion since time of deposition.

Soil development on each landform increases with increasing age with a stage IV laminar

cap reached in the Q1 and Q2 surfaces. Surfaces Q3 and Q4 have stages II to I

respectively and Q5 contains no significant soil development. Soil pendants also increase

in thickness with increasing age. An increase with age of silica accumulation is seen on

the bottoms of clasts and pendants in the Q1-Q4 landforms. Silica accumulations are not

as well developed in the $Q1_D$-$Q4_D$ landforms as the $Q1_V$-$Q4_V$ landforms. Silica is also

found as durinodes in the in the $Q4_V$ and $Q5_V$ profiles. This variation is most likely from

the increased amount of glass shards and other silicious material weathered from the

tephra parent material on the volcanic dominant surfaces. The presence of silica in

profiles of both dolomite and volcanic lithologies suggests that Holocene ash falls may

have provided material for silica dissolution and reaccumulaion within the profile.

Soil pendants that have formed in the Quaternary landforms of the northern

Pahranagat Valley exhibit formation characteristics that have not been documented in

previous studies. Features viewed with macromorphic and micromorphic techniques

provide evidence for a new style of formation. The dominant feature contributing to this

process is a linear void found on 68 % of the clast-pendant contacts on samples viewed in

this study. At the clast-pendant contact, the linear void shows evidence of dissolution

and more importantly, precipitation of calcium carbonate and other materials such as

silica and silicate clays. Large portions of parent-clast material are incorporated in the

carbonate matrix in 28% of the pendants observed. Some parent clast grains or detrital

grains incorporated into the pendant undergo displacement and/or dissolution in soils

from the older (Q1-Q3) landforms. Evidence for displacement from the growth of calcite

crystals includes the appearance of angular grains that fit together like a puzzle. These

"puzzle pieces" are separated by pedogenic carbonate. Evidence for dissolution includes

angular voids, grains with dissolved or etched grains, and grains surrounded by silica and

sepiolite clay. The presence of dissolved grains and sepiolite clay in the Q1-Q3 pendants

of the study area suggests that these features undergo processes similar to petrocalcic

(stage III or greater) horizons that are Mid-Pleistocene or older in age (Bachmann and

Machette, 1977).

From the occurrence of the above mentioned features in pendants a new model for the

genesis of carbonate pendants is presented. (1) A linear void develops at the clast-pendant

contact that remains open to soil water throughout time. (2) Evaporation of soil water

within the void leads to the supersaturation and eventual precipitation of carbonate and/or other materials. These precipitates do not close the void. Instead, the contact between the pendant and parent clast remains open to soil fluids possibly due to differences in thermal expansion and or freeze-thaw between pedogenic carbonate and the host clast. (3) In some cases, the clast contains a break-up zone where soil fluids can infiltrate within the microfractures, precipitate crystalline or amorphous materials, and cause displacement and fragmentation of the parent clast. Further precipitation of minerals pushes these fragments deeper into the pendant. (4) Continued precipitation in the clast-pendant void as well as precipitation at the pendant terminus can occur simultaneously thus the youngest pedogenic materials can either be located at the terminus (outermost lamina), or at the clast pendant contact (innermost lamina). Precipitation at the pendant terminus can also incorporate detrital grains into the pendant matrix. (5) Dissolution of the incorporated grains by force of crystallization possibly enhanced by local changes in soil pore water chemistry may occur. The products from dissolution of incorporated grains reprecipitates as secondary minerals including sepiolite and/or amorphous silica. (6) Pore water chemistry may change through time affecting the presence and relationship of different pendant constituents. (7) Rounded forms of sepiolite may develop that may signify the beginning of pellet formation. This may be the initial stage of pisolite morphology found in stage V and VI petrocalcic horizons (Bachmann and Machette, 1977).

Recently, studies have been conducted on ^{14}C and Uranium-series dating of the inner and outer lamina of pendants with some success. Dates of some pendants show inner lamina to be younger then the outer lamina. Because those results contradicted the

assumed genesis of soil pendants (outermost laminae are the youngest), dating geomorphic landforms using this technique has been unreliable. This study presents a new mechanism for the genesis of soil pendants that can explain previous studies' results of isotopic dating. The morphologic data presented herein indicates that soil pendants can form through two different mechanisms: (1) one in which the laminae precipitate at either (or both) the clast/pendant contact or the pendant terminus resulting in the youngest laminae occurring as either the innermost laminae and/or the outermost laminae, and (2) the traditionally assummed method in which the pendant grows from the clast outward so that the outermost laminae are the youngest.

This study suggests that close and detailed examination of pendant features with microscopic techniques be conducted before dating to ensure accurate landform ages. With increased study of the mechanisms controlling soil and landform development, greater progress can be made toward assessing seismic hazards, resource conservation, paleoclimate interpretation, and urban and agricultural planning.

REFERENCES

Abtahi, A., 1980, Soil genesis as affected by topography and time in highly calcareous parent materials under semiarid conditions in Iran: SSSA Journal, v 44, p. 329-336.

Aguilar, J., Guardiola, J.L., Barahona, E., Dorronsoro, C., and Santos, F., 1981, Clay illuviation in calcareous soils *in* Bullock, P., and Murphy, C.P., eds., Soil Micromorphology v. 2, Soil Genesis, A B Academic Press, p. 541-550.

Allen, B.L., 1985, Micromorphology of Aridisols *in* Douglas, L.A., and Thompson, M.L., eds., Soil Micromorphology and Soil Classification, Proceedings of the Soil Science Society of America, Anaheim, CA. P. 197-216.

Amundson, R.G., Chadwick, O.A., Sowers, J.M., and Doner, H.E., 1989, The stable isotope chemistry of pedogenic carbonates at Kyle Canyon, Nevada: Soil Science Society of America Journal, v. 53, p. 201-210.

Amundson, R.G., Wang, Y., Chadwick, O., Trumbore, S., McFadden, L., McDonald, E., Wells., S., and DeNiro, M., 1994, Factors and processes governing the ^{14}C content of carbonate in desert soils: Earth and Planetary Science Letters, v. 125, p. 385-405.

Bachman, G.O., Machette, M.W., 1977, Calcic soils and calcretes in the southwestern U.S.: U.S. Geological Society Open-File Report 77-794, 163p.

Bigham, J.M., Jaynes, W.F., andf Allen, B.L., 1980, Pedogenic degradation of sepiolite and palygorskite on the Texas High Plains: Soil Science Society of America Journal, v. 44, p. 159-167.

Birkeland, P.W., 1999, Soils and Geomorphology, 3rd edition, Oxford University Press, New York, New York, 430 p.

Blank, R.R., and Fosberg, M.A., 1990, Micromorphology and classification of secondary calcium carbonate accumulations that surround or occur on the undersides of coarse fragments in Idaho, USA *in* Douglas, L.A., ed., Soil Micromorphology: A Basic and Applied Science, Developments in Soil Science 19, Elsevier Science, p. 341-346.

Boettinger, J.L., and Southard, R.J., 1990, Micromorphology and mineralogy of a calcareous duripan formed in granitic residuum, Mojave Desert, California, USA *in*

Douglas, L.A., ed., Developments in Soil Science 19, Soil Micromorphology: A basic and applied science, p. 409-415.

Boettinger, J.L., and Southard, R.J., 1995, Phyllosilicate distribution and origin in aridisols on a granitic pediment, western Mojave Desert: Soil Science Society of America Journal v. 59, p. 1189-1198.

Borchardt, G., 1989, Smectites *in* Dixon, J.B., Weed, S.B, eds.,Soil Science Society of America Book Series, Soil Science Society of America, Madison, WI., p. 675-727.

Buol, S.W., Hole, F.D., McCracken, R.J., and Southard, R.J., 1997, Soil genesis and classification, Fourth Edition, Iowa State University Press, Ames, Iowa, 527 p.

Bull, W.B., 1991, Geomorphic response to climate change: Oxford University Press, New York, NY., 326 p.

Chadwick, O.A., 1985, Incipient silica cementation in central Nevada alluvial soils influenced by tephra [Ph.D. thesis]: University of Arizona, 175 p.

Chadwick, O.A., Hendricks, D.M., and Nettleton, W.D., 1987, Silica in duric soils: I. A depositional model: Soil Science Society of America Journal, v. 51, p. 975-982.

Chadwick, O.A., Sowers, J.M., Amundson, R.G., 1988, Morphology of calcite crystals in clast coatings from four soils of the Mojave Desert Region: Soil Science Society of America Journal, v. 52, p. 211-219.

Chadwick, O.A., Hendricks, D.M., and Nettleton, W.D., 1989, Silicification of Holocene soils in northern Monitor Valley, Nevada: Soil Science Society of America Journal, v. 53, p. 158-164.

Courtey, M.A., Marlin, C., Dever, L., Tremblay, P., and Vachier, P., 1994, The properties, genesis and environmental significance of calcitic pendents from the High Arctic (Spitsbergen): Geoderma, v. 61., p. 71-102.

Drees, L.R., Wilding, L.P., Smeck, N.E., and Senkayi, A.L., 1989, Silica in soils: Quartz and dissordered silica polymorphs *in* Dixon, J.B.,and Weed, S.B., eds., Soil Science Society of America Minerals in Soil Environments, Soil Science Society of America Book Series n.1, 1244p.

Ducloux, J., and Laouina, A., 1989, The pendant calcretes in semi-arid climate: an example located near Taforalt, NW Morocco: Catena v. 16, p. 237-322.

Eghbal., M.K., and Southard, R.J., 1993, Micromorphological evidence of polygenesis of three Aridisols, western Mojave Desert, California: Soil Science Society of America Journal, v. 57, p. 1041-1050.

Forman, S.L., and Miller, G.H., 1984, Time dependant soil morphologies and pedogenic processes on raised beaches, Broggerhalvoya, Spitsbergen, Svalbard Archipelago: Arctic and Alpine Research, v. 16, p. 381-394.

Gee, G.W., and Bauder, J.W., 1986, Particle-size analysis *in* Methods of Soil Analysis part 1—Physical and Mineralogical Methods: Soil Science Society of America Book Series, 5, American Society of Agronomy, Inc. Madison, Wisconsin, p. 383-411.

Gile, L.H., and Grossman, R.B., 1968, Morphology of the argillic horizon in desert soils of southern New Mexico: Soil Science, v. 106, p. 6-15.

Gile, L.H., Hawley, J.W., and Grossman, R.B., 1981, Soils and geomorphology in the Basin and Range area of southern New Mexico—Guidebook to the Desert Project: New Mexico Bureau of Mines and Mineral Resources. Memoir 39, 222p.

Gile, L.H., Peterson, F.F., Grossman, R.B., 1965, The K horizon: A master soil horizon of carbonate accumulation: Soil Science, v. 99, p. 74-82.

Gile, L.H., Peterson, F.F., Grossman, R.B., 1966, Morphological and genetic sequences of carbonate accumulation in desert soils: Soil Science v. 101, p. 347-360.

Guzel, N., and Wilson, M.J., 1985, High-magnesium clays from alluvial soils of the Acipayam Plain, southern Turkey: 5th meeting of the European Clay Groups, Prague, 1983, p. 117-123.

Halitem, A., Robert,M., and Berrier, J., 1981, A microscopic study of quartz evolution in arid areas *in* Bullock, P., and Murphy, C.P., eds., Soil Micromorphology v2 Soil Genesis, AB Academic Press, p. 615-621.

Harden, J.W., Taylor, E.M., Reheis, M.C., and McFadden, L.D., 1991, Calcic, gypsic, and siliceous soil chronosequences in arid and semi-arid environments *in* Occurrence, Characteristics, and genesis of carbonate, gypsum and silica accumulations in soils: Soil Science Society of America Special Publication no. 26, p. 1-16.

Hay, R.L., and Wiggins, 1980, Pellets, ooids, sepiolite and silica in three calcretes of the southwestern United States: Sedimentology, v. 27. p. 559-576.

Hutchison, C.S., 1974, Laboratory handbook of Petrographic techniques: John Wiley and Sons, NY, NY. p. 25-26.

Isaacs, C.M., and Tharp, V.L., 1996, Proceedings of the thirteenth annual pacific climate (PACLIM) workshop: Technical Report 53, Asilomar, C.A., ed. P. 65-77.

Jones, B.F., 1983, Occurrence of clay minerals in surficial deposits of southwestern Nevada: Sciences G'eologiques Memoirs, v. 72, p. 81-92.

Jones, R.C., and Uehara, G., 1973, Amorphous coatings on mineral surfaces: Soil Science Society of America Proceedings, v. 37, p. 792-798.

Khademi, H., and Mermut, A.R., 1999, Submicroscopy and stable isotope geochemistry of carbonates and associated palygorskite in Iranian Aridisols: European Journal of Soil Sciences, v. 50, p. 207-216.

Levine, S.J., and Hendricks, D.M., 1990, Carbonate forms in residual horizons of limestone derived soils in northern Arizona *in* Douglas, L.A., ed., Developments in Soil Science 19, Soil Micromorphology: A Basic and Applied Science, p. 373-380.

Ludwig, K.R., and Paces, J.B., 2002, Uranium-series dating of pedogenic silica and carbonate, Crater Flat, Nevada: Geochemica et Cosmochemica Acta, v. 66. p. 487-506.

Mackenzie, R.C., Wilson, M.J., and Mashhady, A.S., 1984, Origin of Palygorskite in some soils of the Arabian Peninsula *in* Singer, A., and Galan, E., eds., Palygorskite-Sepiolite: Occurrences, Genesis and uses: Developments in Sedimentology, v. 37., p. 177-186.

Machette, M.N., 1985, Calcic soils of the southwestern United States: Geological Society of America Special Paper 203, 21p.

Maliva, R.G., and Siever, R., 1988, Diagenic replacement controlled by force of crystallization: Geology, v. 16, p. 655-691.

McFadden, L.D., Wells, S.G., Jercinovich, M.J., 1987, Influences of eolian and pedogenic processes on the origin and evolution of desert pavements: Geology, v. 15, p. 504-508.

McFadden, L.D., Amundson, R.G., and Chadwick, O.A., 1991, Numerical modeling, chemical, and isotopic studies of carbonate accumulation in soils of arid regions *in* Occurrence, Characteristics, and Genesis of Carbonate, Gypsum, and Silica Accumulations in Soils. Soil Science Society of America Special Publication no. 26. p. 17-35.

McFadden, L.D., McDonald, E.V., Wells, S.G., Anderson, K., Quade, J., and Forman, S.L., 1998, The vesicular layer and carbonate collars of desert soils and pavements: formation, age and relation to climate change: Geomorphology, v. 24, p. 101-145.

McFadden, L.D., and Tinsley, J.C., 1985, Rate and depth of pedogenic-carbonate accumulation in soils: Formulation and testing of a compartment model: Geological Society of America Special Paper 203, p. 23-122.

Monger, C.H., and Adams, H.P., 1996, Micromorphology of calcite-silica deposits, Yucca Mountain, Nevada: Soil Science Society of America Journal, v. 60, p. 519-530.

Monger, C.H., and Daugherty, L.A., 1991, Neoformation of Palygorskite in a southern New Mexico Aridisol: Soil Science Society of America Journal, v. 55, p. 1646-1650.

Monger, C.H., Daugherty, L.A., and Gile, L.H., 1991, A microscopic examination of pedogenic calcite in an Aridisol of southern New Mexico *in* Occurrence, Characteristics, and Genesis of Carbonate, Gypsum and Silica Accumulations in Soils: Soil Science Society of America Special Publication no. 26, p. 37-60.

Munk, L.P., and Southard, R.J., 1993, Pedogenic implications of opaline pendants in some California Late-Pleistocene Palexeralfs: Soil Science Society of America Journal, v. 57, p. 149-154.

Papke, K.G., 1972, A sepiolite-rich playa deposit in southern Nevada: Clays and Clay Minerals, v. 20, p. 211-215.

Peterson, F.F., 1981, Landforms of the Basin and Range Province; Defined for soil survey: Technical Bulletin 28. 52 p.

Pierce, K.L., 1985, Quaternary history of faulting on the Arco segment of the Lost River Fault, Central Idaho: U.S. Geological Survey Open-File Report 85-290, p. 195-206.

Pierce, K.L., and Scott, W.E., 1982, Pleistocene episodes of alluvial-gravel deposition, southeastern Idaho *in* Bonnichsen, B. and Breckenridge, R.M., eds., Cenozoic Geology of Idaho: Idaho Bureau of Mines and Geology Bulletin 26, p. 685-702.

Rabenhorst, M.C., Wilding, L.P., 1986, Pedogenesis on the Edwards Plateau, Texas: III New Model for the formation of pedrocalcic horizons: Soil Science Society of America Journal, v. 50., p. 693-699.

Reheis, M.C., 1988, Pedogenic replacement of aluminosilicate grains by $CaCO_3$ in Ustolic Haplargids, South-Central Montana, USA: Geoderma, v. 41, p. 243-261.

Reheis, M.C., Sowers, J.M., Taylor, E.M., McFadden, L.D., and Harden, J.W., 1992, Morphology and genesis of carbonate soils on the Kyle Canyon fan, Nevada, U.S.A.: Geoderma, v. 52, p. 303-342.

Rogers, L.E., Quirk, J.P., and Norrish, K., 1956, Occurrence of an aluminum-sepiolite in a soil having unusual water relationships: Journal of Soil Science, v. 7, p. 175-184.

Schoenberger, P.J., Wysocki, D.A., Benham, E.C., and Broderson, W.D., 1998, Field Book for Describing and Sampling Soils, vs. 1.1, USDA, NRCS

Singer, A., 1984, Pedogenic palygorskite in the arid environment *in* Singer, A., and
Galan, E., eds., Palygorskite-Sepiolite: Ocurrences, genesis and uses: Developments
in Sedimentology, v. 37. p. 177-186.

Sletten, R.S., 1988, The formation of pedogenic carbonates on Svalbard: The influence
of cold temperatures and freezing: Proceedings of the 5th international conference on
permafrost: Trondheim, Norway. Aug. 2-5, p. 467-394.

Soil Survey Staff, 1996, Soil Survey Laboratory Methods Manual: Soil Survey
Investigations Report no. 42. USDA.

Soil Survey Staff, 1998, Keys to Soil Taxonomy, Eighth Edition, USDA, NRCS, 326p.

Soil Survey Staff, 2000, Soil Survey of Lincoln County, Nevada, South Part: USDA,
NRCS, Part I and II.

Sowers, J.M., Harden, J.W., Robinson, S.W., McFadden, L.D., Amundson, R.G., Jull,
A.J.T., Reheis, M.C., Taylor, E.M., Szabo, B.J., Chadwick, O.A., Ku, T.L., 1988,
Geomorphology and pedology on the Kyle Canyon alluvial fan, southern Nevada *in*
Weide, D.L., and Faber, M.L., eds., This extended land, Geological Journeys in the
southern basin and range: Geological Society of America, Cordilleran Section, Field
Trip Guidebook, p. 137-157.

Spaulding, W.G., 1985, Vegetation and climates of the last 45,000 years in the vicinity of
the Nevada Test Site, south-central Nevada: USGS Professional Paper, Report P
1329, 83p.

Swett, K., 1974, Calcrete crusts in an arctic permafrost environment: American Journal of
Science, v. 274, p. 1059-1063.

Switzer, D.D., 1996, The geology and structures in the northern Hiko Range, Lincoln
County, Nevada [Master's thesis]: Las Vegas, University of Nevada, Las Vegas,
129p.

Taylor, W.J., Switzer, D.D., Hammond., K.J., 1998, Definition of fault segments on
young normal faults: Geometry, offset and scarps of the Hurricane Fault, UT and
Hiko Fault, NV: Utah Geological Survey, v. 98-2., p. 45.

Treadwell-Steitz, C., and McFadden, L.D., 2000, Influence of parent material and grain
size on carbonate coatings in gravelly soils, Palo Duro Wash, New Mexico:
Geoderma v. 94, p. 1-22.

Tschantz, C.M., and Pampeyan, E.H., 1970, Geology and mineral deposits of Lincoln
County, Nevada: Nevada Bureau of Mines and Geology Bulletin 73, 188p.

Turner, R.M., 1982, Mojave desertscrub *in* Brown, D.E., ed. Desert Plants, Biotic Communities of the American Southwest United States and Mexico v. 4, University of Arizona Press, p. 145-155.

Vanden Heuvel, R.C., 1966, The occurrence of sepiolite and attapulgite in the calcareous zone of a soil near Las Cruces, New Mexico: Proceedings of the National Conference on clays and clay minerals, v. 13, p. 193-207.

Velde, B., 1985, Sepiolite—Palygorskite *in* Clay Minerals: A Physical—Chemical Explanation of their occurrence, Elseveir, Amsterdam, p. 225-256.

Velde, B., 1992, Introduction to clay minerals. Chemistry, origins, uses and environmental significance: Chapman and Hall, London. 198 p.

Vincent, K.R., Bull, W.B., and Chadwick, O.A., 1994, Construction of a soil chronosequence using the thickness of pedogenic carbonate coatings: Journal of Geological Education v. 42, p. 316-324.

Wang, D., and Anderson, D.W., 1998, Stable carbon isotopes of carbonate pendants from Chernozemic soils of Saskatchewan,Canada: Geoderma, v. 84, p. 309-322.

Wang, Y., Nahon, D., and Merino, E., 1994, Dynamic model of the genesis of calcretes replacing silicate rocks in semi-arid regions: Geochimica et Cosmochimica Acta, v. 58, p. 5131-5145.

Watts, N.L., 1978, Displacive calcite: Evidence from recent and ancient calcretes: Geology, v. 6, p. 699-703.

Weyl, P.K., 1959, Pressure solution and the force of crystallization—A phenomenological theory: Journal of Geophysical Research, v. 64, p. 2001-2025.

Wieder, M., and Yaalon, D.H., 1974, Effect of matrix composition on carbonate nodule crystallization: Geoderma, v. 11, p. 95-121.

Winkler, E.M., and Singer, P.C., 1972, Crystallization pressure of salts in stone and concrete: Geological Society of Americal Bulletin, v. 83, p. 3509-3514.

VITA

Graduate College
University of Nevada, Las Vegas

Amy L. Brock

Local Address:
   3159 Key Largo Dr. #101
   Las Vegas, NV 89120

Home Address:
   Rt. 3 Box 223-A
   Comanche, OK 73529

Degrees:
   Bachelor of Science, Geology 1999
   Oklahoma State University

Special Honors and Awards:
   Bernada E. French Scholarship, Dept. of Geoscience, UNLV (Summer 2000, 2001)
   UNLV Graduate Student Association Grants (Summer 2000, 2001, Fall 2000)
   Arizona Nevada Academy of Science Annual Meeting, Best Poster (2000)
   UNLV Graduate Student Association Research Forum, 2nd Place Poster (Spring 2001)

Publications:
   Brock, Amy and Buck, Brenda J., 2001, Pedogenic Silica and Carbonate Along a
   Chronosequence in Northern Pahranagat Valley, Nevada: Geological Society of
   America Abstracts with Programs, v33, n6, p 436.

   Brock, A.L., Orndorff, R., and Buck, B.J., 2000, Preliminary Assessment of Tectonic
   And Climatic Influences on White River Terraces in the Pahranagat Valley, Lincoln
   Co., Nevada: Geological Society of America Abstracts with Programs, v 32, n7, p 27.

Thesis Title: Genesis and morphology of soil pendants in Quaternary landforms of
Pahranagat Valley, Nevada

Thesis Examination Committee:
   Chairperson, Dr. Brenda J. Buck, PhD
   Committee Member, Dr. Frederick Bachhuber, PhD
   Committee Member, Dr. Richard Orndorff, PhD
   Graduate Faculty Representative, Dr. Kathryn Stave, PhD